UNIVERSIDAD DE CONCEPCIÓN

Centro de Investigación en
Ingeniería Matemática (CI^{2}MA)

A posteriori error analysis of Banach spaces-based fully-mixed finite element methods for Boussinesq-type models

Gabriel N. Gatica, Cristian Inzunza,
Ricardo Ruiz-Baier, Felipe Sandoval

PREPRINT 2021-20

SERIE DE PRE-PUBLICACIONES

A posteriori error analysis of Banach spaces-based fully-mixed finite element methods for Boussinesq-type models*

GABRIEL N. GATICA† CRISTIAN INZUNZA‡
RICARDO RUIZ-BAIER§ FELIPE SANDOVAL¶

Abstract

In this paper we consider Banach spaces-based fully-mixed variational formulations that has been recently proposed for the Boussinesq and the Oberbeck-Boussinesq models, and develop reliable and efficient residual-based a posteriori error estimators for the 2D and 3D versions of the associated mixed finite element schemes. For the reliability analysis, we employ the global inf-sup condition for each equation defining the model, namely Navier-Stokes and heat equations in the case of Boussinesq, along with suitable Helmholtz decomposition in nonstandard Banach spaces, the approximation properties of the Raviart-Thomas and Clément interpolants, further regularity on the continuous solutions, and smallness assumptions on the data. In turn, the efficiency estimates follow from inverse inequalities and the localization technique through bubble functions in adequately defined local L^p spaces. Finally, several numerical results including natural convection in 3D differentially heated enclosures, are reported with the aim of confirming the theoretical properties of the estimators and illustrating the performance of the associated adaptive algorithm.

Key words: Boussinesq-Oberbeck flows, Navier–Stokes equations, heat and mass transfer, fully-mixed finite element methods, a posteriori error analysis

Mathematics subject classifications (2000): 65N30, 65N12, 65N15, 35Q79, 80A20, 76R05, 76D07

1 Introduction

We have recently introduced in [24] and [25] new fully-mixed finite element methods for the stationary Boussinesq and Oberbeck-Boussinesq problems in R^n, $n \in \{2, 3\}$, with temperature-dependent viscosities. The first model deals with the fluid motion generated by density differences due to temperature

*This research was supported in part by ANID-Chile through the project CENTRO DE MODELAMIENTO MATEMÁTICO (AFB170001) of the PIA Program: Concurso Apoyo a Centros Científicos y Tecnológicos de Excelencia con Financiamiento Basal, and the Becas Chile Programme for national students; by Centro de Investigación en Ingeniería Matemática (CI^{2}MA), Universidad de Concepción; by the Monash Mathematics Research Fund S05802-3951284; by the HPC-Europa3 Transnational Access programme through grant HPC175QA9K; by the Ministry of Science and Higher Education of the Russian Federation within the framework of state support for the creation and development of World-Class Research Centers "Digital biodesign and personalized healthcare" No. 075-15-2020-926; and by the Monash eResearch Centre and eSolutions-Research Support Services through the use of the MonARCH HPC Cluster.

†CI^{2}MA and Departamento de Ingeniería Matemática, Universidad de Concepción, Casilla 160-C, Concepción, Chile, email: ggatica@ci2ma.udec.cl.

‡CI^{2}MA and Departamento de Ingeniería Matemática, Universidad de Concepción, Casilla 160-C, Concepción, Chile, email: crinzunza@udec.cl.

§School of Mathematics, Monash University, 9 Rainforest Walk, Clayton 3800 VIC, Australia; and Institute of Computer Science and Mathematical Modelling, Sechenov University, Moscow, Russian Federation; and Universidad Adventista de Chile, Casilla 7-D, Chillán, Chile, email: ricardo.ruizbaier@monash.edu.

¶CI^{2}MA and Departamento de Ingeniería Matemática, Universidad de Concepción, Casilla 160-C, Concepción, Chile, email: fsandovals@udec.cl.

gradients, and it consists of the Navier–Stokes equations with a buoyancy term depending on the temperature, coupled to the heat equation with a convective term depending on the velocity of the fluid. In turn, the second one refers to natural convection in porous media when temperature and concentration differences occur simultaneously, and it is described by the incompressible Navier-Stokes/Brinkman equations nonlinearly coupled, via convective mass and heat transfer, to advection-diffusion equations for solute's concentration and temperature.

Regarding the main features of the aforementioned references, we first stress that the approach in [24] begins by adopting an idea that had been previously applied to the Navier-Stokes equations only (see, e.g., [30], [44]). Indeed, in addition to the velocity gradient, it introduces the Bernoulli stress tensor as a primary variable in the fluid part, which can be interpreted as an incomplete version of the usual stress tensor whose divergence yields the full equilibrium equation. Then, the novelty of [24] lies on the fact that this very same idea is applied to the heat equation forming part of the Boussinesq model as well, so that, instead of using there the classical primal or dual-mixed methods, the gradient of temperature and a vector version of the Bernoulli tensor are incorporated as further unknowns, thus yielding a modified mixed formulation. As a consequence, and besides eliminating the pressure, which can be computed later on via a postprocessing formula, the resulting continuous scheme does not need any augmentation term, as it has been usual in several previous contributions (see, e.g., [5], [6], [8], [26], [27]). In this way, a Banach spaces-based variational formulation, showing exactly the same saddle-point structure in both equations, is obtained, and hence the corresponding continuous and discrete analyses for the fluid and heat models can be performed separately and very much in the same way, which turns into a clear advantage from the theoretical point of view. In particular, Raviart-Thomas spaces of order $k \geq n-1$ for the Bernoulli tensor and its vector version, and piecewise polynomials of degree $\leq k$ for the velocity, the temperature, and both gradients, constitute a feasible choice for the well-posedness of the associated Galerkin scheme.

In turn, the theory developed in [24] is extended in [25] to the case of the Oberbeck-Boussinesq equations. In this case, and besides the aforedescribed unknowns in the fluid equations, the temperature gradient, the concentration gradient and a vector version of the Bernoulli tensor combining advective and diffusive heat and concentration fluxes, are introduced as further field variables. Thus, similarly as in [24], the resulting formulation shows again a saddle-point structure on Banach spaces in both the Navier-Stokes/Brinkman and the thermal energy conservation equations. Consequently, the tools employed in [24], which include basically the Banach and Brouwer fixed-point theorems, along with the respective Babuška-Brezzi theory, are also utilized here for the analysis of the continuous and discrete schemes. In this way, the same finite element subspaces from [24] yield now a well-posed Galerkin scheme for this second model. For related contributions dealing with Banach spaces-based variational formulations and corresponding Galerkin schemes for nonlinear and coupled problems, we refer to [13], [16], [17], [21], [22], [34], [39] and the references therein.

On the other hand, it is well known that adaptive algorithms based on a posteriori error estimators are usually employed to recover optimal rates of convergence of finite element and mixed finite element methods that loose accuracy when applied to highly nonlinear models or to problems under the eventual presence of singularities. In fact, in these cases the successive application of quasi uniform refinements in the entire domain might exhaust the computational capacity without obtaining satisfactory approximations of the solutions. In this regard, and concerning Banach spaces-based mixed finite element methods for nonlinear and coupled problems, as the ones mentioned above, not many contributions on the respective a posteriori error analyses of those numerical procedures are available so far (see, e.g. [15], [20], and [34]). In particular, the usual techniques employed within the Hilbertian framework are extended in [15] to the case of Banach spaces by deriving a reliable and efficient a posteriori error estimator for the momentum conservative mixed finite element method introduced in [16] for the steady-state Navier–Stokes problem. The above includes corresponding local estimates and new Helmholtz decompositions for the reliability, as well as respective inverse inequalities and local estimates of bubble functions for the efficiency. In turn, similar tools to those employed in [15] were previously applied in [20] to develop a residual-based a posteriori error analysis of the primal-mixed finite element method introduced in [17] for the Navier–Stokes/Darcy–Forchheimer coupled problem. The amount of references is certainly much larger for Hilbert spaces-based variational formulations, including augmented ones, of nonlinear and coupled problems, particularly of Navier-Stokes, Boussinesq, and related flow-transport coupling models. A representative list of them is given by [3], [4], [7], [10], [11], [14], [18], [19], [28], [29], [40], and [41].

According to the above discussion, and aiming to continue extending the knowledge on the numerical analysis of nonlinear and coupled problems, in this paper we proceed similarly to [15] and [20] and derive reliable and efficient residual-based a posteriori error estimators in 2D and 3D for the fully-mixed finite element methods introduced in [24] and [25]. In this way, and up to our knowledge, the present work provides the first a posteriori error analyses of non-augmented Banach spaces-based mixed finite element methods for the stationary Boussinesq and Oberbeck-Boussinesq systems.

The rest of the paper is organized as follows. At the end of this section we introduce some notations and definitions to be employed throughout the whole manuscript. In Section 2 we recall from [24] the Boussinesq model, its fully-mixed variational formulation, and the associated mixed finite element scheme. Next, in Section 3 we derive in full details a reliable and efficient residual-based a posteriori error estimator for the 2D version of the Boussinesq equations. This includes preliminary results to be utilized for the derivation of the reliability and efficiency estimates, and then the proofs of the latter themselves, respectively. Then, in Section 4 we establish the 3D version of the a posteriori error estimator provided in Section 3. Being the analysis analogue to the 2D case, the respective details are omitted. In turn, the extension of the main results from Sections 3 and 4 to the Oberbeck-Boussinesq equations are summarized in Section 5. Finally, several numerical results illustrating the reliability and efficiency of the a posteriori error estimators, as well as the good performance of the adaptive algorithms induced by them, and confirming the recovery of optimal rates of convergence, are reported in Section 6.

1.1 Preliminary notations

Let $\Omega \subseteq \mathrm{R}^n$, $n \in \{2,3\}$, be a given bounded domain with polyhedral boundary Γ, and let $\boldsymbol{\nu}$ be the outward unit normal vector on Γ. Standard notation will be adopted for Lebesgue spaces $\mathrm{L}^p(\Omega)$ and $\mathrm{L}^p(\Gamma)$, and Sobolev spaces $\mathrm{W}^{s,p}(\Omega)$ and $\mathrm{W}^{s,p}(\Gamma)$, with $s \in \mathrm{R}$ and $p > 1$, whose corresponding norms, and semi-norms in the case of the latter, either for the scalar, vector, or tensor case, are denoted by $\|\cdot\|_{0,p;\Omega}$, $\|\cdot\|_{0,p;\Gamma}$, $\|\cdot\|_{s,p;\Omega}$, $|\cdot|_{s,p;\Omega}$, $\|\cdot\|_{s,p;\Gamma}$, and $|\cdot|_{s,p;\Gamma}$, respectively. In addition, $\mathrm{W}^{s,2}(\Omega)$ and $\mathrm{W}^{s,2}(\Gamma)$ are also denoted by $\mathrm{H}^s(\Omega)$ and $\mathrm{H}^s(\Gamma)$, and the notations of their norms and semi-norms are simplified to $\|\cdot\|_{s,\Omega}$, $|\cdot|_{s,\Omega}$, $\|\cdot\|_{s,\Gamma}$, and $|\cdot|_{s,\Gamma}$, respectively. In particular, $\mathrm{H}^{1/2}(\Gamma)$ is the space of traces of functions of $\mathrm{H}^1(\Omega)$ and $\mathrm{H}^{-1/2}(\Gamma)$ is its dual. On the other hand, given any generic scalar functional space M, we let $\mathbf{M}$ and $\mathbb{M}$ be the corresponding vectorial and tensorial counterparts, whereas $\|\cdot\|$, with no subscripts, will be employed for the norm of any element or operator whenever there is no confusion about the space to which they belong. Furthermore, as usual $\mathbb{I}$ stands for the identity tensor in $\mathbb{R} := \mathrm{R}^{n\times n}$, and $|\cdot|$ denotes the Euclidean norm in $\mathbf{R} := \mathrm{R}^n$. Also, for any vector fields $\mathbf{v} = (v_i)_{i=1,n}$ and $\mathbf{w} = (w_i)_{i=1,n}$ we set the gradient, divergence, and tensor product operators, as

$$\nabla \mathbf{v} := \left(\frac{\partial v_i}{\partial x_j}\right)_{i,j=1,n}, \quad \operatorname{div}(\mathbf{v}) := \sum_{j=1}^{n} \frac{\partial v_j}{\partial x_j}, \quad \text{and} \quad \mathbf{v}\otimes\mathbf{w} := (v_i\, w_j)_{i,j=1,n}.$$

In turn, for any tensor fields $\boldsymbol{\tau} = (\tau_{ij})_{i,j=1,n}$ and $\boldsymbol{\zeta} = (\zeta_{ij})_{i,j=1,n}$, we let $\mathbf{div}(\boldsymbol{\tau})$ be the divergence operator div acting along the rows of $\boldsymbol{\tau}$, and define the transpose, the trace, the tensor inner product, and the deviatoric tensor, respectively, as

$$\boldsymbol{\tau}^{\mathtt{t}} := (\tau_{ji})_{i,j=1,n}, \quad \mathrm{tr}\,(\boldsymbol{\tau}) := \sum_{i=1}^{n} \tau_{ii}, \quad \boldsymbol{\tau} : \boldsymbol{\zeta} := \sum_{i,j=1}^{n} \tau_{ij}\zeta_{ij}\,, \quad \text{and} \quad \boldsymbol{\tau}^{\mathtt{d}} := \boldsymbol{\tau} - \frac{1}{n}\,\mathrm{tr}\,(\boldsymbol{\tau})\,\mathbb{I}\,.$$

Next, given $p > 1$, we introduce the Banach spaces

$$\mathbf{H}(\mathrm{div}_p;\Omega) := \Big\{ \boldsymbol{\tau} \in \mathbf{L}^2(\Omega) : \quad \mathrm{div}(\boldsymbol{\tau}) \in \mathrm{L}^p(\Omega) \Big\}\,,$$
$$\mathbb{H}(\mathbf{div}_p;\Omega) := \Big\{ \boldsymbol{\tau} \in \mathbb{L}^2(\Omega) : \quad \mathbf{div}(\boldsymbol{\tau}) \in \mathbf{L}^p(\Omega) \Big\}\,,$$

provided with the natural norms

$$\|\boldsymbol{\tau}\|_{\mathrm{div}_p;\Omega} := \|\boldsymbol{\tau}\|_{0,\Omega} + \|\mathrm{div}(\boldsymbol{\tau})\|_{0,p;\Omega} \qquad \forall\, \boldsymbol{\tau} \in \mathbf{H}(\mathrm{div}_p;\Omega)\,,$$

and

$$\|\boldsymbol{\tau}\|_{\mathbf{div}_p;\Omega} := \|\boldsymbol{\tau}\|_{0,\Omega} + \|\mathbf{div}(\boldsymbol{\tau})\|_{0,p;\Omega} \qquad \forall\, \boldsymbol{\tau} \in \mathbb{H}(\mathbf{div}_p;\Omega)\,.$$

Finally, we end this section by mentioning that, throughout the rest of the paper, we employ $\mathbf{0}$ to denote a generic null vector (or tensor), and use C and c, with or without subscripts, bars, tildes or hats, to denote generic constants independent of the discretization parameters, which may take different values at different places.

2 The Boussinesq model

In this section we resort to [24] to introduce the Boussinesq model, its corresponding fully-mixed variational formulation, and the associated mixed finite element method.

2.1 The boundary value problem

The stationary Boussinesq problem consists of a system of equations in which the incompressible Navier-Stokes equation is coupled with the heat equation through a convective term and a buoyancy term typically acting in opposite direction to gravity. More precisely, given a fluid occupying the region Ω, an external force per unit mass $\boldsymbol{g} \in \mathbf{L}^\infty(\Omega)$, and data $\mathbf{u}_D \in \mathbf{H}^{1/2}(\Gamma)$ and $\varphi_D \in \mathrm{H}^{1/2}(\Gamma)$, the model of interest reads: Find a velocity field $\mathbf{u}$, a pressure field p and a temperature field φ such that

$$\begin{gathered} -\mathbf{div}(2\mu(\varphi)\boldsymbol{e}(\mathbf{u})) + (\nabla\mathbf{u})\mathbf{u} + \nabla p = \varphi\boldsymbol{g} \quad \text{in} \quad \Omega, \qquad \mathrm{div}(\mathbf{u}) = 0 \quad \text{in} \quad \Omega\,, \\ \int_\Omega p = 0\,, \quad -\mathrm{div}(\mathbb{K}\nabla\varphi) + \mathbf{u}\cdot\nabla\varphi = 0 \quad \text{in} \quad \Omega\,, \\ \mathbf{u} = \mathbf{u}_D \quad \text{on} \quad \Gamma\,, \quad \text{and} \quad \varphi = \varphi_D \quad \text{on} \quad \Gamma\,, \end{gathered} \tag{2.1}$$

where $\boldsymbol{e}(\mathbf{u})$ is the symmetric part of the velocity gradient $\nabla\mathbf{u}$, also known as the strain rate tensor, and $\mathbb{K} \in \mathbb{L}^\infty(\Omega)$ is a uniformly positive tensor describing the thermal conductivity of the fluid, thus allowing the possibility of anisotropy. In turn, $\mu : \mathrm{R} \longrightarrow \mathrm{R}^+$ is the temperature dependent viscosity, which is assumed to be a Lipschitz-continuous and bounded from above and below function, which means that there exist constants $L_\mu > 0$ and $\mu_1, \mu_2 > 0$, such that

$$|\mu(s) - \mu(t)| \le L_\mu\,|s - t| \quad \text{and} \quad \mu_1 \le \mu(s) \le \mu_2 \qquad \forall\, s, t \ge 0\,. \tag{2.2}$$

We observe here that, because of the incompressibility of the fluid (cf. second eq. of (2.1)) and the Dirichlet boundary condition (cf. fifth eq. of (2.1)), $\mathbf{u}_D$ must satisfy the compatibility condition $\int_\Gamma \mathbf{u}_D \cdot \boldsymbol{\nu} = 0$.

2.2 The fully-mixed variational formulation

Following the approach from [24], we first introduce the velocity gradient $\mathbf{t}$, the Bernoulli stress tensor $\boldsymbol{\sigma}$, the temperature gradient $\widetilde{\mathbf{t}}$, and the pseudoheat flux $\widetilde{\boldsymbol{\sigma}}$ as auxiliary unknowns, that is

$$\begin{aligned} \mathbf{t} \,:=\, \nabla\mathbf{u}, \qquad \boldsymbol{\sigma} \,:=\, 2\mu(\varphi)\mathbf{t}_{sym} - \frac{1}{2}(\mathbf{u}\otimes\mathbf{u}) - p\mathbf{I}\,, \\ \widetilde{\mathbf{t}} \,:=\, \nabla\varphi, \qquad \text{and} \quad \widetilde{\boldsymbol{\sigma}} \,:=\, \mathbb{K}\widetilde{\mathbf{t}} - \frac{1}{2}\varphi\mathbf{u}\,, \end{aligned}$$

where $\mathbf{t}_{sym} := \frac{1}{2}\big(\mathbf{t} + \mathbf{t}^{\mathrm{t}}\big)$ is the symmetric part of $\mathbf{t}$. In this way, the Boussinesq problem (2.1) can be rewritten as

$$\begin{array}{rcll} \nabla\mathbf{u} & = & \mathbf{t} & \text{in} \quad \Omega\,, \\ \operatorname{tr}(\mathbf{t}) & = & 0 & \text{in} \quad \Omega\,, \\ -\mathbf{div}(\boldsymbol{\sigma}) + \dfrac{1}{2}\mathbf{t}\mathbf{u} - \varphi\boldsymbol{g} & = & 0 & \text{in} \quad \Omega\,, \\ 2\mu(\varphi)\mathbf{t}_{sym} - \dfrac{1}{2}(\mathbf{u}\otimes\mathbf{u})^{\mathrm{d}} & = & \boldsymbol{\sigma}^{\mathrm{d}} & \text{in} \quad \Omega\,, \\ \nabla\varphi & = & \widetilde{\mathbf{t}} & \text{in} \quad \Omega\,, \\ \mathbb{K}\widetilde{\mathbf{t}} - \dfrac{1}{2}\varphi\mathbf{u} & = & \widetilde{\boldsymbol{\sigma}} & \text{in} \quad \Omega\,, \\ -\operatorname{div}(\widetilde{\boldsymbol{\sigma}}) + \dfrac{1}{2}\mathbf{u}\cdot\widetilde{\mathbf{t}} & = & 0 & \text{in} \quad \Omega\,, \\ \mathbf{u} = \mathbf{u}_D \quad \text{and} \quad \varphi & = & \varphi_D & \text{on} \quad \Gamma\,, \\ \displaystyle\int_\Omega \operatorname{tr}(2\boldsymbol{\sigma} + \mathbf{u}\otimes\mathbf{u}) & = & 0\,, & \end{array} \tag{2.3}$$

where p is eliminated from the present formulation and computed afterwards in terms of $\boldsymbol{\sigma}$ and $\mathbf{u}$ by using the identity

$$p \,=\, -\frac{1}{2n}\operatorname{tr}\big(2\boldsymbol{\sigma} \,+\, \mathbf{u}\otimes\mathbf{u}\big). \tag{2.4}$$

In what follows we recall from [24] the variational formulation of (2.3), for which we begin by noticing from its first two equations that, if $\mathbf{u}$ is originally sought in $\mathbf{H}^1(\Omega)$, then $\mathbf{t}$ must belong to the space

$$\mathbb{L}^2_{\mathrm{tr}}(\Omega) \,:=\, \Big\{ \mathbf{s} \in \mathbb{L}^2_{\mathrm{tr}}(\Omega) : \quad \operatorname{tr}(\mathbf{s}) \,=\, 0 \Big\}\,.$$

Next, we consider the orthogonal decomposition

$$\mathbb{H}(\mathbf{div}_{4/3};\Omega) = \mathbb{H}_0(\mathbf{div}_{4/3};\Omega) \oplus \mathbb{R}\mathbb{I}, \tag{2.5}$$

where

$$\mathbb{H}_0(\mathbf{div}_{4/3};\Omega) \,:=\, \Big\{ \boldsymbol{\tau} \in \mathbb{H}(\mathbf{div}_{4/3};\Omega) : \quad \int_\Omega \operatorname{tr}\boldsymbol{\tau} = 0 \Big\}\,,$$

and observe, in particular, that the unknown $\boldsymbol{\sigma}$ can be uniquely decomposed, according to (2.5) and the condition $\displaystyle\int_\Omega \operatorname{tr}(2\boldsymbol{\sigma} + \mathbf{u}\otimes\mathbf{u}) = 0$, as

$$\boldsymbol{\sigma} = \boldsymbol{\sigma}_0 + c_0\mathbb{I}, \quad \text{with} \quad \boldsymbol{\sigma}_0 \in \mathbb{H}_0(\mathbf{div}_{4/3};\Omega) \quad \text{and} \quad c_0 := -\frac{1}{2n|\Omega|}\int_\Omega \operatorname{tr}(\mathbf{u}\otimes\mathbf{u}).$$

In this way, and similarly as for the pressure, the constant c_0 can be computed once the velocity is known, and hence it only remains to obtain $\boldsymbol{\sigma}_0$. In this regard, we now stress that the equations of (2.3) involving $\boldsymbol{\sigma}$ remain unchanged if $\boldsymbol{\sigma}$ is replaced by $\boldsymbol{\sigma}_0$, and hence from now on we denote $\boldsymbol{\sigma}_0$ as simply $\boldsymbol{\sigma} \in \mathbb{H}_0(\mathbf{div}_{4/3};\Omega)$. In addition, thanks to the compatibility condition satisfied by the datum $\mathbf{u}_D$ and the fact that $\mathbf{t}$ is sought in $\mathbb{L}^2_{\mathrm{tr}}(\Omega)$, we realize that testing the fourth equation of (2.3) against $\boldsymbol{\tau} \in \mathbb{H}(\mathbf{div}_{4/3};\Omega)$ is equivalent to doing it against $\boldsymbol{\tau} \in \mathbb{H}_0(\mathbf{div}_{4/3};\Omega)$.

Finally, in order to write the announced formulation in a simplified way, we now set the notations

$$(\varphi,\psi)_\Omega := \int_\Omega \varphi\,\psi, \quad (\mathbf{u},\mathbf{v})_\Omega := \int_\Omega \mathbf{u}\cdot\mathbf{v}, \quad (\boldsymbol{\sigma},\boldsymbol{\tau})_\Omega := \int_\Omega \boldsymbol{\sigma}:\boldsymbol{\tau},$$
$$\vec{\mathbf{u}} := (\mathbf{u},\mathbf{t}), \quad \vec{\mathbf{v}} := (\mathbf{v},\mathbf{s}) \in \mathbf{H} := \mathbf{L}^4(\Omega)\times\mathbb{L}^2_{\mathrm{tr}}(\Omega),$$
$$\vec{\varphi} := (\varphi,\widetilde{\mathbf{t}}), \quad \vec{\psi} := (\psi,\widetilde{\mathbf{s}}) \in \widetilde{\mathbf{H}} := \mathrm{L}^4(\Omega)\times\mathbf{L}^2(\Omega),$$
$$\|\vec{\mathbf{u}}\| := \|\mathbf{u}\|_{0,4;\Omega} + \|\mathbf{t}\|_{0,\Omega} \qquad \forall\,\vec{\mathbf{u}} := (\mathbf{u},\mathbf{t}) \in \mathbf{H}, \quad \text{and}$$
$$\|\vec{\varphi}\| := \|\varphi\|_{0,4;\Omega} + \|\widetilde{\mathbf{t}}\|_{0,\Omega} \qquad \forall\,\vec{\varphi} := (\varphi,\widetilde{\mathbf{t}}) \in \widetilde{\mathbf{H}}.$$

In this way, the fully-mixed formulation of our stationary Boussinesq problem reduces to (we refer to [24, Section 3.1] for details): Find $(\vec{\mathbf{u}},\boldsymbol{\sigma}) \in \mathbf{H}\times\mathbb{H}_0(\mathbf{div}_{4/3};\Omega)$ and $(\vec{\varphi},\widetilde{\boldsymbol{\sigma}}) \in \widetilde{\mathbf{H}}\times\mathbf{H}(\mathrm{div}_{4/3};\Omega)$ such that

$$\begin{aligned}
a_\varphi(\vec{\mathbf{u}},\vec{\mathbf{v}}) + c(\mathbf{u};\vec{\mathbf{u}},\vec{\mathbf{v}}) + b(\vec{\mathbf{v}},\boldsymbol{\sigma}) &= F_\varphi(\vec{\mathbf{v}}) &&\forall\,\vec{\mathbf{v}}\in\mathbf{H},\\
b(\vec{\mathbf{u}},\boldsymbol{\tau}) &= G(\boldsymbol{\tau}) &&\forall\,\boldsymbol{\tau}\in\mathbb{H}_0(\mathbf{div}_{4/3};\Omega),\\
\widetilde{a}(\vec{\varphi},\vec{\psi}) + \widetilde{c}_{\mathbf{u}}(\vec{\varphi},\vec{\psi}) + \widetilde{b}(\vec{\psi},\widetilde{\boldsymbol{\sigma}}) &= 0 &&\forall\,\vec{\psi}\in\widetilde{\mathbf{H}},\\
\widetilde{b}(\vec{\varphi},\widetilde{\boldsymbol{\tau}}) &= \widetilde{G}(\widetilde{\boldsymbol{\tau}}) &&\forall\,\widetilde{\boldsymbol{\tau}}\in\mathbf{H}(\mathrm{div}_{4/3};\Omega),
\end{aligned} \tag{2.6}$$

where, given arbitrary $(\mathbf{w},\phi) \in \mathbf{L}^4(\Omega)\times\mathrm{L}^4(\Omega)$, the forms a_ϕ, b, $c(\mathbf{w};\cdot,\cdot)$, $\widetilde{a}$, $\widetilde{b}$, and $\widetilde{c}_{\mathbf{w}}$, the functionals F_ϕ, G, and $\widetilde{G}$, are defined by

$$a_\phi(\vec{\mathbf{u}},\vec{\mathbf{v}}) := (2\mu(\phi)\mathbf{t}_{sym},\mathbf{s})_\Omega, \quad b(\vec{\mathbf{v}},\boldsymbol{\tau}) := -(\boldsymbol{\tau},\mathbf{s})_\Omega - (\mathbf{v},\mathbf{div}(\boldsymbol{\tau}))_\Omega, \tag{2.7}$$

$$c(\mathbf{w};\vec{\mathbf{u}},\vec{\mathbf{v}}) := \frac{1}{2}\left\{(\mathbf{t}\mathbf{w},\mathbf{v})_\Omega - \big((\mathbf{u}\otimes\mathbf{w})^{\mathrm{d}},\mathbf{s}^{\mathrm{d}}\big)_\Omega\right\}, \tag{2.8}$$

for all $\vec{\mathbf{u}} := (\mathbf{u},\mathbf{t})$, $\vec{\mathbf{v}} := (\mathbf{v},\mathbf{s}) \in \mathbf{H}$, $\boldsymbol{\tau} \in \mathbb{H}_0(\mathbf{div}_{4/3};\Omega)$,

$$\widetilde{a}(\vec{\varphi},\vec{\psi}) := (\mathbb{K}\widetilde{\mathbf{t}},\widetilde{\mathbf{s}})_\Omega, \quad \widetilde{b}(\vec{\psi},\widetilde{\boldsymbol{\tau}}) := -(\widetilde{\boldsymbol{\tau}},\widetilde{\mathbf{s}})_\Omega - (\psi,\mathrm{div}(\widetilde{\boldsymbol{\tau}}))_\Omega, \tag{2.9}$$

$$\widetilde{c}_{\mathbf{w}}(\vec{\varphi},\vec{\psi}) := \frac{1}{2}\left\{(\psi\mathbf{w},\widetilde{\mathbf{t}})_\Omega - (\varphi\mathbf{w},\widetilde{\mathbf{s}})_\Omega\right\}, \tag{2.10}$$

for all $\vec{\varphi} := (\varphi,\widetilde{\mathbf{t}})$, $\vec{\psi} := (\psi,\widetilde{\mathbf{s}}) \in \widetilde{\mathbf{H}}$, $\widetilde{\boldsymbol{\tau}} \in \mathbf{H}(\mathrm{div}_{4/3};\Omega)$, and

$$F_\phi(\vec{\mathbf{v}}) := (\phi\boldsymbol{g},\mathbf{v})_\Omega, \quad G(\boldsymbol{\tau}) := -\langle\boldsymbol{\tau}\boldsymbol{\nu},\mathbf{u}_D\rangle_\Gamma, \quad \widetilde{G}(\widetilde{\boldsymbol{\tau}}) := -\langle\widetilde{\boldsymbol{\tau}}\cdot\boldsymbol{\nu},\varphi_D\rangle_\Gamma, \tag{2.11}$$

for all $\vec{\mathbf{v}} := (\mathbf{v}, \mathbf{s}) \in \mathbf{H}$, $\boldsymbol{\tau} \in \mathbb{H}_0(\mathbf{div}_{4/3};\Omega)$, $\widetilde{\boldsymbol{\tau}} \in \mathbf{H}(\mathrm{div}_{4/3};\Omega)$.

The well posedness of (2.6), which makes use of a fixed-point strategy along with the Babuška-Brezzi theory in Banach spaces, is established by [24, Theorem 3.11].

2.3 The finite element method

Let $\{\mathcal{T}_h\}_{h>0}$ be a family of regular triangulations $\mathcal{T}_h$ of $\bar{\Omega}$ made of triangles K (when $n = 2$) or tetrahedra K (when $n = 3$). Then, given $h > 0$, we let $\mathcal{T}_h^b$ be the corresponding barycentric refinement of $\mathcal{T}_h$, and set its meshsize as $h := \max\{h_K : \ K \in \mathcal{T}_h^b\}$, where h_K denotes the diameter of K. In what follows, given an integer $\ell \geq 0$, $\mathrm{P}_\ell(K)$ stands for the space of polynomials of degree $\leq \ell$ defined on K, with vector and tensor versions denoted by $\mathbf{P}_\ell(K) := [\mathrm{P}_\ell(K)]^n$ and $\mathbb{P}_\ell(K) := [\mathrm{P}_\ell(K)]^{n\times n}$, respectively. Then, given an integer $k \geq 0$, we set for each $K \in \mathcal{T}_h^b$ the local Raviart–Thomas space of order k as

$$\mathbf{RT}_k(K) := \mathbf{P}_k(K) \oplus \mathrm{P}_k(K)\mathbf{x},$$

where $\mathbf{x} := (x_1, \ldots, x_n)^{\mathbf{t}}$ is a generic vector of $\mathbb{R}^n$. Next, following [24, Section 5], we assume from now on that $k + 1 \geq n$, and introduce the following finite element subspaces approximating the unknowns $\mathbf{u}$, $\mathbf{t}$, $\boldsymbol{\sigma}$, φ, $\widetilde{\mathbf{t}}$, and $\widetilde{\boldsymbol{\sigma}}$, respectively

$$\begin{aligned}
\mathbf{H}_h^{\mathbf{u}} &:= \Big\{\mathbf{v}_h \in \mathbf{L}^4(\Omega) : \quad \mathbf{v}_h|_K \in \mathbf{P}_k(K) \quad \forall\, K \in \mathcal{T}_h^{\mathrm{b}}\Big\},\\
\mathbb{H}_h^{\mathbf{t}} &:= \Big\{\mathbf{s}_h \in \mathbb{L}^2_{\mathrm{tr}}(\Omega) : \quad \mathbf{s}_h|_K \in \mathbb{P}_k(K) \quad \forall\, K \in \mathcal{T}_h^{\mathrm{b}}\Big\},\\
\mathbb{H}_h^{\boldsymbol{\sigma}} &:= \Big\{\boldsymbol{\tau}_h \in \mathbb{H}_0(\mathbf{div}_{4/3};\Omega) : \quad \mathbf{c}^{\mathbf{t}}\,\boldsymbol{\tau}_h|_K \in \mathbf{RT}_k(K) \quad \forall\, \mathbf{c} \in \mathrm{R}^n, \quad \forall\, K \in \mathcal{T}_h^{\mathrm{b}}\Big\},\\
\mathrm{H}_h^{\varphi} &:= \Big\{\psi_h \in \mathrm{L}^4(\Omega) : \quad \psi_h|_K \in \mathrm{P}_k(K) \quad \forall\, K \in \mathcal{T}_h^{\mathrm{b}}\Big\},\\
\mathbf{H}_h^{\widetilde{\mathbf{t}}} &:= \Big\{\widetilde{\mathbf{s}}_h \in \mathbf{L}^2(\Omega) : \quad \widetilde{\mathbf{s}}_h|_K \in \mathbf{P}_k(K) \quad \forall\, K \in \mathcal{T}_h^{\mathrm{b}}\Big\}, \quad \text{and}\\
\mathbf{H}_h^{\widetilde{\boldsymbol{\sigma}}} &:= \Big\{\widetilde{\boldsymbol{\tau}}_h \in \mathbf{H}(\mathrm{div}_{4/3};\Omega) : \quad \widetilde{\boldsymbol{\tau}}_h|_K \in \mathbf{RT}_k(K) \quad \forall\, K \in \mathcal{T}_h^{\mathrm{b}}\Big\}.
\end{aligned}$$

In addition, and similarly to Section 2.1, we set the notations

$$\begin{aligned}
\vec{\mathbf{u}}_h := (\mathbf{u}_h, \mathbf{t}_h), \quad \vec{\mathbf{v}}_h := (\mathbf{v}_h, \mathbf{s}_h) \in \mathbf{H}_h := \mathbf{H}_h^{\mathbf{u}} \times \mathbb{H}_h^{\mathbf{t}},\\
\vec{\varphi}_h := (\varphi_h, \widetilde{\mathbf{t}}_h), \quad \vec{\psi}_h := (\psi_h, \widetilde{\mathbf{s}}_h) \in \widetilde{\mathbf{H}}_h := \mathrm{H}_h^{\varphi} \times \mathbf{H}_h^{\widetilde{\mathbf{t}}}.
\end{aligned}$$

Hence, the Galerkin scheme associated with 2.6 reads: Find $(\vec{\mathbf{u}}_h, \boldsymbol{\sigma}_h) \in \mathbf{H}_h \times \mathbb{H}_h^{\boldsymbol{\sigma}}$ and $(\vec{\varphi}_h, \widetilde{\boldsymbol{\sigma}}_h) \in \widetilde{\mathbf{H}}_h \times \mathbf{H}_h^{\widetilde{\boldsymbol{\sigma}}}$ such that

$$\begin{aligned}
a_{\varphi_h}(\vec{\mathbf{u}}_h, \vec{\mathbf{v}}_h) + c(\mathbf{u}_h; \vec{\mathbf{u}}_h, \vec{\mathbf{v}}_h) + b(\vec{\mathbf{v}}_h, \boldsymbol{\sigma}_h) &= F_{\varphi_h}(\vec{\mathbf{v}}_h) && \forall\, \vec{\mathbf{v}}_h \in \mathbf{H}_h,\\
b(\vec{\mathbf{u}}_h, \boldsymbol{\tau}_h) &= G(\boldsymbol{\tau}_h) && \forall\, \boldsymbol{\tau}_h \in \mathbb{H}_h^{\boldsymbol{\sigma}},\\
\widetilde{a}(\vec{\varphi}_h, \vec{\psi}_h) + \widetilde{c}_{\mathbf{u}_h}(\vec{\varphi}_h, \vec{\psi}_h) + \widetilde{b}(\vec{\psi}_h, \widetilde{\boldsymbol{\sigma}}_h) &= 0 && \forall\, \vec{\psi}_h \in \widetilde{\mathbf{H}}_h,\\
\widetilde{b}(\vec{\varphi}_h, \widetilde{\boldsymbol{\tau}}_h) &= \widetilde{G}(\widetilde{\boldsymbol{\tau}}_h) && \forall\, \widetilde{\boldsymbol{\tau}}_h \in \mathbf{H}_h^{\widetilde{\boldsymbol{\sigma}}}.
\end{aligned} \tag{2.12}$$

The solvability analysis and the derivation of the a priori error bounds for (2.12), which employ a fixed-point strategy as well, along with the discrete version of the Babuška-Brezzi theory in Banach spaces, are provided in [24, Theorems 4.11 and 6.2].

3 A posteriori error analysis: The 2D case

In this section, we proceed to derive a reliable and efficient residual-based a posteriori error estimator for the two-dimensional version of (2.12). The corresponding a posteriori error analysis for the 3D case, which follows from minor modifications of the one to be presented next, will be addressed in Section 4.

3.1 Preliminaries for reliability

We begin by introducing a few useful notations for describing local information on elements and edges. Given $K \in \mathcal{T}_h^b$, we let $\mathcal{E}_h(K)$ be the set of its edges e, and let $\mathcal{E}_h$ be the set of all the edges e of $\mathcal{T}_h^b$, with corresponding diameters denoted by h_e. Then, we set $\mathcal{E}_h = \mathcal{E}_h(\Omega) \cup \mathcal{E}_h(\Gamma)$, where $\mathcal{E}_h(\Omega) := \{e \in \mathcal{E}_h : \quad e \subset \Omega\}$ and $\mathcal{E}_h(\Gamma) := \{e \in \mathcal{E}_h : \quad e \subset \Gamma\}$. Also for each $e \in \mathcal{E}_h$ we fix unit normal and tangential vectors to e denoted by $\boldsymbol{\nu}_e := (\nu_1, \nu_2)^{\mathrm{t}}$ and $\mathbf{s}_e := (-\nu_2, \nu_1)^{\mathrm{t}}$, respectively. However, when no confusion arises, we simply write $\boldsymbol{\nu}$ and $\mathbf{s}$ instead of $\boldsymbol{\nu}_e$ and $\mathbf{s}_e$, respectively. In addition, the usual jump operator $[\![\cdot]\!]$ across an internal edge $e \in \mathcal{E}_h(\Omega)$ is defined for piecewise continuous tensor, vector, or scalar-valued functions ζ as simply $[\![\zeta]\!] := \zeta|_K - \zeta|_{K'}$, where K and K' are the triangles of $\mathcal{T}_h^b$ having e as a common edge. Furthermore, given scalar, vector and matrix valued fields ϕ, $\mathbf{v} = (v_1, v_2)^{\mathrm{t}}$ and $\boldsymbol{\tau} := (\tau_{ij})_{2\times 2}$, respectively, we set

$$\mathbf{curl}\,(\phi) := \left(\frac{\partial \phi}{\partial x_2}, -\frac{\partial \phi}{\partial x_1}\right)^{\mathrm{t}}, \quad \underline{\mathbf{curl}}(\mathbf{v}) := \begin{pmatrix} \mathbf{curl}\,(v_1)^{\mathrm{t}} \\ \mathbf{curl}\,(v_2)^{\mathrm{t}} \end{pmatrix},$$

$$\mathrm{rot}\,(\mathbf{v}) := \frac{\partial v_2}{\partial x_1} - \frac{\partial v_1}{\partial x_2}, \quad \text{and} \quad \mathbf{rot}\,(\boldsymbol{\tau}) := \begin{pmatrix} \mathrm{rot}\,(\tau_{11}, \tau_{12}) \\ \mathrm{rot}\,(\tau_{21}, \tau_{22}) \end{pmatrix},$$

where the derivatives involved are taken in the distributional sense.

Let us now recall the main properties of the Raviart-Thomas and Clément interpolation operators (cf. [33], [23]). We begin by defining for each $p \geq \frac{2n}{n+2}$ the spaces

$$\mathbf{H}_p := \left\{\boldsymbol{\tau} \in \mathbf{H}(\mathrm{div}_p; \Omega) : \quad \boldsymbol{\tau}|_K \in \mathbf{W}^{1,p}(K) \quad \forall\, K \in \mathcal{T}_h^{\mathsf{b}}\right\}, \tag{3.1}$$

and

$$\widehat{\mathbf{H}}_h^{\boldsymbol{\sigma}} := \left\{\boldsymbol{\tau} \in \mathbf{H}(\mathrm{div}_p; \Omega) : \quad \boldsymbol{\tau}|_K \in \mathbf{RT}_k(K) \quad \forall\, K \in \mathcal{T}_h^{\mathsf{b}}\right\}. \tag{3.2}$$

In addition, we let $\Pi_h^k : \mathbf{H}_p \to \widehat{\mathbf{H}}_h^{\boldsymbol{\sigma}}$ be the Raviart-Thomas interpolation operator, which is characterized for each $\boldsymbol{\tau} \in \mathbf{H}_p$ by the identities (see e.g. [33, Section 1.2.7])

$$\int_e (\Pi_h^k(\boldsymbol{\tau}) \cdot \boldsymbol{\nu})\, \xi \;=\; \int_e (\boldsymbol{\tau} \cdot \boldsymbol{\nu})\, \xi \qquad \forall\, \xi \in \mathrm{P}_k(e), \quad \forall\, \text{edge or face } e \text{ of } \mathcal{T}_h^{\mathsf{b}}\,, \tag{3.3}$$

when $k \geq 0$, and

$$\int_K \Pi_h^k(\boldsymbol{\tau}) \cdot \psi \;=\; \int_K \boldsymbol{\tau} \cdot \psi \qquad \forall\, \psi \in \mathbf{P}_{k-1}(K)\,, \quad \forall\, K \in \mathcal{T}_h^{\mathsf{b}}\,,$$

when $k \geq 1$. In turn, given $q > 1$ such that $\frac{1}{p} + \frac{1}{q} = 1$, we let

$$\mathrm{H}_h^{\mathbf{u}} := \left\{v \in \mathrm{L}^q(\Omega) : \quad v|_K \in \mathrm{P}_k(K) \quad \forall\, K \in \mathcal{T}_h^{\mathsf{b}}\right\}, \tag{3.4}$$

and recall from [33, Lemma 1.41] that there holds

$$\mathrm{div}\big(\Pi_h^k(\boldsymbol{\tau})\big) \;=\; \mathcal{P}_h^k\big(\mathrm{div}(\boldsymbol{\tau})\big) \qquad \forall\, \boldsymbol{\tau} \in \mathbf{H}_p\,,$$

where $\mathcal{P}_h^k : \mathrm{L}^p(\Omega) \to \mathrm{H}_h^{\mathbf{u}}$ is the usual orthogonal projector with respect to the $\mathrm{L}^2(\Omega)$-inner product, which satisfies the following error estimate (see [33, Proposition 1.135]): there exists a positive constant C_0, independent of h, such that for $0 \le l \le k+1$ and $1 \le p \le \infty$ there holds

$$\|w - \mathcal{P}_h^k(w)\|_{0,p;\Omega} \,\le\, C_0\, h^l\, \|w\|_{l,p;\Omega} \qquad \forall\, w \in \mathrm{W}^{l,p}(\Omega)\,.$$

We stress that $\mathcal{P}_h^k(w)|_K \,=\, \mathcal{P}_K^k(w|_K) \;\; \forall\, w \in \mathrm{L}^p(\Omega)$, where $\mathcal{P}_K^k : \mathrm{L}^p(K) \to \mathrm{P}_k(K)$ is the corresponding local orthogonal projector. In addition, denoting by $\mathbf{H}_h^{\mathbf{u}}$ the vector version of $\mathrm{H}_h^{\mathbf{u}}$ (cf. (3.4)), we let $\boldsymbol{\mathcal{P}}_h^k : \mathbf{L}^p(\Omega) \to \mathbf{H}_h^{\mathbf{u}}$ be the vector version of $\mathcal{P}_h^k$.

Next, we collect some approximation properties of Π_h^k.

Lemma 3.1 *Given $p > 1$, there exist positive constants C_1, C_2, independent of h, such that for $0 \le l \le k$ and for each $K \in \mathcal{T}_h^b$ there holds*

$$\|\boldsymbol{\tau} - \Pi_h^k(\boldsymbol{\tau})\|_{0,p;K} \,\le\, C_1\, h_K^{l+1}\, |\boldsymbol{\tau}|_{l+1,p;K} \qquad \forall\, \boldsymbol{\tau} \in \mathbf{W}^{l+1,p}(K)\,. \tag{3.5}$$

and

$$\|\boldsymbol{\tau}\cdot\nu - \Pi_h^k(\boldsymbol{\tau})\cdot\nu\|_{0,p;e} \,\le\, C_2\, h_e^{1-1/p} |\boldsymbol{\tau}|_{1,p;K} \qquad \forall\, \boldsymbol{\tau} \in \mathbf{W}^{1,p}(K)\,, \quad \forall e \in \mathcal{E}_h(K). \tag{3.6}$$

Proof. The estimate (3.5) follows from straightforward applications of [33, Lemma B.67] and [33, Lemma 1.101] (see, e.g. [24, Lemma 5.3, eq. (5.38)]), whereas for (3.6) we refer to [15, Lemma 4.2]. □

Furthermore, denoting by $\mathbb{H}_p$ and $\widehat{\mathbb{H}}_h^{\boldsymbol{\sigma}}$ the tensor versions of $\mathbf{H}_p$ (cf. (3.1)) and $\widehat{\mathbf{H}}_h^{\boldsymbol{\sigma}}$ (cf. (3.2)), respectively, we let $\boldsymbol{\Pi}_h^k : \mathbb{H}_p \to \widehat{\mathbb{H}}_h^{\boldsymbol{\sigma}}$ be the operator Π_h^k acting row-wise. Then, according to the decomposition (2.5), for each $\boldsymbol{\tau} \in \mathbb{H}_p$ there holds

$$\boldsymbol{\Pi}_h^k(\boldsymbol{\tau}) \,=\, \boldsymbol{\Pi}_{h,0}^k(\boldsymbol{\tau}) + d\,\mathbb{I}\,, \quad \text{with} \quad d := \frac{1}{n|\Omega|}\int_\Omega \mathrm{tr}(\boldsymbol{\Pi}_h^k(\boldsymbol{\tau})) \,\in\, \mathrm{R}$$
$$\text{and} \quad \boldsymbol{\Pi}_{h,0}^k(\boldsymbol{\tau}) := \boldsymbol{\Pi}_h^k(\boldsymbol{\tau}) - d\,\mathbb{I} \in \mathbb{H}_h^{\boldsymbol{\sigma}}\,.$$

We now recall from [15] a stable Helmholtz decomposition for the Banach space $\mathbf{H}(\mathrm{div}_p;\Omega)$, whose particular case given by $p = 4/3$ will be selected in the forthcoming analysis. More precisely, we have the following result.

Lemma 3.2 *Given $p \in (1,+\infty)$, there exists a positive constant C_p such that for each $\boldsymbol{\tau} \in \mathbf{H}(\mathrm{div}_p;\Omega)$ there exist $\boldsymbol{\eta} \in \mathbf{W}^{1,p}(\Omega)$ and $\xi \in \mathrm{H}^1(\Omega)$ satisfying*

$$\boldsymbol{\tau} \,=\, \boldsymbol{\eta} + \mathbf{curl}\,(\xi) \quad \text{in} \quad \Omega \qquad \text{and} \qquad \|\boldsymbol{\eta}\|_{1,p;\Omega} + \|\xi\|_{1,\Omega} \,\le\, C_p\,\|\boldsymbol{\tau}\|_{\mathrm{div}_p;\Omega}\,.$$

Proof. See [15, Lemma 4.4]. □

We stress here that the foregoing theorem is certainly valid for the tensor version $\mathbb{H}(\mathbf{div}_p;\Omega)$ of $\mathbf{H}(\mathrm{div}_p;\Omega)$ as well, and hence in particular for $\mathbb{H}_0(\mathbf{div}_p;\Omega)$. In other words, for each $\boldsymbol{\tau} \in \mathbb{H}_0(\mathbf{div}_p;\Omega)$ there exist $\boldsymbol{\eta} \in \mathbb{W}^{1,p}(\Omega)$ and $\boldsymbol{\xi} \in \mathbf{H}^1(\Omega)$ such that

$$\boldsymbol{\tau} = \boldsymbol{\eta} + \underline{\mathbf{curl}}\,(\boldsymbol{\xi}) \quad \text{in} \quad \Omega \qquad \text{and} \qquad \|\boldsymbol{\eta}\|_{1,p;\Omega} + \|\boldsymbol{\xi}\|_{1,\Omega} \,\le\, C_p\,\|\boldsymbol{\tau}\|_{\mathbf{div}_p;\Omega}\,. \tag{3.7}$$

On the other hand, defining $X_h := \big\{v_h \in C(\overline{\Omega}) : \quad v|_K \in \mathrm{P}_1(K) \quad \forall\, K \in \mathcal{T}_h^b\big\}$ and denoting by $\mathbf{X}_h$ its vector version, we let $\mathrm{I}_h : \mathrm{H}^1(\Omega) \to X_h$ and $\mathbf{I}_h : \mathbf{H}^1(\Omega) \to \mathbf{X}_h$ be the usual Clément interpolation operator and its vector version, respectively. Some local properties of I_h, and hence of $\mathbf{I}_h$, which correspond to the particular case of [33, Lemma 1.127] that arises by choosing there $m = 0$, $p = 2$, and $\ell = 1$, are established in the following lemma.

Lemma 3.3 *There exist positive constants C_1 and C_2, such that*

$$\|v - \mathrm{I}_h v\|_{0,K} \,\le\, C_1 h_K \, \|v\|_{1,\Delta(K)} \qquad \forall\, K \in \mathcal{T}_h^b\,,$$

and

$$\|v - \mathrm{I}_h v\|_{0,e} \,\le\, C_2 h_e^{1/2} \, \|v\|_{1,\Delta(e)} \qquad \forall\, e \in \mathcal{E}_h\,,$$

where $\Delta(K) := \cup\big\{K' \in \mathcal{T}_h^b : \quad K' \cap K \neq \emptyset\big\}$ *and* $\Delta(e) := \cup\big\{K' \in \mathcal{T}_h^b : \quad K' \cap e \neq \emptyset\big\}$.

Proof. See [23] for details. □

3.2 Reliability

Recall that

$$\vec{\boldsymbol{\sigma}} := ((\vec{\mathbf{u}}, \boldsymbol{\sigma}), (\vec{\varphi}, \widetilde{\boldsymbol{\sigma}})) \in \mathbb{X} := \mathbf{H} \times \mathbb{H}_0(\mathbf{div}_{4/3};\Omega) \times \widetilde{\mathbf{H}} \times \mathbf{H}(\mathrm{div}_{4/3};\Omega)$$

is the unique solution of problem (2.6), and that

$$\vec{\boldsymbol{\sigma}}_h := ((\vec{\mathbf{u}}_h, \boldsymbol{\sigma}_h), (\vec{\varphi}_h, \widetilde{\boldsymbol{\sigma}}_h)) \in \mathbb{X}_h := \mathbf{H}_h \times \mathbb{H}_h^{\boldsymbol{\sigma}} \times \widetilde{\mathbf{H}}_h \times \mathbf{H}_h^{\widetilde{\boldsymbol{\sigma}}}$$

is a solution of problem (2.12). Then, assuming from now on that $\mathbf{u}_D \in \mathbf{H}^1(\Gamma) \cap \mathbf{L}^4(\Gamma)$ and $\varphi_D \in \mathrm{H}^1(\Gamma) \cap \mathrm{L}^4(\Gamma)$, which allows, in particular, to define their tangential derivatives $\nabla \mathbf{u}_D\, \mathbf{s}$ and $\nabla \varphi_D \cdot \mathbf{s}$, we introduce for each $K \in \mathcal{T}_h^b$ the local error indicators

$$\widetilde{\Theta}_K^{4/3} := \big\| -\mathbf{div}(\boldsymbol{\sigma}_h) + \frac{1}{2}\mathbf{t}_h\, \mathbf{u}_h - \varphi_h\, \boldsymbol{g}\big\|_{0,4/3;K}^{4/3} + \big\| -\mathrm{div}(\widetilde{\boldsymbol{\sigma}}_h) + \frac{1}{2}\mathbf{u}_h \cdot \widetilde{\mathbf{t}}_h\big\|_{0,4/3;K}^{4/3}\,, \tag{3.8}$$

$$\begin{aligned}\bar{\Theta}_K^2 := &\big\|2\mu(\varphi_h)\mathbf{t}_{h,sym} - \frac{1}{2}(\mathbf{u}_h \otimes \mathbf{u}_h)^{\mathtt{d}} - \boldsymbol{\sigma}_h^{\mathtt{d}}\big\|_{0,K}^2 + \big\|\mathbb{K}\widetilde{\mathbf{t}}_h - \frac{1}{2}\varphi_h \mathbf{u}_h - \widetilde{\boldsymbol{\sigma}}_h\big\|_{0,K}^2 \\ &+ h_K^2 \|\mathbf{rot}\,(\mathbf{t}_h)\|_{0,K}^2 + h_K^2 \|\mathrm{rot}\,(\widetilde{\mathbf{t}}_h)\|_{0,K}^2 + \sum_{e\in\mathcal{E}_h(K)\cap\mathcal{E}_h(\Omega)} h_e \Big\{ \big\|[\![\mathbf{t}_h\,\mathbf{s}]\!]\big\|_{0,e}^2 + \big\|[\![\widetilde{\mathbf{t}}_h \cdot \mathbf{s}]\!]\big\|_{0,e}^2 \Big\} \\ &+ \sum_{e\in\mathcal{E}_h(K)\cap\mathcal{E}_h(\Gamma)} h_e \Big\{ \|\mathbf{t}_h \mathbf{s} - \nabla \mathbf{u}_D\, \mathbf{s}\|_{0,e}^2 + \|\widetilde{\mathbf{t}}_h \cdot \mathbf{s} - \nabla \varphi_D \cdot \mathbf{s}\|_{0,e}^2 \Big\}\,,\end{aligned}$$

and

$$\begin{aligned}\widehat{\Theta}_K^4 := &\, h_K^4 \|\mathbf{t}_h - \nabla \mathbf{u}_h\|_{0,4;K}^4 + h_K^4 \|\widetilde{\mathbf{t}}_h - \nabla \varphi_h\|_{0,4;K}^4 \\ &+ \sum_{e\in\mathcal{E}_h(K)\cap\mathcal{E}_h(\Gamma))} h_e \Big\{ \|\mathbf{u}_D - \mathbf{u}_h\|_{0,4;e}^4 + \|\varphi_D - \varphi_h\|_{0,4;e}^4 \Big\}\,,\end{aligned} \tag{3.9}$$

so that the global a posteriori error estimator is defined as

$$\Theta = \Big\{ \sum_{K\in\mathcal{T}_h^b} \widetilde{\Theta}_K^{4/3} \Big\}^{3/4} + \Big\{ \sum_{K\in\mathcal{T}_h^b} \bar{\Theta}_K^2 \Big\}^{1/2} + \Big\{ \sum_{K\in\mathcal{T}_h^b} \widehat{\Theta}_K^4 \Big\}^{1/4}. \tag{3.10}$$

The residual character of each one of the terms defining the foregoing indicators becomes clear from a simple inspection of the strong problem (2.3) and thanks to the regularity of the continuous solution.

The main result of this section, which establishes the reliability of Θ, reads as follows.

Theorem 3.4 *Assume that the data are sufficiently small (as indicated below in Lemma* 3.7*). Then, there exists a positive constant $C_{\mathtt{rel}}$, independent of h, such that*

$$\|\vec{\boldsymbol{\sigma}} - \vec{\boldsymbol{\sigma}}_h\|_{\mathbb{X}} \,\le\, C_{\mathtt{rel}}\, \Theta\,. \tag{3.11}$$

The proof of (3.11) is performed throughout the rest of the section by means of several consecutive steps. We begin by recalling from [24, Section 3.2] the definitions of two suitable operators, namely $S : \mathbf{L}^4(\Omega)\times \mathrm{L}^4(\Omega) \to \mathbf{H}$ and $\widetilde{S} : \mathbf{L}^4(\Omega) \to \widetilde{\mathbf{H}}$. In fact, for each $(\mathbf{w},\phi) \in \mathbf{L}^4(\Omega)\times \mathrm{L}^4(\Omega)$ we let $S(\mathbf{w},\phi) := \vec{\mathbf{u}} = (\mathbf{u},\mathbf{t}) \in \mathbf{H}$, where $(\vec{\mathbf{u}},\boldsymbol{\tau})$ is the solution of the problem arising from the first two equations of (2.6) after replacing a_φ and $c(\mathbf{u};\cdot,\cdot)$ by a_ϕ and $c(\mathbf{w};\cdot,\cdot)$, respectively, that is, $(\vec{\mathbf{u}},\boldsymbol{\tau}) \in \mathbf{H}\times \mathbb{H}_0(\mathbf{div}_{4/3};\Omega)$ is such that

$$\begin{aligned} a_\phi(\vec{\mathbf{u}},\vec{\mathbf{v}}) \,+\, c(\mathbf{w};\vec{\mathbf{u}},\vec{\mathbf{v}}) \,+\, b(\vec{\mathbf{v}},\boldsymbol{\sigma}) \;&=\; F_\phi(\vec{\mathbf{v}}) \qquad \forall\, \vec{\mathbf{v}} \in \mathbf{H}\,, \\ b(\vec{\mathbf{u}},\boldsymbol{\tau}) \;&=\; G(\boldsymbol{\tau}) \qquad \forall\, \boldsymbol{\tau} \in \mathbb{H}_0(\mathbf{div}_{4/3};\Omega)\,. \end{aligned} \tag{3.12}$$

In turn, for each $\mathbf{w} \in \mathbf{L}^4(\Omega)$ we let $\widetilde{S}(\mathbf{w}) := \vec{\varphi} \in \widetilde{\mathbf{H}}$, where $(\vec{\varphi},\widetilde{\boldsymbol{\sigma}})$ is the solution of the problem arising from the last two equations of (2.6) after replacing $\mathbf{u}$ by $\mathbf{w}$, that is, $(\vec{\varphi},\widetilde{\boldsymbol{\sigma}}) \in \widetilde{\mathbf{H}}\times \mathbf{H}(\mathrm{div}_{4/3};\Omega)$ is such that

$$\begin{aligned} \widetilde{a}(\vec{\varphi},\vec{\psi}) + \widetilde{c}_{\mathbf{w}}(\vec{\varphi},\vec{\psi}) + \widetilde{b}(\vec{\psi},\widetilde{\boldsymbol{\sigma}}) \;&=\; 0 \qquad \forall\, \vec{\psi} \in \widetilde{\mathbf{H}}\,, \\ \widetilde{b}(\vec{\varphi},\widetilde{\boldsymbol{\tau}}) \;&=\; \widetilde{G}(\widetilde{\boldsymbol{\tau}}) \qquad \forall\, \widetilde{\boldsymbol{\tau}} \in \mathbf{H}(\mathrm{div}_{4/3};\Omega)\,. \end{aligned} \tag{3.13}$$

We now recall from [24, Lemmas 3.5 and 3.6] that (3.12) and (3.13) are well-posed for each $(\mathbf{w},\phi) \in \mathbf{L}^4(\Omega)\times \mathrm{L}^4(\Omega)$ and for each $\mathbf{w} \in \mathbf{L}^4(\Omega)$, respectively, which implies that the bilinear forms arising after adding the corresponding left-hand sides satisfy global inf-sup conditions uniformly. In other words, denoting from now on $\mathbf{W} := \mathbf{H}\times \mathbb{H}_0(\mathbf{div}_{4/3};\Omega)$ and $\widetilde{\mathbf{W}} := \widetilde{\mathbf{H}}\times \mathbf{H}(\mathrm{div}_{4/3};\Omega)$, there exist positive constants γ, and $\widetilde{\gamma}$, independent of $(\mathbf{w},\phi)$ and $\mathbf{w}$, respectively, such that

$$\gamma\,\|(\vec{\mathbf{z}},\boldsymbol{\zeta})\|_{\mathbf{W}} \,\le\, \sup_{\substack{(\vec{\mathbf{v}},\boldsymbol{\tau})\in\mathbf{W}\\ (\vec{\mathbf{v}},\boldsymbol{\tau})\neq\mathbf{0}}} \frac{a_\phi(\vec{\mathbf{z}},\vec{\mathbf{v}}) + c(\mathbf{w};\vec{\mathbf{z}},\vec{\mathbf{v}}) + b(\vec{\mathbf{v}},\boldsymbol{\zeta}) + b(\vec{\mathbf{z}},\boldsymbol{\tau})}{\|(\vec{\mathbf{v}},\boldsymbol{\tau})\|_{\mathbf{W}}} \qquad \forall\,(\vec{\mathbf{z}},\boldsymbol{\zeta}) \in \mathbf{W}\,, \tag{3.14}$$

and

$$\widetilde{\gamma}\,\|(\vec{\phi},\widetilde{\boldsymbol{\zeta}})\|_{\widetilde{\mathbf{W}}} \,\le\, \sup_{\substack{(\vec{\psi},\widetilde{\boldsymbol{\tau}})\in\widetilde{\mathbf{W}}\\ (\vec{\psi},\widetilde{\boldsymbol{\tau}})\neq\mathbf{0}}} \frac{\widetilde{a}(\vec{\phi},\vec{\psi}) + \widetilde{c}_{\mathbf{w}}(\vec{\phi},\vec{\psi}) + \widetilde{b}(\vec{\psi},\widetilde{\boldsymbol{\zeta}}) + \widetilde{b}(\vec{\phi},\widetilde{\boldsymbol{\tau}})}{\|(\vec{\psi},\widetilde{\boldsymbol{\tau}})\|_{\widetilde{\mathbf{W}}}} \qquad \forall\,(\vec{\phi},\widetilde{\boldsymbol{\zeta}}) \in \widetilde{\mathbf{W}}\,. \tag{3.15}$$

Next, proceeding exactly as in [24, Section 3.4], we suppose further regularity on the solutions of the problem defining the operator S (cf. (3.12)). Indeed, we assume that $\mathbf{u}_D \in \mathbf{H}^{1/2+\epsilon}(\Gamma)$ for some $\epsilon \in [1/2,1)$ (when $n=2$) or $\epsilon \in [3/4,1)$ (when $n=3$), and that for each $(\mathbf{w},\phi) \in \mathbf{L}^4(\Omega)\times \mathrm{L}^4(\Omega)$ there holds

$$S(\mathbf{w},\phi) := \vec{\mathbf{u}} = (\mathbf{u},\mathbf{t}) \in \mathbf{W}^{\epsilon,4}(\Omega) \times \big(\mathbb{L}^2_{\mathrm{tr}}(\Omega) \cap \mathbb{H}^\epsilon(\Omega)\big)\,, \tag{3.16}$$

and (cf. [24, eq. (3.62)])

$$\|\mathbf{u}\|_{\epsilon,4;\Omega} \,+\, \|\mathbf{t}\|_{\epsilon,\Omega} \,\le\, c_S\Big\{\|\phi\|_{0,4;\Omega}\,\|\boldsymbol{g}\|_{0,\infty;\Omega} \,+\, \big(1 \,+\, \|\mathbf{w}\|_{0,4;\Omega}\big)\,\|\mathbf{u}_D\|_{1/2+\epsilon,\Gamma}\Big\}\,, \tag{3.17}$$

with a positive constant c_S independent of the given $(\mathbf{w},\phi)$. In particular, taking $\|(\mathbf{w},\phi)\| \le r$, with $r > 0$ given, there holds

$$\|\mathbf{u}\|_{\epsilon,4;\Omega} \,+\, \|\mathbf{t}\|_{\epsilon,\Omega} \,\le\, c_S\Big\{r\,\|\boldsymbol{g}\|_{0,\infty;\Omega} \,+\, (1+r)\,\|\mathbf{u}_D\|_{1/2+\epsilon,\Gamma}\Big\}\,. \tag{3.18}$$

Our first estimate aiming to prove (3.11) is established as follows.

Lemma 3.5 *There exists $C_1 > 0$, independent of h, such that*

$$\begin{aligned}\|(\vec{\mathbf{u}},\boldsymbol{\sigma}) - (\vec{\mathbf{u}}_h,\boldsymbol{\sigma}_h)\|_{\mathbf{W}} \,&\le\, C_1 \Big\{ \big\| -\mathbf{div}(\boldsymbol{\sigma}_h) + \tfrac{1}{2}\mathbf{t}_h\mathbf{u}_h - \varphi_h \boldsymbol{g}\big\|_{0,4/3;\Omega} \\ &+ \quad \big\|2\mu(\varphi_h)\mathbf{t}_{h,sym} - \frac{1}{2}(\mathbf{u}_h\otimes\mathbf{u}_h)^{\mathrm{d}} - \boldsymbol{\sigma}_h^{\mathrm{d}}\big\|_{0,\Omega} + \|\vec{\mathbf{u}}_h\|_{\mathbf{H}}\,\|\mathbf{u}-\mathbf{u}_h\|_{0,4;\Omega} \\ &+ \quad \big(\|\boldsymbol{g}\|_{0,\infty;\Omega} + \|\mathbf{t}\|_{\epsilon,\Omega}\big)\|\varphi-\varphi_h\|_{0,4;\Omega} \,+\, \|\mathcal{R}\| \Big\}\,,\end{aligned} \tag{3.19}$$

where $\mathcal{R} : \mathbb{H}_0(\mathbf{div}_{4/3};\Omega) \to \mathrm{R}$ is the functional defined by

$$\mathcal{R}(\boldsymbol{\tau}) \,:=\, (\mathbf{t}_h,\boldsymbol{\tau})_\Omega + \big(\mathbf{u}_h, \mathbf{div}(\boldsymbol{\tau})\big)_\Omega - \langle \boldsymbol{\tau\nu}, \mathbf{u}_D\rangle_\Gamma \qquad \forall\,\boldsymbol{\tau}\in\mathbb{H}_0(\mathbf{div}_{4/3};\Omega)\,. \tag{3.20}$$

Proof. We begin by applying (3.14) to $(\mathbf{w},\phi) = (\mathbf{u},\varphi)$ and $(\vec{\mathbf{z}},\boldsymbol{\zeta}) = (\vec{\mathbf{u}},\boldsymbol{\sigma}) - (\vec{\mathbf{u}}_h,\boldsymbol{\sigma}_h)$. In this way, and additionally employing the first two equations of (2.6), we arrive at

$$\gamma\|(\vec{\mathbf{u}},\boldsymbol{\sigma}) - (\vec{\mathbf{u}}_h,\boldsymbol{\sigma}_h)\|_{\mathbf{W}} \,\le\, \sup_{\substack{(\vec{\mathbf{v}},\boldsymbol{\tau})\in\mathbf{W}\\ (\vec{\mathbf{v}},\boldsymbol{\tau})\neq\mathbf{0}}} \frac{\mathcal{Q}(\vec{\mathbf{v}}) + \mathcal{R}(\boldsymbol{\tau})}{\|(\vec{\mathbf{v}},\boldsymbol{\tau})\|_{\mathbf{W}}}\,, \tag{3.21}$$

where

$$\mathcal{Q}(\vec{\mathbf{v}}) := F_\varphi(\vec{\mathbf{v}}) - \Big\{ a_\varphi(\vec{\mathbf{u}}_h,\vec{\mathbf{v}}) + c(\mathbf{u};\vec{\mathbf{u}}_h,\vec{\mathbf{v}}) + b(\vec{\mathbf{v}},\boldsymbol{\sigma}_h)\Big\} \qquad \forall\,\vec{\mathbf{v}}\in\mathbf{H}\,,$$

and

$$\mathcal{R}(\boldsymbol{\tau}) \,:=\, G(\boldsymbol{\tau}) \,-\, b(\vec{\mathbf{u}}_h,\boldsymbol{\tau}) \qquad \forall\,\boldsymbol{\tau}\in\mathbb{H}_0(\mathbf{div}_{4/3};\Omega)\,,$$

which, according to the definitions of G (cf. (2.11)) and b (cf. (2.7)), yields (3.20). Next, adding and subtracting $F_{\varphi_h}(\vec{\mathbf{v}})$, $a_{\varphi_h}(\vec{\mathbf{u}}_h,\vec{\mathbf{v}})$, and $c(\mathbf{u}_h;\vec{\mathbf{u}}_h,\vec{\mathbf{v}})$, we obtain

$$\mathcal{Q}(\vec{\mathbf{v}}) \,:=\, \mathcal{Q}_1(\vec{\mathbf{v}}) + F_{\varphi-\varphi_h}(\vec{\mathbf{v}}) + a_{\varphi_h}(\vec{\mathbf{u}}_h,\vec{\mathbf{v}}) - a_\varphi(\vec{\mathbf{u}}_h,\vec{\mathbf{v}}) + c(\mathbf{u}_h;\vec{\mathbf{u}}_h,\vec{\mathbf{v}}) - c(\mathbf{u};\vec{\mathbf{u}}_h,\vec{\mathbf{v}})\,, \tag{3.22}$$

with

$$\mathcal{Q}_1(\vec{\mathbf{v}}) \,:=\, F_{\varphi_h}(\vec{\mathbf{v}}) - a_{\varphi_h}(\vec{\mathbf{u}}_h,\vec{\mathbf{v}}) - c(\mathbf{u}_h;\vec{\mathbf{u}}_h,\vec{\mathbf{v}}) - b(\vec{\mathbf{v}},\boldsymbol{\sigma}_h)\,.$$

Then, bearing in mind the definitions of the forms and functionals involved (cf. (2.7), (2.8), and (2.11)), and applying the Hölder and Cauchy-Schwarz inequalities, we find that

$$\begin{aligned}|\mathcal{Q}_1(\vec{\mathbf{v}})| \,\le\, &\Big\{ \big\| -\mathbf{div}(\boldsymbol{\sigma}_h) + \frac{1}{2}\mathbf{t}_h\mathbf{u}_h - \varphi_h\boldsymbol{g}\big\|_{0,4/3;\Omega} \\ &+ \big\|2\mu(\varphi_h)\mathbf{t}_{h,sym} - \frac{1}{2}(\mathbf{u}_h\otimes\mathbf{u}_h)^{\mathrm{d}} - \boldsymbol{\sigma}_h^{\mathrm{d}}\big\|_{0,\Omega}\Big\}\,\|\vec{\mathbf{v}}\|_{\mathbf{H}}\,,\end{aligned} \tag{3.23}$$

$$|F_{\varphi-\varphi_h}(\vec{\mathbf{v}})| \,\le\, |\Omega|^{1/2}\|\boldsymbol{g}\|_{0,\infty;\Omega}\,\|\varphi-\varphi_h\|_{0,4;\Omega}\,\|\vec{\mathbf{v}}\|_{\mathbf{H}}\,, \tag{3.24}$$

and

$$|c(\mathbf{u}_h;\vec{\mathbf{u}}_h,\vec{\mathbf{v}}) - c(\mathbf{u};\vec{\mathbf{u}}_h,\vec{\mathbf{v}})| \,\le\, \|\vec{\mathbf{u}}_h\|_{\mathbf{H}}\,\|\mathbf{u}-\mathbf{u}_h\|_{0,4;\Omega}\,\|\vec{\mathbf{v}}\|_{\mathbf{H}}\,. \tag{3.25}$$

In turn, proceeding as in the proof of [24, Lemma 3.8], that is using the Lipschitz-continuity of μ (cf. (2.2)), the Cauchy-Schwarz and Hölder inequalities again, and the regularity assumption on the operator S (cf. (3.16)), we obtain (cf. [24, eqs. (3.67) y (3.68)])

$$|a_{\varphi_h}(\vec{\mathbf{u}}_h,\vec{\mathbf{v}}) - a_\varphi(\vec{\mathbf{u}}_h,\vec{\mathbf{v}})| \,\le\, 2L_\mu\,\|i_\epsilon\|\,c(\epsilon,n,|\Omega|)\,\|\mathbf{t}\|_{\epsilon,\Omega}\,\|\varphi-\varphi_h\|_{0,4;\Omega}\,\|\vec{\mathbf{v}}\|_{\mathbf{H}}\,, \tag{3.26}$$

where i_ϵ denotes the continuous injection of $\mathbb{H}^\epsilon(\Omega)$ into $\mathbb{L}^{\epsilon^*}(\Omega)$, with $\epsilon^* := 2/(1-\epsilon)$, and $c(\epsilon, n, |\Omega|)$ is a positive constant depending on ϵ, n, and $|\Omega|$. Hence, employing (3.23), (3.24), (3.25), and (3.26) to bound $|\mathcal{Q}(\vec{\mathbf{v}})|$ (cf. (3.22)), and replacing the resulting estimate back into (3.21), we get (3.19) with $C_1 := \gamma^{-1} \max\{1, |\Omega|^{1/2}, 2L_\mu \|i_\epsilon\| c(\epsilon, n, |\Omega|)\}$, which completes the proof. □

The bound for $\|(\vec{\varphi}, \widetilde{\boldsymbol{\sigma}}) - (\vec{\varphi}_h, \widetilde{\boldsymbol{\sigma}}_h)\|_{\widetilde{\mathbf{W}}}$ is provided next.

Lemma 3.6 *There exists $C_2 > 0$, independent of h, such that*

$$\begin{aligned}\|(\vec{\varphi}, \widetilde{\boldsymbol{\sigma}}) - (\vec{\varphi}_h, \widetilde{\boldsymbol{\sigma}}_h)\|_{\widetilde{\mathbf{W}}} \,\le\, C_2 \Big\{ &\big\| -\operatorname{div}(\widetilde{\boldsymbol{\sigma}}_h) + \frac{1}{2}\mathbf{u}_h \cdot \widetilde{\mathbf{t}}_h \big\|_{0,4/3;\Omega} \\ &+ \big\|\mathbb{K}\widetilde{\mathbf{t}}_h - \frac{1}{2}\varphi_h \mathbf{u}_h - \widetilde{\boldsymbol{\sigma}}_h\big\|_{0,\Omega} + \|\vec{\varphi}_h\|_{\widetilde{\mathbf{H}}} \|\mathbf{u} - \mathbf{u}_h\|_{0,4;\Omega} + \|\widetilde{\mathcal{R}}\| \Big\},\end{aligned} \tag{3.27}$$

where $\widetilde{\mathcal{R}} : \mathbf{H}(\operatorname{div}_{4/3};\Omega) \to \mathrm{R}$ is the functional defined by

$$\widetilde{\mathcal{R}}(\widetilde{\boldsymbol{\tau}}) := (\widetilde{\mathbf{t}}_h, \widetilde{\boldsymbol{\tau}})_\Omega + (\varphi_h, \operatorname{div}(\widetilde{\boldsymbol{\tau}}))_\Omega - \langle \widetilde{\boldsymbol{\tau}} \cdot \nu, \varphi_D \rangle_\Gamma \qquad \forall\, \boldsymbol{\tau} \in \mathbf{H}(\operatorname{div}_{4/3};\Omega)\,. \tag{3.28}$$

Proof. It proceeds similarly to the proof of Lemma 3.5, but now applying the global inf-sup condition (3.15) to $\mathbf{w} = \mathbf{u}$ and $(\vec{\phi}, \widetilde{\boldsymbol{\zeta}}) = (\vec{\varphi}, \widetilde{\boldsymbol{\sigma}}) - (\vec{\varphi}_h, \widetilde{\boldsymbol{\sigma}}_h)$, and then employing the last two equations of (2.6), along with the definitions and boundedness properties of the forms and functionals involved (cf. (2.9), (2.10), and (2.11)). Further details are omitted. □

Thanks to Lemmas 3.5 and 3.6, we are able to state now a preliminary estimate for the global error

$$\|\vec{\boldsymbol{\sigma}} - \vec{\boldsymbol{\sigma}}_h\|_{\mathbb{X}} \,=\, \|(\vec{\mathbf{u}}, \boldsymbol{\sigma}) - (\vec{\mathbf{u}}_h, \boldsymbol{\sigma}_h)\|_{\mathbf{W}} \,+\, \|(\vec{\varphi}, \widetilde{\boldsymbol{\sigma}}) - (\vec{\varphi}_h, \widetilde{\boldsymbol{\sigma}}_h)\|_{\widetilde{\mathbf{W}}}\,.$$

Indeed, it follows straightforwardly from (3.19) and (3.27) that

$$\begin{aligned}\|\vec{\boldsymbol{\sigma}} - \vec{\boldsymbol{\sigma}}_h\|_{\mathbb{X}} \,\le\, C_3 \Big\{ &\big\| -\mathbf{div}(\boldsymbol{\sigma}_h) + \frac{1}{2}\mathbf{t}_h \mathbf{u}_h - \varphi_h \boldsymbol{g}\big\|_{0,4/3;\Omega} + \big\| -\operatorname{div}(\widetilde{\boldsymbol{\sigma}}_h) + \frac{1}{2}\mathbf{u}_h \cdot \widetilde{\mathbf{t}}_h\big\|_{0,4/3;\Omega} \\ &+ \big\|2\mu(\varphi_h)\mathbf{t}_{h,sym} - \frac{1}{2}(\mathbf{u}_h \otimes \mathbf{u}_h)^{\mathrm{d}} - \boldsymbol{\sigma}_h^{\mathrm{d}}\big\|_{0,\Omega} + \big\|\mathbb{K}\widetilde{\mathbf{t}}_h - \frac{1}{2}\varphi_h \mathbf{u}_h - \widetilde{\boldsymbol{\sigma}}_h\big\|_{0,\Omega} \\ &+ \big(\|\vec{\mathbf{u}}_h\|_{\mathbf{H}} + \|\vec{\varphi}_h\|_{\widetilde{\mathbf{H}}}\big) \|\mathbf{u} - \mathbf{u}_h\|_{0,4;\Omega} + \big(\|\boldsymbol{g}\|_{0,\infty;\Omega} + \|\mathbf{t}\|_{\epsilon,\Omega}\big) \|\varphi - \varphi_h\|_{0,4;\Omega} + \|\mathcal{R}\| + \|\widetilde{\mathcal{R}}\| \Big\},\end{aligned}$$

with $C_3 := \max\{C_1, C_2\}$. Then, according to the a priori estimates for $\|\vec{\mathbf{u}}_h\|_{\mathbf{H}}$ and $\|\vec{\varphi}_h\|_{\widetilde{\mathbf{H}}}$ provided by [24, Theorem 4.11, eqns. (4.24) and (4.25)], there exist positive constants $C_{S,\mathtt{d}}$ and $C_{\widetilde{S},\mathtt{d}}$, independent of h, such that

$$\|\vec{\mathbf{u}}_h\|_{\mathbf{H}} \,\le\, C_{S,\mathtt{d}} \Big\{ r\, \|\boldsymbol{g}\|_{0,\infty;\Omega} \,+\, \big(1 + r\big)\, \|\mathbf{u}_D\|_{1/2,\Gamma} \Big\}, \tag{3.29}$$

and

$$\|\vec{\varphi}_h\|_{\widetilde{\mathbf{H}}} \,\le\, C_{\widetilde{S},\mathtt{d}} \Big\{ 1 \,+\, \|\mathbb{K}\|_{0,\infty;\Omega} \,+\, r \Big\} \|\varphi_D\|_{1/2,\Gamma}\,,$$

whereas the regularity estimate (3.18) yields a corresponding bound for $\|\mathbf{t}\|_{\epsilon,\Omega}$. Thus, it follows that

$$\begin{aligned} C_3 \Big\{ \big(\|\vec{\mathbf{u}}_h\|_{\mathbf{H}} + \|\vec{\varphi}_h\|_{\widetilde{\mathbf{H}}}\big) \|\mathbf{u} - \mathbf{u}_h\|_{0,4;\Omega} + \big(\|\boldsymbol{g}\|_{0,\infty;\Omega} + \|\mathbf{t}\|_{\epsilon,\Omega}\big) \|\varphi - \varphi_h\|_{0,4;\Omega} \Big\} \\ \le\, \max\{C(\mathtt{data}), C_\epsilon(\mathtt{data})\} \|\vec{\boldsymbol{\sigma}} - \vec{\boldsymbol{\sigma}}_h\|_{\mathbb{X}}\,,\end{aligned}$$

where $C(\mathtt{data})$ and $C_\epsilon(\mathtt{data})$ are the data-depending constants given by

$$C(\mathtt{data}) \,:=\, C_3\, C_{S,\mathtt{d}} \Big\{ r\, \|\boldsymbol{g}\|_{0,\infty;\Omega} \,+\, \big(1+r\big)\, \|\mathbf{u}_D\|_{1/2,\Gamma} \Big\} \\ + C_3\, C_{\widetilde{S},\mathtt{d}} \Big\{ 1 \,+\, \|\mathbb{K}\|_{0,\infty;\Omega} \,+\, r \Big\}\, \|\varphi_D\|_{1/2,\Gamma}\,,$$

and

$$C_\epsilon(\mathtt{data}) \,:=\, C_3\, \|\boldsymbol{g}\|_{0,\infty;\Omega} + C_3\, c_S \Big\{ r\|\boldsymbol{g}\|_{0,\infty;\Omega} + (1+r)\|\mathbf{u}_D\|_{1/2+\epsilon,\Gamma} \Big\}\,.$$

As a consequence, we readily deduce the following result.

Lemma 3.7 *Assume that*

$$\max\big\{C(\mathtt{data}), C_\epsilon(\mathtt{data})\big\} \,\leq\, \frac{1}{2}\,,$$

and let $\widetilde{C} := 2C_3$. *Then there holds*

$$\|\vec{\boldsymbol{\sigma}} - \vec{\boldsymbol{\sigma}}_h\|_{\mathbb{X}} \,\leq\, \widetilde{C} \Big\{ \big\| -\mathbf{div}(\boldsymbol{\sigma}_h) + \frac{1}{2}\mathbf{t}_h\mathbf{u}_h - \varphi_h\boldsymbol{g}\big\|_{0,4/3;\Omega} + \big\| -\mathrm{div}(\widetilde{\boldsymbol{\sigma}}_h) + \frac{1}{2}\mathbf{u}_h\cdot\widetilde{\mathbf{t}}_h\big\|_{0,4/3;\Omega} \\ + \big\|2\mu(\varphi_h)\mathbf{t}_{h,sym} - \frac{1}{2}(\mathbf{u}_h\otimes\mathbf{u}_h)^{\mathrm{d}} - \boldsymbol{\sigma}_h^{\mathrm{d}}\big\|_{0,\Omega} + \big\|\mathbb{K}\widetilde{\mathbf{t}}_h - \frac{1}{2}\varphi_h\mathbf{u}_h - \widetilde{\boldsymbol{\sigma}}_h\big\|_{0,\Omega} + \|\mathcal{R}\| + \|\widetilde{\mathcal{R}}\| \Big\}\,. \tag{3.30}$$

According to (3.30), and in order to complete the derivation of our residual-based estimator, we need to bound the norms of the residual functionals $\mathcal{R}$ and $\widetilde{\mathcal{R}}$. In this regard, we now notice from the second and fourth equations of the Galerkin scheme (2.12) that $\mathcal{R}(\boldsymbol{\tau}_h) = 0$ for all $\boldsymbol{\tau}_h \in \mathbb{H}_h^{\boldsymbol{\sigma}}$ and $\widetilde{\mathcal{R}}(\widetilde{\boldsymbol{\tau}}_h) = 0$ for all $\widetilde{\boldsymbol{\tau}}_h \in \mathbf{H}_h^{\widetilde{\boldsymbol{\sigma}}}$, respectively, whence the aforementioned norms can be redefined as

$$\|\mathcal{R}\| := \sup_{\substack{\boldsymbol{\tau}\in\mathbb{H}_0(\mathbf{div}_{4/3};\Omega)\\ \boldsymbol{\tau}\neq\mathbf{0}}} \frac{\mathcal{R}(\boldsymbol{\tau}-\boldsymbol{\tau}_h)}{\|\boldsymbol{\tau}\|_{\mathbf{div}_{4/3};\Omega}} \quad\text{and}\quad \|\widetilde{\mathcal{R}}\| := \sup_{\substack{\widetilde{\boldsymbol{\tau}}\in\mathbf{H}(\mathrm{div}_{4/3};\Omega)\\ \widetilde{\boldsymbol{\tau}}\neq\mathbf{0}}} \frac{\widetilde{\mathcal{R}}(\widetilde{\boldsymbol{\tau}}-\widetilde{\boldsymbol{\tau}}_h)}{\|\widetilde{\boldsymbol{\tau}}\|_{\mathrm{div}_{4/3};\Omega}}\,, \tag{3.31}$$

where the functions $\boldsymbol{\tau}_h$ and $\widetilde{\boldsymbol{\tau}}_h$ are chosen within the suprema of (3.31) so that they depend on the corresponding $\boldsymbol{\tau} \in \mathbb{H}_0(\mathbf{div}_{4/3};\Omega)$ and $\widetilde{\boldsymbol{\tau}} \in \mathbf{H}(\mathrm{div}_{4/3};\Omega)$. More precisely, they are suitably defined in what follows by employing the Helmholtz decompositions provided by Lemma 3.2 and (3.7) with $p = 4/3$. Indeed, letting $\boldsymbol{\eta} \in \mathbb{W}^{1,4/3}(\Omega)$, $\boldsymbol{\xi} \in \mathbf{H}^1(\Omega)$, $\eta \in \mathbf{W}^{1,4/3}(\Omega)$, and $\xi \in \mathrm{H}^1(\Omega)$, such that

$$\boldsymbol{\tau} \,:=\, \boldsymbol{\eta} + \underline{\mathbf{curl}}(\boldsymbol{\xi}) \quad\text{and}\quad \widetilde{\boldsymbol{\tau}} \,:=\, \eta + \mathbf{curl}\,(\xi) \quad\text{in}\quad \Omega\,, \tag{3.32}$$

with

$$\|\boldsymbol{\eta}\|_{1,4/3;\Omega} + \|\boldsymbol{\xi}\|_{1,\Omega} \,\leq\, C_{4/3}\, \|\boldsymbol{\tau}\|_{\mathbf{div}_{4/3};\Omega} \quad\text{and}\quad \|\eta\|_{1,4/3;\Omega} + \|\xi\|_{1,\Omega} \,\leq\, C_{4/3}\, \|\tau\|_{\mathrm{div}_{4/3};\Omega}\,, \tag{3.33}$$

we set

$$\boldsymbol{\tau}_h \,:=\, \boldsymbol{\Pi}_h^k(\boldsymbol{\eta}) \,+\, \underline{\mathbf{curl}}(\mathbf{I}_h\boldsymbol{\xi}) \,+\, c\,\mathbb{I} \in \mathbb{H}_h^{\boldsymbol{\sigma}} \quad\text{and}\quad \widetilde{\boldsymbol{\tau}}_h \,:=\, \Pi_h^k(\eta) \,+\, \mathbf{curl}\,(\mathrm{I}_h\xi) \in \mathbf{H}_h^{\widetilde{\boldsymbol{\sigma}}}\,, \tag{3.34}$$

where the constant c is chosen so that $\mathrm{tr}\,(\boldsymbol{\tau}_h)$ has a null mean value, and hence $\boldsymbol{\tau}_h$ does belong to $\mathbb{H}_h^{\boldsymbol{\sigma}}$. Note that $\boldsymbol{\tau}_h$ and $\widetilde{\boldsymbol{\tau}}_h$ can be seen as discrete Helmholtz decompositions of $\boldsymbol{\tau}$ and $\widetilde{\boldsymbol{\tau}}$, respectively. In this way, using that $\mathcal{R}(c\mathbb{I}) \,=\, 0$, and denoting

$$\widehat{\boldsymbol{\eta}} \,:=\, \boldsymbol{\eta} - \boldsymbol{\Pi}_h^k(\boldsymbol{\eta})\,, \quad \widehat{\boldsymbol{\xi}} \,:=\, \boldsymbol{\xi} - \mathbf{I}_h\boldsymbol{\xi}\,, \quad \widehat{\eta} \,:=\, \eta - \Pi_h^k(\eta)\,, \quad\text{and}\quad \widehat{\xi} \,:=\, \xi - \mathrm{I}_h\xi\,,$$

it follows from (3.32) and (3.34) that

$$\mathcal{R}(\boldsymbol{\tau}) \,=\, \mathcal{R}(\boldsymbol{\tau}-\boldsymbol{\tau}_h) \,=\, \mathcal{R}(\widehat{\boldsymbol{\eta}}) \,+\, \mathcal{R}(\underline{\mathbf{curl}}(\widehat{\boldsymbol{\xi}}))\,, \tag{3.35}$$

and

$$\widetilde{\mathcal{R}}(\widetilde{\boldsymbol{\tau}}) \,=\, \widetilde{\mathcal{R}}(\widetilde{\boldsymbol{\tau}}-\widetilde{\boldsymbol{\tau}}_h) \,=\, \widetilde{\mathcal{R}}(\widehat{\eta}) \,+\, \widetilde{\mathcal{R}}(\mathbf{curl}\,(\widehat{\xi}))\,, \tag{3.36}$$

where, according to the definitions of $\mathcal{R}$ and $\widetilde{\mathcal{R}}$ (cf. (3.20) and (3.28)), we find that

$$\mathcal{R}(\widehat{\boldsymbol{\eta}}) \,=\, (\mathbf{t}_h,\widehat{\boldsymbol{\eta}})_\Omega \,+\, (\mathbf{u}_h,\mathbf{div}(\widehat{\boldsymbol{\eta}}))_\Omega \,-\, \langle \widehat{\boldsymbol{\eta}}\boldsymbol{\nu},\mathbf{u}_D\rangle_\Gamma\,, \tag{3.37}$$

$$\mathcal{R}(\underline{\mathbf{curl}}(\widehat{\boldsymbol{\xi}})) \,=\, (\mathbf{t}_h,\underline{\mathbf{curl}}(\widehat{\boldsymbol{\xi}}))_\Omega \,-\, \langle \underline{\mathbf{curl}}(\widehat{\boldsymbol{\xi}})\boldsymbol{\nu},\mathbf{u}_D\rangle_\Gamma\,, \tag{3.38}$$

$$\widetilde{\mathcal{R}}(\widehat{\eta}) \,=\, (\widetilde{\mathbf{t}}_h,\widehat{\eta})_\Omega \,+\, (\varphi_h,\mathrm{div}(\widehat{\eta}))_\Omega \,-\, \langle \widehat{\eta}\cdot\boldsymbol{\nu},\varphi_D\rangle_\Gamma\,,$$

and

$$\widetilde{\mathcal{R}}(\mathbf{curl}\,(\widehat{\xi})) \,=\, (\widetilde{\mathbf{t}}_h,\mathbf{curl}\,(\widehat{\xi}))_\Omega \,-\, \langle \mathbf{curl}\,(\widehat{\xi})\cdot\boldsymbol{\nu},\varphi_D\rangle_\Gamma\,.$$

The following lemma establishes the residual upper bound for $\|\mathcal{R}\|$.

Lemma 3.8 *There exists a positive constant C, independent of h, such that*

$$\|\mathcal{R}\| \,\leq\, C\left\{\bar{\boldsymbol{\Phi}} \,+\, \widehat{\boldsymbol{\Phi}}\right\}, \tag{3.39}$$

where

$$\bar{\boldsymbol{\Phi}}^2 \,:=\, \sum_{K\in\mathcal{T}_h^b} \bar{\Phi}_K^2 \quad \textit{and} \quad \widehat{\boldsymbol{\Phi}}^4 \,:=\, \sum_{K\in\mathcal{T}_h^b} \widehat{\Phi}_K^4\,,$$

with

$$\bar{\Phi}_K^2 \,:=\, h_K^2\,\|\mathbf{rot}\,(\mathbf{t}_h)\|_{0,K}^2 \,+\, \sum_{e\in\mathcal{E}_h(K)\cap\mathcal{E}_h(\Omega)} h_e\,\|[\![\mathbf{t}_h\,\mathbf{s}]\!]\|_{0,e}^2 \,+\, \sum_{e\in\mathcal{E}_h(K)\cap\mathcal{E}_h(\Gamma)} h_e\,\|\mathbf{t}_h\mathbf{s}-\nabla\mathbf{u}_D\,\mathbf{s}\|_{0,e}^2\,,$$

and

$$\widehat{\Phi}_K^4 \,:=\, h_K^4\,\|\mathbf{t}_h-\nabla\mathbf{u}_h\|_{0,4;K}^4 \,+\, \sum_{e\in\mathcal{E}_h(K)\cap\mathcal{E}_h(\Gamma)} h_e\,\|\mathbf{u}_D-\mathbf{u}_h\|_{0,4;e}^4\,.$$

Proof. According to (3.35), we begin by estimating $\mathcal{R}(\widehat{\boldsymbol{\eta}})$ (cf. (3.37)). Let us first observe that, for each $e\in\mathcal{E}_h$, the identity (3.3) and the fact that $\mathbf{u}_h|_e\in\mathbf{P}_k(e)$ yield $\displaystyle\int_e \widehat{\boldsymbol{\eta}}\boldsymbol{\nu}\cdot\mathbf{u}_h = 0$. Hence, locally integrating by parts the second term in (3.37), we readily obtain

$$\mathcal{R}(\widehat{\boldsymbol{\eta}}) = (\mathbf{t}_h-\nabla\mathbf{u}_h,\widehat{\boldsymbol{\eta}})_\Omega - \sum_{e\in\mathcal{E}_h(\Gamma)}\int_e \mathbf{u}_D\cdot\widehat{\boldsymbol{\eta}}\boldsymbol{\nu} = (\mathbf{t}_h-\nabla\mathbf{u}_h,\widehat{\boldsymbol{\eta}})_\Omega - \sum_{e\in\mathcal{E}_h(\Gamma)}\int_e (\mathbf{u}_D-\mathbf{u}_h)\cdot\widehat{\boldsymbol{\eta}}\boldsymbol{\nu}\,,$$

from which, applying the Hölder inequality along with the approximation properties (3.5) and (3.6) (cf. Lemma 3.1) with $p=4/3$ and $l=0$, we find that

$$\begin{aligned}|\mathcal{R}(\widehat{\boldsymbol{\eta}})| \,&\leq\, \sum_{K\in\mathcal{T}_h^b}\|\mathbf{t}_h-\nabla\mathbf{u}_h\|_{0,4;K}\,\|\widehat{\boldsymbol{\eta}}\|_{0,4/3;K} \,+\, \sum_{e\in\mathcal{E}_h(\Gamma)}\|\mathbf{u}_D-\mathbf{u}_h\|_{0,4;e}\,\|\widehat{\boldsymbol{\eta}}\boldsymbol{\nu}\|_{0,4/3;e}\\ &\leq\, \widehat{C}_1\left\{\sum_{K\in\mathcal{T}_h^b} h_K\,\|\mathbf{t}_h-\nabla\mathbf{u}_h\|_{0,4;K}\,|\boldsymbol{\eta}|_{1,4/3;K} \,+\, \sum_{e\in\mathcal{E}_h(\Gamma)} h_e^{1/4}\,\|\mathbf{u}_D-\mathbf{u}_h\|_{0,4;e}\,|\boldsymbol{\eta}|_{1,4/3;K_e}\right\},\end{aligned}$$

where, given $e \in \mathcal{E}_h(\Gamma)$, K_e is the triangle of $\mathcal{T}_h^b$ having e as an edge. Then, employing the discrete Hölder inequality in the above sums and then the first stability estimate of (3.33), we arrive at

$$|\mathcal{R}(\widehat{\boldsymbol{\eta}})| \,\le\, \widehat{C}_2 \left\{ \sum_{K\in\mathcal{T}_h^b} h_K^4 \, \|\mathbf{t}_h - \nabla \mathbf{u}_h\|_{0,4;K}^4 \,+\, \sum_{e\in\mathcal{E}_h(\Gamma)} h_e \, \|\mathbf{u}_D - \mathbf{u}_h\|_{0,4;e}^4 \right\}^{1/4} \|\boldsymbol{\tau}\|_{\mathbf{div}_{4/3};\Omega} \,. \tag{3.40}$$

Next, we estimate $\mathcal{R}(\underline{\mathbf{curl}}(\widehat{\boldsymbol{\xi}}))$ (cf. (3.38)). In fact, regarding its second term, a suitable boundary integration by parts formula (cf. [31, eq. (3.35), Lemma 3.5]) yields

$$\langle \underline{\mathbf{curl}}(\widehat{\boldsymbol{\xi}})\boldsymbol{\nu}, \mathbf{u}_D\rangle_\Gamma \,=\, -\langle \nabla \mathbf{u}_D\,\mathbf{s}, \widehat{\boldsymbol{\xi}}\rangle_\Gamma \,. \tag{3.41}$$

In turn, locally integrating by parts the first term of $\mathcal{R}(\underline{\mathbf{curl}}(\widehat{\boldsymbol{\xi}}))$, we get

$$(\mathbf{t}_h, \underline{\mathbf{curl}}(\widehat{\boldsymbol{\xi}}))_\Omega \,=\, \sum_{K\in\mathcal{T}_h^b} \int_K \mathbf{rot}\,(\mathbf{t}_h)\cdot\widehat{\boldsymbol{\xi}} \,-\, \sum_{e\in\mathcal{E}_h(\Omega)} \int_e [\![\mathbf{t}_h\mathbf{s}]\!]\cdot\widehat{\boldsymbol{\xi}} \,-\, \sum_{e\in\mathcal{E}_h(\Gamma)} \int_e \mathbf{t}_h\mathbf{s}\cdot\widehat{\boldsymbol{\xi}} \,,$$

which, together with (3.41), imply

$$\mathcal{R}(\underline{\mathbf{curl}}(\widehat{\boldsymbol{\xi}})) \,=\, \sum_{K\in\mathcal{T}_h^b} \int_K \mathbf{rot}\,(\mathbf{t}_h)\cdot\widehat{\boldsymbol{\xi}} \,-\, \sum_{e\in\mathcal{E}_h(\Omega)} \int_e [\![\mathbf{t}_h\mathbf{s}]\!]\cdot\widehat{\boldsymbol{\xi}} \,-\, \sum_{e\in\mathcal{E}_h(\Gamma)} \int_e (\mathbf{t}_h\mathbf{s} - \nabla\mathbf{u}_D\,\mathbf{s})\cdot\widehat{\boldsymbol{\xi}} \,. \tag{3.42}$$

In this way, applying the Cauchy-Schwarz inequality, the approximation properties provided by Lemma 3.3, and again the first stability estimate of (3.33), we deduce from (3.42) that

$$\begin{aligned} |\mathcal{R}(\underline{\mathbf{curl}}(\widehat{\boldsymbol{\xi}}))| \,\le\, \widehat{C}_3 \Bigg\{ & \sum_{K\in\mathcal{T}_h^b} h_K^2 \|\mathbf{rot}\,(\mathbf{t}_h)\|_{0,K}^2 + \sum_{e\in\mathcal{E}_h(\Omega)} h_e \|[\![\mathbf{t}_h\mathbf{s}]\!]\|_{0,e}^2 \\ & + \sum_{e\in\mathcal{E}_h(\Gamma)} h_e \|\mathbf{t}_h\mathbf{s} - \nabla\mathbf{u}_D\,\mathbf{s}\|_{0,e}^2 \Bigg\}^{1/2} \|\boldsymbol{\tau}\|_{\mathbf{div}_{4/3};\Omega} \,. \end{aligned} \tag{3.43}$$

Finally, it is easy to see that (3.31), (3.35), (3.40), and (3.43) give (3.39), which ends the proof. $\square$

The derivation of the residual upper bound for $\|\widetilde{\mathcal{R}}\|$ proceeds analogously to the proof of the previous lemma. We omit further details and state the corresponding result as follows.

Lemma 3.9 *There exists a positive constant C, independent of h, such that*

$$\|\widetilde{\mathcal{R}}\| \,\le\, C \left\{ \bar{\mathbf{\Psi}} + \widehat{\mathbf{\Psi}} \right\},$$

where

$$\bar{\mathbf{\Psi}}^2 \,:=\, \sum_{K\in\mathcal{T}_h^b} \bar{\Psi}_K^2 \quad \textit{and} \quad \widehat{\mathbf{\Psi}}^4 \,:=\, \sum_{K\in\mathcal{T}_h^b} \widehat{\Psi}_K^4 \,,$$

with

$$\bar{\Psi}_K^2 \,:=\, h_K^2 \|\mathrm{rot}\,(\widetilde{\mathbf{t}}_h)\|_{0,K}^2 + \sum_{e\in\mathcal{E}_h(K)\cap\mathcal{E}_h(\Gamma)} h_e \, \|[\![\widetilde{\mathbf{t}}_h\cdot\mathbf{s}]\!]\|_{0,e}^2 + \sum_{e\in\mathcal{E}_h(K)\cap\mathcal{E}_h(\Gamma)} h_e \, \|\widetilde{\mathbf{t}}_h\cdot\mathbf{s} - \nabla\varphi_D\cdot\mathbf{s}\|_{0,e}^2 \,,$$

and

$$\widehat{\Psi}_K^4 \,:=\, h_K^4 \, \|\widetilde{\mathbf{t}}_h - \nabla\varphi_h\|_{0,4;K}^4 + \sum_{e\in\mathcal{E}_h(K)\cap\mathcal{E}_h(\Gamma)} h_e \, \|\varphi_D - \varphi_h\|_{0,4;e}^4 \,.$$

We end this section by stressing that the reliability of the estimator Θ (cf. (3.10)), that is the proof of Theorem 3.4, is a direct consequence of Lemmas 3.7, 3.8, and 3.9.

3.3 Preliminaries for efficiency

For the efficiency analysis of Θ (cf. (3.10)) we proceed as in [7], [10], [11], [15], [20], [27] and [40], and apply the localization technique based on bubble functions, along with inverse and discrete trace inequalities. For the former, given $K \in \mathcal{T}_h^b$, we let ψ_K be the usual element-bubble function (cf. [46, eqs. (1.5) and (1.6)]), which satisfies

$$\psi_K \in \mathrm{P}_3(K),\ \mathrm{supp}(\psi_K) \subseteq K,\ \psi_K = 0 \quad \text{on} \quad \partial T \quad \text{and} \quad 0 \le \psi_K \le 1 \quad \text{in} \quad K\,.$$

The specific properties of ψ_K to be employed in what follows, are collected in the following lemma, for whose proof we refer to [46, Lemma 3.3 and Remark 3.2].

Lemma 3.10 *Let k be a non-negative integer, and let* $\mathrm{p}, \mathrm{q} \in (1,+\infty)$ *conjugate to each other, that is such that* $1/\mathrm{p} + 1/\mathrm{q} = 1$, *and* $K \in \mathcal{T}_h^b$. *Then, there exist positive constants c_1, c_2, and c_3, independent of h and K, but depending on the shape-regularity of the triangulations (minimum angle condition) and k, such that for each $u \in \mathrm{P}_k(K)$ there hold*

$$c_1\, \|u\|_{0,\mathrm{p};K} \,\le\, \sup_{\substack{v\in \mathrm{P}_k(K)\\ v\neq 0}} \frac{\displaystyle\int_K u\,\psi_K v}{\|v\|_{0,\mathrm{q};K}} \,\le\, \|u\|_{0,\mathrm{p};K}\,, \tag{3.44}$$

and

$$c_2\, h_K^{-1}\, \|\psi_K u\|_{0,\mathrm{q};K} \,\le\, \|\nabla(\psi_K u)\|_{0,\mathrm{q};K} \,\le\, c_3\, h_K^{-1}\, \|\psi_K u\|_{0,\mathrm{q};K}\,. \tag{3.45}$$

In turn, the aforementioned inverse inequality is stated as follows (cf. [33, Lemma 1.138]).

Lemma 3.11 *Let k, ℓ, and m be non-negative integers such that $m \le \ell$, and let r, $s \in [1,+\infty]$, and $K \in \mathcal{T}_h^b$. Then, there exists $c > 0$, independent of h, K, r, and s, but depending on k, ℓ, m, and the shape regularity of the triangulations, such that*

$$\|v\|_{l,r;K} \,\le\, c\, h_K^{m-\ell+n(1/r-1/s)}\, \|v\|_{m,s;K} \qquad \forall\, v \in \mathrm{P}_k(K)\,. \tag{3.46}$$

Finally, proceeding as in [1, Theorem 3.10], that is employing the usual scaling estimates with respect to a fixed reference element $\widehat{K}$, and applying the trace inequality in $\mathrm{W}^{1,p}(\widehat{K})$, for a given $p \in (1,+\infty)$, one is able to establish the following discrete trace inequality.

Lemma 3.12 *Let $p \in (1,+\infty)$. Then, there exits $c > 0$, depending only on the shape regularity of the triangulations, such that for each $K \in \mathcal{T}_h^b$ and $e \in \mathcal{E}(K)$, there holds*

$$\|v\|_{0,p;e}^p \,\le\, c\,\Big\{ h_K^{-1}\, \|v\|_{0,p;K}^p \,+\, h_K^{p-1}\, |v|_{1,p;K}^p \Big\} \qquad \forall\, v \in \mathrm{W}^{1,p}(K)\,. \tag{3.47}$$

3.4 Efficiency

In this section we prove the efficiency of Θ (cf. (3.10)), which is stated as follows.

Theorem 3.13 *Assume, for simplicity, that $\mathbf{u}_D$ and φ_D are piecewise polynomials. Then, there exists a positive constant $C_{\mathtt{eff}}$, independent of h, such that*

$$C_{\mathtt{eff}}\, \Theta + \text{h.o.t.} \,\le\, \|\vec{\boldsymbol{\sigma}} - \vec{\boldsymbol{\sigma}}_h\|_{\mathbb{X}}\,, \tag{3.48}$$

where h.o.t. *stands for one or several terms of higher order.*

The proof of (3.48) is carried out throughout the rest of this section. We begin with the following result.

Lemma 3.14 *There exist positive constants c, $\widetilde{c}$, C, and $\widetilde{C}$, independent of h, such that*

$$\begin{aligned}&\big\| -\mathbf{div}(\boldsymbol{\sigma}_h) + \frac{1}{2}\mathbf{t}_h\,\mathbf{u}_h - \varphi_h\,\boldsymbol{g}\big\|_{0,4/3;\Omega}\\ &\quad\leq\, c\Big\{\|\boldsymbol{\sigma}-\boldsymbol{\sigma}_h\|_{\mathbf{div}_{4/3};\Omega} + \|\mathbf{u}-\mathbf{u}_h\|_{0,4;\Omega} + \|\mathbf{t}-\mathbf{t}_h\|_{0,\Omega} \,+\, \|\varphi-\varphi_h\|_{0,4;\Omega}\Big\}\,,\end{aligned}\tag{3.49}$$

$$\begin{aligned}&\big\|2\mu(\varphi_h)\mathbf{t}_{h,sym} - \frac{1}{2}(\mathbf{u}_h\otimes\mathbf{u}_h)^{\mathtt{d}} - \boldsymbol{\sigma}_h^{\mathtt{d}}\big\|_{0,\Omega}\\ &\quad\leq\, C\Big\{\|\boldsymbol{\sigma}-\boldsymbol{\sigma}_h\|_{\mathbf{div}_{4/3};\Omega} + \|\mathbf{t}-\mathbf{t}_h\|_{0,\Omega} + \|\mathbf{u}-\mathbf{u}_h\|_{0,4,\Omega} \,+\, \|\varphi-\varphi_h\|_{0,4;\Omega}\Big\}\,,\end{aligned}\tag{3.50}$$

$$\big\| -\mathrm{div}(\widetilde{\boldsymbol{\sigma}}_h) + \frac{1}{2}\mathbf{u}_h\cdot\widetilde{\mathbf{t}}_h\big\|_{0,4/3;\Omega} \,\leq\, \widetilde{c}\Big\{\|\widetilde{\boldsymbol{\sigma}}-\widetilde{\boldsymbol{\sigma}}_h\|_{\mathrm{div}_{4/3};\Omega} + \|\widetilde{\mathbf{t}}-\widetilde{\mathbf{t}}_h\|_{0,\Omega} + \|\mathbf{u}-\mathbf{u}_h\|_{0,4;\Omega}\Big\}\,,\tag{3.51}$$

and

$$\big\|\mathbb{K}\widetilde{\mathbf{t}}_h - \frac{1}{2}\varphi_h\mathbf{u}_h - \widetilde{\boldsymbol{\sigma}}_h\big\|_{0,\Omega} \,\leq\, \widetilde{C}\Big\{\|\widetilde{\boldsymbol{\sigma}}-\widetilde{\boldsymbol{\sigma}}_h\|_{\mathrm{div}_{4/3};\Omega} + \|\widetilde{\mathbf{t}}-\widetilde{\mathbf{t}}_h\|_{0,\Omega} + \|\mathbf{u}-\mathbf{u}_h\|_{0,4;\Omega} + \|\varphi-\varphi_h\|_{0,4;\Omega}\Big\}.\tag{3.52}$$

Proof. Let us begin with the proof of (3.49). According to the third row of (2.3), and applying the triangle inequality and the continuous injection of $\mathrm{L}^4(\Omega)$ into $\mathrm{L}^{4/3}(\Omega)$, we readily find that

$$\begin{aligned}\big\| -\mathbf{div}(\boldsymbol{\sigma}_h) + \frac{1}{2}\mathbf{t}_h\mathbf{u}_h - \varphi_h\boldsymbol{g}\big\|_{0,4/3;\Omega} &= \Big\|\mathbf{div}(\boldsymbol{\sigma}-\boldsymbol{\sigma}_h) - \frac{1}{2}(\mathbf{t}\mathbf{u}-\mathbf{t}_h\mathbf{u}_h) + (\varphi-\varphi_h)\boldsymbol{g}\Big\|_{0,4/3;\Omega}\\ &\leq\, \|\boldsymbol{\sigma}-\boldsymbol{\sigma}_h\|_{\mathbf{div}_{4/3};\Omega} + \frac{1}{2}\|\mathbf{t}\mathbf{u}-\mathbf{t}_h\mathbf{u}_h\|_{0,4/3;\Omega} + \|\boldsymbol{g}\|_{0,\infty;\Omega}\,\|\varphi-\varphi_h\|_{0,4;\Omega}\,.\end{aligned}\tag{3.53}$$

Then, subtracting and adding $\mathbf{t}\mathbf{u}_h$, and employing the triangle and Hölder inequalities, the latter with conjugate exponents given by $3/2$ and 3, we obtain

$$\begin{aligned}\|\mathbf{t}\mathbf{u}-\mathbf{t}_h\mathbf{u}_h\|_{0,4/3;\Omega} &\leq\, \|\mathbf{t}(\mathbf{u}-\mathbf{u}_h)\|_{0,4/3;\Omega} \,+\, \|(\mathbf{t}-\mathbf{t}_h)\mathbf{u}_h\|_{0,4/3;\Omega}\\ &\leq\, \|\mathbf{t}\|_{0,\Omega}\,\|\mathbf{u}-\mathbf{u}_h\|_{0,4;\Omega} \,+\, \|\mathbf{t}-\mathbf{t}_h\|_{0,\Omega}\,\|\mathbf{u}_h\|_{0,4;\Omega}\,.\end{aligned}\tag{3.54}$$

Next, using the bounds for $\|\mathbf{t}\|_{0,\Omega}$ and $\|\mathbf{u}_h\|_{0,4;\Omega}$ provided by [24, Theorem 3.11, eq. (3.79)] and (3.29) (cf. [24, Theorem 4.11, eq. (4.24)]), respectively, we deduce from (3.54) the existence of a positive constant C, depending only on data, but independent of h, such that

$$\|\mathbf{t}\mathbf{u}-\mathbf{t}_h\mathbf{u}_h\|_{0,4/3;\Omega} \,\leq\, C\Big\{\|\mathbf{u}-\mathbf{u}_h\|_{0,4;\Omega} \,+\, \|\mathbf{t}-\mathbf{t}_h\|_{0,\Omega}\Big\}\,,$$

which, replaced back into (3.53), yields (3.49). In turn, for the proof of (3.50), we first make use of the fourth row of (2.3) and the triangle inequality to obtain

$$\begin{aligned}&\big\|2\mu(\varphi_h)\mathbf{t}_{h,sym} - \frac{1}{2}(\mathbf{u}_h\otimes\mathbf{u}_h)^{\mathtt{d}} - \boldsymbol{\sigma}_h^{\mathtt{d}}\big\|_{0,\Omega}\\ &\quad= \big\|2\big\{\mu(\varphi_h)\mathbf{t}_{h,sym} - \mu(\varphi)\mathbf{t}_{sym}\big\} + \frac{1}{2}\big\{(\mathbf{u}\otimes\mathbf{u})^{\mathtt{d}} - (\mathbf{u}_h\otimes\mathbf{u}_h)^{\mathtt{d}}\big\} + \boldsymbol{\sigma}^{\mathtt{d}} - \boldsymbol{\sigma}_h^{\mathtt{d}}\big\|_{0,\Omega}\\ &\quad\leq\, 2\Big\{\|\mu(\varphi_h)\mathbf{t}_{h,sym} - \mu(\varphi)\mathbf{t}_{sym}\|_{0,\Omega} + \|(\mathbf{u}\otimes\mathbf{u}) - (\mathbf{u}_h\otimes\mathbf{u}_h)\|_{0,\Omega} + \|\boldsymbol{\sigma}-\boldsymbol{\sigma}_h\|_{0,\Omega}\Big\}\,.\end{aligned}\tag{3.55}$$

Then, subtracting and adding $\mu(\varphi_h)\mathbf{t}_{sym}$, using the upper bound of μ (cf. (2.2)), proceeding as for the derivation of (3.26) (see also [24, eq. (3.68)]), and employing the regularity estimate for $\|\mathbf{t}\|_{\epsilon,\Omega}$ provided by (3.18), we find that

$$\begin{aligned}\|\mu(\varphi_h)\mathbf{t}_{h,sym} - \mu(\varphi)\mathbf{t}_{sym}\|_{0,\Omega} &\le \|\mu(\varphi_h)\big(\mathbf{t}_{sym} - \mathbf{t}_{h,sym}\big)\|_{0,\Omega} + \|\big(\mu(\varphi) - \mu(\varphi_h)\big)\,\mathbf{t}_{sym}\|_{0,\Omega} \\ &\le C\Big\{\|\mathbf{t} - \mathbf{t}_h\|_{0,\Omega} + \|\varphi - \varphi_h\|_{0,4;\Omega}\Big\},\end{aligned} \tag{3.56}$$

where C is a positive constant depending only on data and independent of h. Similarly, subtracting and adding $\mathbf{u}_h$ in one factor of $\mathbf{u}\otimes\mathbf{u}$, and then applying Hölder's inequality, we get

$$\|(\mathbf{u}\otimes\mathbf{u}) - (\mathbf{u}_h\otimes\mathbf{u}_h)\|_{0,\Omega} \le \|\mathbf{u}\|_{0,4;\Omega}\,\|\mathbf{u}-\mathbf{u}_h\|_{0,4;\Omega} + \|\mathbf{u}_h\|_{0,4;\Omega}\,\|\mathbf{u}-\mathbf{u}_h\|_{0,4;\Omega}, \tag{3.57}$$

from which, making use of the bounds for $\|\mathbf{u}\|_{0,4;\Omega}$ and $\|\mathbf{u}_h|_{0,4;\Omega}$ given by [24, Theorem 3.11, eq. (3.79)] and (3.29) (see also [24, Theorem 4.11, eq. (4.24)], respectively, it follows that

$$\|(\mathbf{u}\otimes\mathbf{u}) - (\mathbf{u}_h\otimes\mathbf{u}_h)\|_{0,\Omega} \le C\,\|\mathbf{u}-\mathbf{u}_h\|_{0,4;\Omega}, \tag{3.58}$$

with another positive constant C depending only on data and independent of h as well. In this way, replacing the bounds from (3.56) and (3.58) in (3.55), we are lead to (3.50). The proofs of (3.51) and (3.52), being similar to those of (3.49) and (3.50), are omitted. □

The local efficiency estimates to be stated by the next two lemmas have already been proved in the literature by using localization through bubble functions, and hence we simply refer to their respective proofs.

Lemma 3.15 *There exist positive constants c, $\widetilde{c}$, C, and $\widetilde{C}$, such that*

$$h_K^2\,\|\mathbf{rot}\,(\mathbf{t}_h)\|_{0,K}^2 \le c\,\|\mathbf{t}-\mathbf{t}_h\|_{0,K}^2 \quad \text{and} \quad h_K^2\,\|\mathrm{rot}\,(\widetilde{\mathbf{t}}_h)\|_{0,K}^2 \le \widetilde{c}\,\|\widetilde{\mathbf{t}}-\widetilde{\mathbf{t}}_h\|_{0,K}^2 \quad \forall\, K\in\mathcal{T}_h^b,$$

$$h_e\,\|[\![\mathbf{t}_h\mathbf{s}]\!]\|_{0,e}^2 \le C\,\|\mathbf{t}-\mathbf{t}_h\|_{0,\omega_e}^2 \quad \text{and} \quad h_e\,\|[\![\widetilde{\mathbf{t}}_h\cdot\mathbf{s}]\!]\|_{0,e}^2 \le \widetilde{C}\,\|\widetilde{\mathbf{t}}-\widetilde{\mathbf{t}}_h\|_{0,\omega_e}^2 \quad \forall\, e\in\mathcal{E}_h(\Omega),$$

where ω_e is the union of the two elements of $\mathcal{T}_h^b$ sharing the edge e.

Proof. See [12, Lemmas 4.3 and 4.4]. □

Lemma 3.16 *Assume that $\mathbf{u}_D$ and φ_D are piecewise polynomials. Then, there exist positive constants c and $\widetilde{c}$, such that for each $e\in\mathcal{E}_h(\Gamma)$ there hold*

$$h_e\,\|\mathbf{t}_h\mathbf{s} - \nabla\mathbf{u}_D\,\mathbf{s}\|_{0,e}^2 \le c\,\|\mathbf{t}-\mathbf{t}_h\|_{0,K_e}^2 \quad \text{and} \quad h_e\,\|\widetilde{\mathbf{t}}_h\cdot\mathbf{s} - \nabla\varphi_D\cdot\mathbf{s}\|_{0,e}^2 \le \widetilde{c}\,\|\widetilde{\mathbf{t}}-\widetilde{\mathbf{t}}_h\|_{0,K_e}^2,$$

where K_e is the triangle of $\mathcal{T}_h^b$ having e as an edge.

Proof. See [38, Lemma 4.15]. □

The inequalities supplied by Lemma 3.10 are invoked in the proof of the following lemma.

Lemma 3.17 *There exist positive constants c and $\widetilde{c}$, independent of h, such that*

$$h_K^4\,\|\mathbf{t}_h - \nabla\mathbf{u}_h\|_{0,4;K}^4 \le c\Big\{\|\mathbf{u}-\mathbf{u}_h\|_{0,4;K}^4 + h_K^2\|\mathbf{t}-\mathbf{t}_h\|_{0,K}^4\Big\} \qquad \forall\, K\in\mathcal{T}_h^b,$$

and

$$h_K^4\,\|\widetilde{\mathbf{t}}_h - \nabla\varphi_h\|_{0,4;K}^4 \le \widetilde{c}\Big\{\|\varphi-\varphi_h\|_{0,4;K}^4 + h_K^2\|\widetilde{\mathbf{t}}-\widetilde{\mathbf{t}}_h\|_{0,K}^4\Big\} \qquad \forall\, K\in\mathcal{T}_h^b.$$

Proof. For the first inequality we proceed as in the proof of [20, Lemma 5.15]. In fact, given $K \in \mathcal{T}_h^b$, we begin by applying the vector version of the left hand side inequality of (3.44), with $p = 4$ and $q = 4/3$, to the local polynomial $\boldsymbol{\chi}_K := \mathbf{t}_h - \nabla \mathbf{u}_h \in \mathbf{P}_k(K)$, which gives

$$c_1 \, \|\boldsymbol{\chi}_K\|_{0,4;K} \,\le\, \sup_{\substack{\mathbf{v}\in\mathbf{P}_k(K)\\ \mathbf{v}\neq\mathbf{0}}} \frac{\displaystyle\int_K \boldsymbol{\chi}_K \cdot \psi_K \mathbf{v}}{\|\mathbf{v}\|_{0,4/3;K}} \,. \tag{3.59}$$

Then, using that $\mathbf{t} = \nabla \mathbf{u}$ in Ω, and integrating by parts, we find that

$$\int_K \boldsymbol{\chi}_K \cdot \psi_K \mathbf{v} = \int_K \Big\{ \nabla(\mathbf{u} - \mathbf{u}_h) - (\mathbf{t} - \mathbf{t}_h) \Big\} \cdot \psi_K \mathbf{v} = - \int_K (\mathbf{u} - \mathbf{u}_h)\,\mathrm{div}(\psi_K \mathbf{v}) - \int_K (\mathbf{t} - \mathbf{t}_h) \cdot \psi_K \mathbf{v} \,,$$

from which, employing the Hölder and Cauchy-Schwarz inequalities, noting that $\|\mathrm{div}(\psi_K \mathbf{v})\|_{0,4/3;\Omega} \le \|\nabla(\psi_K \mathbf{v})\|_{0,4/3;\Omega}$, and then applying the right hand side inequality of (3.45), along with the fact that $0 \le \psi_K \le 1$, we obtain

$$\int_K \boldsymbol{\chi}_K \cdot \psi_K \mathbf{v} \,\le\, C \Big\{ h_K^{-1} \, \|\mathbf{u} - \mathbf{u}_h\|_{0,4;K} \, \|\mathbf{v}\|_{0,4/3;K} + \|\mathbf{t} - \mathbf{t}_h\|_{0,K} \, \|\mathbf{v}\|_{0,K} \Big\} \,. \tag{3.60}$$

In turn, according to the local inverse inequality (3.46) with $n = 2$, $\ell = m = 0$, $r = 2$, and $s = 4/3$, there holds $\|\mathbf{v}\|_{0,K} \le c\, h_K^{-1/2} \, \|\mathbf{v}\|_{0,4/3;K}$, and thus (3.60) becomes

$$\int_K \boldsymbol{\chi}_K \cdot \psi_K \mathbf{v} \,\le\, C \Big\{ h_K^{-1} \, \|\mathbf{u} - \mathbf{u}_h\|_{0,4;K} + h_K^{-1/2} \, \|\mathbf{t} - \mathbf{t}_h\|_{0,K} \Big\} \, \|\mathbf{v}\|_{0,4/3;K} \,. \tag{3.61}$$

In this way, replacing (3.61) back into (3.59), and multiplying the resulting inequality by h_K, we get

$$h_K \, \|\mathbf{t}_h - \nabla \mathbf{u}_h\|_{0,4;K} \,\le\, \|\mathbf{u} - \mathbf{u}_h\|_{0,4;K} + h_K^{1/2} \, \|\mathbf{t} - \mathbf{t}_h\|_{0,K} \,,$$

so that taking the foregoing inequality to the power 4 the required efficiency estimate is obtained. The derivation of the second inequality follows an analogue reasoning, and hence we omit further details. □

The remaining local efficiency estimates are established as follows.

Lemma 3.18 *Assume that $\mathbf{u}_D$ and φ_D are piecewise polynomials. Then, there exist positive constants C and $\widetilde{C}$, independent of h, such that*

$$h_e \, \|\mathbf{u}_D - \mathbf{u}_h\|_{0,4;e}^4 \,\le\, C \Big\{ \|\mathbf{u} - \mathbf{u}_h\|_{0,4;K_e}^4 + h_{K_e}^2 \, \|\mathbf{t} - \mathbf{t}_h\|_{0,K_e}^4 \Big\} \qquad \forall\, e \in \mathcal{E}_h(\Gamma) \,,$$

and

$$h_e \, \|\varphi_D - \varphi_h\|_{0,4;e}^4 \,\le\, \widetilde{C} \Big\{ \|\varphi - \varphi_h\|_{0,4;K_e}^4 + h_{K_e}^2 \, \|\widetilde{\mathbf{t}} - \widetilde{\mathbf{t}}_h\|_{0,K_e}^4 \Big\} \qquad \forall\, e \in \mathcal{E}_h(\Gamma) \,,$$

where K_e is the triangle of $\mathcal{T}_h^b$ having e as an edge.

Proof. Being both inequalities proved in an analogous way, we only show the first one. In fact, given $e \in \mathcal{E}_h(\Gamma)$, we first observe that the local inverse inequality (3.46) with $n = 1$, $\ell = m = 0$, $r = 4$, and $s = 2$ yields $\|\mathbf{u}_D - \mathbf{u}_h\|_{0,4;e} \le c\, h_e^{-1/4} \, \|\mathbf{u}_D - \mathbf{u}_h\|_{0,e}$. Hence, taking the above to the power 4, using that $\mathbf{u} = \mathbf{u}_D$ on Γ, applying the vector version of the discrete trace inequality (3.47) (cf. Lemma 3.12) with $p = 2$, recalling that $\mathbf{t} = \nabla \mathbf{u}$, and employing the triangle inequality, we find that

$$\begin{aligned} h_e \|\mathbf{u}_D - \mathbf{u}_h\|_{0,4;e}^4 &\le C \|\mathbf{u} - \mathbf{u}_h\|_{0,e}^4 \le C \left\{ h_{K_e}^{-1} \|\mathbf{u} - \mathbf{u}_h\|_{0,K_e}^2 + h_{K_e} \|\mathbf{t} - \nabla \mathbf{u}_h\|_{0,K_e}^2 \right\}^2 \\ &\le C \left\{ h_{K_e}^{-1} \|\mathbf{u} - \mathbf{u}_h\|_{0,K_e}^2 + h_{K_e} \|\mathbf{t} - \mathbf{t}_h\|_{0,K_e}^2 + h_{K_e} \|\mathbf{t}_h - \nabla \mathbf{u}_h\|_{0,K_e}^2 \right\}^2 . \end{aligned} \tag{3.62}$$

Next, using, thanks to the Cauchy-Schwarz inequality, that

$$\|\mathbf{w}\|_{0,K_e}^2 \le |K_e|^{1/2} \|\mathbf{w}\|_{0,4;K_e}^2 \le c\, h_{K_e} \|\mathbf{w}\|_{0,4;K_e}^2 \qquad \forall\, \mathbf{w} \in \mathbf{L}^4(K_e) ,$$

it follows from (3.62) that

$$\begin{aligned} h_e \|\mathbf{u}_D - \mathbf{u}_h\|_{0,4;e}^4 &\le C \left\{ \|\mathbf{u} - \mathbf{u}_h\|_{0,4;K_e}^2 + h_{K_e} \|\mathbf{t} - \mathbf{t}_h\|_{0,K_e}^2 + h_{K_e}^2 \|\mathbf{t}_h - \nabla \mathbf{u}_h\|_{0,4;K_e}^2 \right\}^2 \\ &\le c \left\{ \|\mathbf{u} - \mathbf{u}_h\|_{0,4;K_e}^4 + h_{K_e}^2 \|\mathbf{t} - \mathbf{t}_h\|_{0,K_e}^4 + h_{K_e}^4 \|\mathbf{t}_h - \nabla \mathbf{u}_h\|_{0,4;K_e}^4 \right\} . \end{aligned}$$

Finally, owing to the first estimate from Lemma 3.17 we can bound the last term in the foregoing inequality, and this step concludes the proof. □

At this point we stress that if $\mathbf{u}_D$ and φ_D were not piecewise polynomials but sufficiently smooth, then higher order terms given by the errors arising from suitable polynomial approximations of these functions would appear in the efficiency estimates provided by Lemmas 3.16 and 3.18. This fact explains the eventual expression h.o.t. in the global efficiency estimate (3.48).

We end this section by remarking that the proof of (3.48) follows straightforwardly from Lemmas 3.14–3.18, and after summing up the local efficiency estimates over all $K \in \mathcal{T}_h^b$. Further details are omitted.

4 A posteriori error analysis: the 3D case

In this section we extend the results from Section 3 to the three-dimensional version of (2.12). Similarly as in the previous section, given a tetrahedron $K \in \mathcal{T}_h^b$, we let $\mathcal{E}(K)$ be the set of its faces, and let $\mathcal{E}_h$ be the set of all faces of the triangulation $\mathcal{T}_h^b$. Then, we write $\mathcal{E}_h = \mathcal{E}_h(\Omega) \cup \mathcal{E}_h(\Gamma)$ with $\mathcal{E}_h(\Omega)$ and $\mathcal{E}_h(\Gamma)$ defined as in Section 3.1. Also, for each face $e \in \mathcal{E}_h$ we fix a unit normal $\boldsymbol{\nu}_e$ to e. Now, let $\mathbf{v} \in \mathbf{L}^2(\Omega)$ such that $\mathbf{v}|_K \in \mathbf{C}(K)$ on each $K \in \mathcal{T}_h^b$. Then, given $e \in \mathcal{E}(K) \cap \mathcal{E}_h(\Omega)$, we denote by $[\![\mathbf{v} \times \boldsymbol{\nu}_e]\!]$ the tangential jump of $\mathbf{v}$ across e, that is, $[\![\mathbf{v} \times \boldsymbol{\nu}_e]\!] := (\mathbf{v}|_K - \mathbf{v}|_{K'})|_e \times \boldsymbol{\nu}_e$, where K and K' are the tetrahedron of $\mathcal{T}_h^b$ having e as a common face. In addition, for $\boldsymbol{\tau} \in \mathbb{L}^2(\Omega)$ such that $\boldsymbol{\tau}|_K \in \mathbb{C}(K)$, we let $[\![\boldsymbol{\tau} \times \boldsymbol{\nu}_e]\!]$ be the tangential jump of $\boldsymbol{\tau}$ across e, that is, $[\![\boldsymbol{\tau} \times \boldsymbol{\nu}_e]\!] := (\boldsymbol{\tau}|_K - \boldsymbol{\tau}|_{K'})|_e \times \boldsymbol{\nu}_e$. In what follows, when no confusion arises, we simply write $\boldsymbol{\nu}$ instead of $\boldsymbol{\nu}_e$. On the other hand, we recall that the curl of a 3D vector $\mathbf{v} := (v_1, v_2, v_3)$ is the 3D vector

$$\mathbf{curl}\,(\mathbf{v}) = \nabla \times \mathbf{v} := \left(\frac{\partial v_3}{\partial x_2} - \frac{\partial v_2}{\partial x_3}, \frac{\partial v_1}{\partial x_3} - \frac{\partial v_3}{\partial x_1}, \frac{\partial v_2}{\partial x_1} - \frac{\partial v_1}{\partial x_2} \right) ,$$

and that, given a tensor function $\boldsymbol{\tau} := (\tau_{ij})_{3\times 3}$, the operator $\underline{\mathbf{curl}}\,(\boldsymbol{\tau})$ is the 3×3 tensor whose rows are given by

$$\underline{\mathbf{curl}}\,(\tau) := \begin{pmatrix} \mathbf{curl}\,(\tau_{11}, \tau_{12}, \tau_{13}) \\ \mathbf{curl}\,(\tau_{21}, \tau_{22}, \tau_{23}) \\ \mathbf{curl}\,(\tau_{31}, \tau_{32}, \tau_{33}) \end{pmatrix} .$$

In addition, $\boldsymbol{\tau} \times \boldsymbol{\nu}$ stands for the 3×3 tensor whose rows are given by the tangential components of each row of $\boldsymbol{\tau}$, that is,

$$\boldsymbol{\tau} \times \boldsymbol{\nu}_e := \begin{pmatrix} (\tau_{11}, \tau_{12}, \tau_{13}) \times \boldsymbol{\nu}_e \\ (\tau_{21}, \tau_{22}, \tau_{23}) \times \boldsymbol{\nu}_e \\ (\tau_{31}, \tau_{32}, \tau_{33}) \times \boldsymbol{\nu}_e \end{pmatrix}.$$

In turn, the tangential curl operator $\mathbf{curl}_{\mathbf{s}}$ and a tensor version of it, denoted $\underline{\mathbf{curl}}_{\mathbf{s}}$, which is defined component-wise by $\mathbf{curl}_{\mathbf{s}}$, will also be used (see [18, Section 3] for details).

Thus, we define for each $K \in \mathcal{T}_h^b$

$$\begin{aligned} \bar{\Theta}_K^2 &:= \left\|2\mu(\varphi_h)\mathbf{t}_{h,sym} - \frac{1}{2}(\mathbf{u}_h \otimes \mathbf{u}_h)^{\mathtt{d}} - \boldsymbol{\sigma}_h^{\mathtt{d}}\right\|_{0,K}^2 + \left\|\mathbb{K}\widetilde{\mathbf{t}}_h - \frac{1}{2}\varphi_h \mathbf{u}_h - \widetilde{\boldsymbol{\sigma}}_h\right\|_{0,K}^2 \\ &+ h_K^2 \, \|\underline{\mathbf{curl}}(\mathbf{t}_h)\|_{0,K}^2 + h_K^2 \|\mathbf{curl}\,(\widetilde{\mathbf{t}}_h)\|_{0,K}^2 + \sum_{e \in \mathcal{E}_h(\Omega)} h_e \Big\{ \big\|[\![\mathbf{t}_h \times \boldsymbol{\nu}]\!]\big\|_{0,e}^2 + \big\|[\![\widetilde{\mathbf{t}}_h \times \boldsymbol{\nu}]\!]\big\|_{0,e}^2 \Big\} \\ &+ \sum_{e \in \mathcal{E}_h(K) \cap \mathcal{E}_h(\Gamma)} h_e \Big\{ \|\mathbf{t}_h \times \boldsymbol{\nu} - \underline{\mathbf{curl}}_{\mathbf{s}}(\mathbf{u}_D)\|_{0,e}^2 + \|\widetilde{\mathbf{t}}_h \times \boldsymbol{\nu} - \mathbf{curl}_{\mathbf{s}}(\varphi_D)\|_{0,e}^2 \Big\}. \end{aligned} \tag{4.1}$$

Hence, bearing in mind the definitions of $\widetilde{\Theta}_K^{4/3}$ (cf. (3.8)) and $\widehat{\Theta}_K^4$ (cf. (3.9)), which are also valid in the present 3D case, the associated global a posteriori error estimator is defined as

$$\Theta = \left\{ \sum_{K \in \mathcal{T}_h^b} \widetilde{\Theta}_K^{4/3} \right\}^{3/4} + \left\{ \sum_{K \in \mathcal{T}_h^b} \bar{\Theta}_K^2 \right\}^{1/2} + \left\{ \sum_{K \in \mathcal{T}_h^b} \widehat{\Theta}_K^4 \right\}^{1/4}. \tag{4.2}$$

In this way, the corresponding reliability and efficiency estimates, which constitute the analogue of Theorems 3.4 and 3.13, are stated as follows.

Theorem 4.1 *Assume that the data are sufficiently small (similarly as indicated in Lemma* 3.7*), and suppose that* $\mathbf{u}_D$ *and* φ_D *are piecewise polynomials. Then, there exist positive constants* $C_{\mathtt{rel}}$ *and* $C_{\mathtt{eff}}$*, independent of* h*, such that*

$$C_{\mathtt{eff}}\,\Theta + \text{h.o.t.} \,\le\, \|\vec{\boldsymbol{\sigma}} - \vec{\boldsymbol{\sigma}}_h\|_{\mathbb{X}} \,\le\, C_{\mathtt{rel}}\,\Theta\,.$$

The proof of Theorem 4.1 follows very closely the analysis of Section 3, except a few issues to be described throughout the following discussion. Indeed, we first observe that the general a posteriori error estimate given by Lemma 3.7 is also valid in 3D. Then, we follow [36, Theorem 3.2] to derive a 3D version for arbitrary polyhedral domains of the Helmholtz decomposition provided by Lemma 3.2. Next, the associated discrete Helmholtz decomposition and the functionals $\mathcal{R}$ and $\widetilde{\mathcal{R}}$ are set and rewritten exactly as in (3.34), (3.35), and (3.36), respectively. Furthermore, in order to derive the new upper bounds of $\|\mathcal{R}\|$ and $\|\widetilde{\mathcal{R}}\|$, we now need the 3D analogue of the integration by parts formula on the boundary given by (3.41). In fact, by applying the identities from [43, Chapter I, eq. 2.17, and Theorem 2.11], we deduce that in this case there holds

$$\langle \mathbf{curl}\,\boldsymbol{\xi}\cdot\boldsymbol{\nu}, \theta\rangle_\Gamma \,=\, -\langle \mathbf{curl}_{\mathbf{s}}\theta, \boldsymbol{\xi}\rangle_\Gamma \qquad \forall\,\boldsymbol{\xi} \in \mathbf{H}^1(\Omega)\,, \quad \forall\,\theta \in \mathrm{H}^{1/2}(\Gamma)\,.$$

In addition, the integration by parts formula on each tetrahedron $K \in \mathcal{T}_h^b$, which is used in the proof of the 3D analogue of Lemma 3.8, becomes (cf. [43, Chapter I, Theorem 2.11])

$$\int_K \mathbf{curl}\,\mathbf{q}\cdot\boldsymbol{\xi} - \int_K \mathbf{q}\cdot\mathbf{curl}\,\boldsymbol{\xi} = \langle \mathbf{q}\times\boldsymbol{\nu}, \boldsymbol{\xi}\rangle_{\partial K} \qquad \forall\,\mathbf{q} \in \mathbf{H}(\mathbf{curl}\,;\Omega), \quad \forall\,\boldsymbol{\xi} \in \mathbf{H}^1(\Omega)\,,$$

where $\langle\cdot,\cdot\rangle_{\partial K}$ is the duality pairing between $\mathbf{H}^{-1/2}(\partial K)$ and $\mathbf{H}^{1/2}(\partial K)$, and, as usual, $\mathbf{H}(\mathbf{curl}\,,\Omega)$ is the space of vectors in $\mathbf{L}^2(\Omega)$ whose $\mathbf{curl}$ lies also in $\mathbf{L}^2(\Omega)$. Note that, unlike the 2D case, it is not necessary for the reliability to assume that $\mathbf{u}_D \in \mathbf{H}^1(\Gamma)$ and $\varphi_D \in \mathrm{H}^1(\Gamma)$, since the $\mathbf{curl}_{\mathbf{s}}$ is defined into $\mathrm{H}^{1/2}(\Gamma)$.

Finally, in order to prove the efficiency of Θ (cf. (4.2)), we first observe that the terms defining $\widetilde{\Theta}_K^{4/3}$ (cf. (3.8)) and the first two defining $\bar{\Theta}_K^2$ (cf. (4.1)) are estimated exactly as done for the 2D case in Lemma 3.14. For the remaining terms, we have the following lemma.

Lemma 4.2 *Assume that $\mathbf{u}_D$ and ϕ_D are piecewise polynomials. Then, there exist positive constants C_i, $i \in \{1, ..., 10\}$, all independent of h, such that*

a) $h_K^4\|\mathbf{t}_h - \nabla\mathbf{u}_h\|_{0,4;K}^4 \le C_1\Big\{\|\mathbf{u}-\mathbf{u}_h\|_{0,4;K}^4 + h_K\|\mathbf{t}-\mathbf{t}_h\|_{0,K}^4\Big\} \qquad \forall\, K \in \mathcal{T}_h^b,$

b) $h_K^4\|\widetilde{\mathbf{t}}_h - \nabla\varphi_h\|_{0,4;K}^4 \le C_2\Big\{\|\varphi-\varphi_h\|_{0,4;K}^4 + h_K\|\widetilde{\mathbf{t}}-\widetilde{\mathbf{t}}_h\|_{0,K}^4\Big\} \qquad \forall\, K \in \mathcal{T}_h^b,$

c) $h_e\|\mathbf{u}_D - \mathbf{u}_h\|_{0,4;e}^4 \le C_3\Big\{\|\mathbf{u}-\mathbf{u}_h\|_{0,4;K_e}^4 + h_{K_e}\|\mathbf{t}-\mathbf{t}_h\|_{0,K_e}^4\Big\} \qquad \forall\, e \in \mathcal{E}_h(\Gamma),$

d) $h_e\|\varphi_D - \varphi_h\|_{0,4;e}^4 \le C_4\Big\{\|\varphi-\varphi_h\|_{0,4;K_e}^4 + h_{K_e}\|\widetilde{\mathbf{t}}-\widetilde{\mathbf{t}}_h\|_{0,K_e}^4\Big\} \qquad \forall\, e \in \mathcal{E}_h(\Gamma),$

e) $h_K^2\|\underline{\mathbf{curl}}(\mathbf{t}_h)\|_{0,K}^2 \le C_5\|\mathbf{t}-\mathbf{t}_h\|_{0,K}^2 \qquad \forall\, K \in \mathcal{T}_h^b,$

f) $h_K^2\|\mathbf{curl}\,(\widetilde{\mathbf{t}}_h)\|_{0,K}^2 \le C_6\|\widetilde{\mathbf{t}}-\widetilde{\mathbf{t}}_h\|_{0,K}^2 \qquad \forall\, K \in \mathcal{T}_h^b,$

g) $\big\|[\![\mathbf{t}_h \times \boldsymbol{\nu}]\!]\big\|_{0,e}^2 \le C_7\|\mathbf{t}-\mathbf{t}_h\|_{0,\omega_e}^2 \qquad \forall\, e \in \mathcal{E}_h(\Omega),$

h) $\big\|[\![\widetilde{\mathbf{t}}_h \times \boldsymbol{\nu}]\!]\big\|_{0,e}^2 \le C_8\|\widetilde{\mathbf{t}}-\widetilde{\mathbf{t}}_h\|_{0,\omega_e}^2 \qquad \forall\, e \in \mathcal{E}_h(\Omega),$

i) $h_e\|\mathbf{t}_h \times \boldsymbol{\nu} - \underline{\mathbf{curl}}_{\mathbf{s}}(\mathbf{u}_D)\|_{0,e}^2 \le C_9\|\mathbf{t}-\mathbf{t}_h\|_{0,K_e}^2 \qquad \forall\, e \in \mathcal{E}_h(\Gamma),$

j) $h_e\|\widetilde{\mathbf{t}}_h - \mathbf{curl}_{\mathbf{s}}(\varphi_D)\|_{0,e}^2 \le C_{10}\|\widetilde{\mathbf{t}}-\widetilde{\mathbf{t}}_h\|_{0,K_e}^2 \qquad \forall\, e \in \mathcal{E}_h(\Gamma).$

Proof. The proof of a) and b) follows as in Lemma 3.17 by using now the local inverse inequality (3.46) with $n = 3$. Analogously, c) and d) follow from Lemma 3.18 and the present estimates a) and b). In turn, for the proof of e), f), g), and h), we refer to [37, Lemmas 4.9 and 4.10]. Finally, i) and j) are consequence of a straightforward adaptation of the proof of [38, Lemma 4.15], along with the definitions of $\underline{\mathbf{curl}}_{\mathbf{s}}$ and $\mathbf{curl}_{\mathbf{s}}$, respectively. □

5 Extension to the Oberbeck–Boussinesq problem

The same tools and techniques employed in the previous sections can be applied to develop the a posteriori error analysis of the fully-mixed finite element introduced in [25] for the steady state Oberbeck–Boussinesq model. The resulting a posteriori error estimators for the 2D and 3D cases are summarized in Sections 5.3 and 5.4 below after recalling next the model problem and its associated continuous and discrete formulations.

5.1 The Oberbeck–Boussinesq problem

The stationary Oberbeck-Boussinesq problem consists of the incompressible Navier-Stokes-Brinkman equations coupled with the heat and mass transfer equations through a convective term and a buoyancy term acting in opposite direction to gravity. More precisely, given an external force per unit mass $\boldsymbol{g} \in \mathbf{L}^\infty(\Omega)$, and Dirichlet data $\mathbf{u}_D \in \mathbf{H}^{1/2}(\Gamma)$, and $\varphi_{1,D}$, $\varphi_{2,D} \in \mathrm{H}^{1/2}(\Gamma)$, the model reduces to: Find a velocity field $\mathbf{u}$, a pressure field p, a temperature field φ_1, and a concentration field φ_2, both defining a vector $\boldsymbol{\varphi} := \big(\varphi_1, \varphi_2\big)$, such that

$$
\begin{gathered}
\gamma\mathbf{u} - \mathbf{div}(2\mu(\boldsymbol{\varphi})\boldsymbol{e}(\mathbf{u})) + (\nabla\mathbf{u})\mathbf{u} + \nabla p = (\boldsymbol{\vartheta}\cdot\boldsymbol{\varphi})\boldsymbol{g} \quad \text{in} \quad \Omega, \qquad \operatorname{div}(\mathbf{u}) = 0 \quad \text{in} \quad \Omega\,, \\
-\operatorname{div}(\mathbb{K}_1\nabla\varphi_1) + \mathbf{u}\cdot\nabla\varphi_1 = 0 \quad \text{in} \quad \Omega\,, \quad -\operatorname{div}(\mathbb{K}_2\nabla\varphi_2) + \mathbf{u}\cdot\nabla\varphi_2 = 0 \quad \text{in} \quad \Omega\,, \\
\mathbf{u} = \mathbf{u}_D \quad \text{on} \quad \Gamma\,, \quad \varphi_1 = \varphi_{1,D} \quad \text{on} \quad \Gamma\,, \quad \varphi_2 = \varphi_{2,D} \quad \text{on} \quad \Gamma\,,
\end{gathered}
\tag{5.1}
$$

where γ is a positive constant inversely proportional to the reciprocal of the Darcy number Da, $\mu : \mathrm{R}\times\mathrm{R}^+ \longrightarrow \mathrm{R}^+$ is the viscosity of the fluid, $\boldsymbol{e}(\mathbf{u})$ is the symmetric part of the velocity gradient $\nabla\mathbf{u}$, also known as the rate of strain tensor, $\boldsymbol{\vartheta} := (\vartheta_1, \vartheta_2)$ is a vector containing expansion coefficients, and $\mathbb{K}_j \in \mathbb{L}^\infty(\Omega)$, with $j \in \{1,2\}$, are uniformly positive definite tensors describing the thermal conductivity of the fluid. In addition, μ is assumed bounded and Lipschitz continuous, which means that there exist constants μ_1, μ_2, $L_\mu > 0$, such that

$$
\mu_1 \,\le\, \mu(\boldsymbol{\phi}) \,\le\, \mu_2 \quad \text{and} \quad |\mu(\boldsymbol{\phi}) - \mu(\boldsymbol{\psi})| \,\le\, L_\mu\,|\boldsymbol{\phi} - \boldsymbol{\psi}| \qquad \forall\,\boldsymbol{\phi},\,\boldsymbol{\psi} \in \mathrm{R}\times\mathrm{R}^+\,,
$$

where $|\cdot|$ denotes from on the euclidean norm of R^n, $n \in \big\{1,2,3\big\}$. We remark here that, because of the incompressibility of the fluid (cf. second eq. of (5.1)) and the Dirichlet boundary condition (cf. fifth eq. of (5.1)), $\mathbf{u}_D$ must satisfy the compatibility condition $\int_\Gamma \mathbf{u}_D\cdot\boldsymbol{\nu} = 0$. Then, using some of the auxiliary unknowns defined in Section 2.2, introducing the new ones that are set implicitly next, denoting $\boldsymbol{\varphi}_D := \big(\varphi_{1,D}, \varphi_{2,D}\big)$, and eliminating the pressure p, as we did in Section 2.2, the Oberbeck–Boussinesq problem (5.1) can be re-stated as follows: Find $(\mathbf{u}, \mathbf{t}, \boldsymbol{\sigma})$ and $(\varphi_j, \widetilde{\mathbf{t}}_j, \widetilde{\boldsymbol{\sigma}}_j)$, $j \in \big\{1,2\big\}$, in suitable spaces to be indicated below such that

$$
\begin{array}{rcll}
\nabla\mathbf{u} & = & \mathbf{t} & \text{in} \quad \Omega\,, \\
\gamma\mathbf{u} - \mathbf{div}\,\boldsymbol{\sigma} + \dfrac{1}{2}\,\mathbf{t}\mathbf{u} - (\boldsymbol{\vartheta}\cdot\varphi)\boldsymbol{g} & = & \mathbf{0} & \text{in} \quad \Omega\,, \\
2\mu(\varphi)\mathbf{t}_{sym} - \dfrac{1}{2}(\mathbf{u}\otimes\mathbf{u})^{\mathrm{d}} & = & \boldsymbol{\sigma}^{\mathrm{d}} & \text{in} \quad \Omega\,, \\
\nabla\varphi_j & = & \widetilde{\mathbf{t}}_j & \text{in} \quad \Omega\,, \\
\mathbb{K}_j\widetilde{\mathbf{t}}_j - \dfrac{1}{2}\varphi_j\,\mathbf{u} & = & \widetilde{\boldsymbol{\sigma}}_j & \text{in} \quad \Omega\,, \\
-\mathbf{div}\,\widetilde{\boldsymbol{\sigma}}_j + \dfrac{1}{2}\widetilde{\mathbf{t}}_j\cdot\mathbf{u} & = & 0 & \text{in} \quad \Omega\,, \\
\displaystyle\int_\Omega \operatorname{tr}(2\boldsymbol{\sigma} + \mathbf{u}\otimes\mathbf{u}) = 0\,, \quad \mathbf{u} = \mathbf{u}_D \quad \text{and} \quad \boldsymbol{\varphi} & = & \boldsymbol{\varphi}_D & \text{on} \quad \Gamma\,,
\end{array}
\tag{5.2}
$$

5.2 The continuous and discrete formulations

Bearing in mind the definitions and notations from Section 2.2, and according to the derivation provided in [25, Section 3.1], the fully-mixed variational formulation of the coupled problem (5.2) reads: Find $(\vec{\mathbf{u}}, \boldsymbol{\sigma}) \in \mathbf{H}\times\mathbb{H}_0(\mathbf{div}_{4/3};\Omega)$ and $(\vec{\varphi}_j, \widetilde{\boldsymbol{\sigma}}_j) \in \widetilde{\mathbf{H}}\times\mathbf{H}(\operatorname{div}_{4/3};\Omega)$, $j \in \{1,2\}$ such that

$$
\begin{array}{rcll}
\widehat{a}_{\boldsymbol{\varphi}}(\vec{\mathbf{u}}, \vec{\mathbf{v}}) + c(\mathbf{u}; \vec{\mathbf{u}}, \vec{\mathbf{v}}) + b(\vec{\mathbf{v}}, \boldsymbol{\sigma}) & = & \widehat{F}_{\boldsymbol{\varphi}}(\vec{\mathbf{v}}) & \forall\,\vec{\mathbf{v}} \in \mathbf{H}\,, \\
b(\vec{\mathbf{u}}, \boldsymbol{\tau}) & = & G(\boldsymbol{\tau}) & \forall\,\boldsymbol{\tau} \in \mathbb{H}_0(\mathbf{div}_{4/3};\Omega)\,, \\
\widetilde{a}_j(\vec{\varphi}_j, \vec{\psi}_j) + \widetilde{c}_{\mathbf{u}}(\vec{\varphi}_j, \vec{\psi}_j) + \widetilde{b}(\vec{\psi}_j, \widetilde{\boldsymbol{\sigma}}_j) & = & 0 & \forall\,\vec{\psi}_j \in \widetilde{\mathbf{H}}\,, \\
\widetilde{b}(\vec{\varphi}_j, \widetilde{\boldsymbol{\tau}}_j) & = & \widetilde{G}(\widetilde{\boldsymbol{\tau}}_j) & \forall\,\widetilde{\boldsymbol{\tau}}_j \in \mathbf{H}(\operatorname{div}_{4/3};\Omega)\,,
\end{array}
\tag{5.3}
$$

where, given $\boldsymbol{\phi} \in \mathbf{L}^4(\Omega)$, the forms $\widehat{a}_{\boldsymbol{\phi}}$ and $\widetilde{a}_j$, and the functional $\widehat{F}_{\boldsymbol{\phi}}$, are defined by

$$\widehat{a}_{\boldsymbol{\phi}}(\vec{\mathbf{u}},\vec{\mathbf{v}}) := (\gamma\mathbf{u},\mathbf{v})_\Omega + (2\mu(\boldsymbol{\phi})\mathbf{t}_{\mathrm{sym}},\mathbf{s})_\Omega\,, \quad \widetilde{a}_j(\vec{\varphi}_j,\vec{\psi}_j) := (\mathbb{K}_j\widetilde{\mathbf{t}}_j,\widetilde{\mathbf{s}}_j)_\Omega\,, \quad \widehat{F}_{\boldsymbol{\phi}}(\vec{\mathbf{v}}) := ((\boldsymbol{\vartheta}\cdot\boldsymbol{\phi})\boldsymbol{g},\mathbf{v})_\Omega$$

for all $\vec{\mathbf{u}} := (\mathbf{u},\mathbf{t})$, $\vec{\mathbf{v}} := (\mathbf{v},\mathbf{s}) \in \mathbf{H}$, for all $\boldsymbol{\tau} \in \mathbb{H}_0(\mathbf{div}_{4/3};\Omega)$, for all $\vec{\varphi}_j := (\varphi_j,\widetilde{\mathbf{t}}_j)$, $\vec{\psi}_j := (\psi_j,\widetilde{\mathbf{s}}_j) \in \widetilde{\mathbf{H}}$, and for all $\widetilde{\boldsymbol{\tau}}_j \in \mathbf{H}(\mathrm{div}_{4/3};\Omega)$. In turn, as stated at the beginning of this section, the forms b, c, $\widetilde{b}$, and $\widetilde{c}_{\mathbf{w}}$, the latter for a given $\mathbf{w} \in \mathbf{L}^4(\Omega)$, and the functionals G and $\widetilde{G}$, are defined in Section 2.2.

In turn, using the same finite element subspaces defined in Section 2.3, the Galerkin scheme associated with (5.3) reads: Find $(\vec{\mathbf{u}}_h,\boldsymbol{\sigma}_h) \in \mathbf{H}_h \times \mathbb{H}_h^{\boldsymbol{\sigma}}$ and $(\vec{\varphi}_{j,h},\widetilde{\boldsymbol{\sigma}}_{j,h}) \in \widetilde{\mathbf{H}}_h \times \mathbf{H}_h^{\widetilde{\boldsymbol{\sigma}}}$, $j \in \{1,2\}$ such that

$$\begin{aligned}
\widehat{a}_{\boldsymbol{\varphi}_h}(\vec{\mathbf{u}}_h,\vec{\mathbf{v}}_h) + c(\mathbf{u}_h;\vec{\mathbf{u}}_h,\vec{\mathbf{v}}_h) + b(\vec{\mathbf{v}}_h,\boldsymbol{\sigma}_h) &= \widehat{F}_{\boldsymbol{\varphi}_h}(\vec{\mathbf{v}}_h) && \forall\,\vec{\mathbf{v}}_h \in \mathbf{H}_h\,,\\
b(\vec{\mathbf{u}}_h,\boldsymbol{\tau}_h) &= G(\boldsymbol{\tau}_h) && \forall\,\boldsymbol{\tau}_h \in \mathbb{H}_h^{\boldsymbol{\sigma}}\,,\\
\widetilde{a}_j(\vec{\varphi}_{j,h},\vec{\psi}_{j,h}) + \widetilde{c}_{\mathbf{u}_h}(\vec{\varphi}_{j,h},\vec{\psi}_{j,h}) + \widetilde{b}(\vec{\psi}_{j,h},\widetilde{\boldsymbol{\sigma}}_{j,h}) &= 0 && \forall\,\vec{\psi}_h \in \widetilde{\mathbf{H}}_h\,,\\
\widetilde{b}(\vec{\varphi}_{j,h},\widetilde{\boldsymbol{\tau}}_{j,h}) &= \widetilde{G}(\widetilde{\boldsymbol{\tau}}_{j,h}) && \forall\,\widetilde{\boldsymbol{\tau}}_h \in \mathbf{H}_h^{\widetilde{\boldsymbol{\sigma}}}\,.
\end{aligned} \tag{5.4}$$

For the well-posedness of (5.3) and (5.4) we refer to [25, Theorem 3.9] and [25, Theorem 4.7], respectively, whereas the a priori error estimates and corresponding rates of convergence are established in [25, Theorems 5.1 and 5.2].

5.3 The a posteriori error estimator in 2D

Recall that

$$\vec{\boldsymbol{\sigma}} = ((\vec{\mathbf{u}},\boldsymbol{\sigma}),(\vec{\varphi}_1,\widetilde{\boldsymbol{\sigma}}_1),(\vec{\varphi}_2,\widetilde{\boldsymbol{\sigma}}_2)) \in \widehat{\mathbb{X}} := \mathbf{H}\times\mathbb{H}_0(\mathbf{div}_{4/3};\Omega)\times\widetilde{\mathbf{H}}\times\mathbf{H}(\mathrm{div}_{4/3};\Omega)\times\widetilde{\mathbf{H}}\times\mathbf{H}(\mathrm{div}_{4/3};\Omega)$$

is the unique solution of problem (5.3), and that

$$\vec{\boldsymbol{\sigma}}_h = ((\vec{\mathbf{u}}_h,\boldsymbol{\sigma}_h),(\vec{\varphi}_{1,h},\widetilde{\boldsymbol{\sigma}}_{1,h}),(\vec{\varphi}_{2,h},\widetilde{\boldsymbol{\sigma}}_{2,h})) \in \widehat{\mathbb{X}}_h := \mathbf{H}_h\times\mathbb{H}_h^{\boldsymbol{\sigma}}\times\widetilde{\mathbf{H}}_h\times\mathbf{H}_h^{\widetilde{\boldsymbol{\sigma}}}\times\widetilde{\mathbf{H}}_h\times\mathbf{H}_h^{\widetilde{\boldsymbol{\sigma}}}$$

is a solution of problem (5.4). Then, assuming as in Section 3.2, that $\mathbf{u}_D \in \mathbf{H}^1(\Gamma)\cap\mathbf{L}^4(\Gamma)$ and $\varphi_{j,D} \in \mathrm{H}^1(\Gamma)\cap\mathrm{L}^4(\Gamma)$, for $j \in \{1,2\}$, we define for each $K \in \mathcal{T}_h^b$ the local error indicators

$$\widetilde{\Psi}_K^{4/3} := \big\|\gamma\mathbf{u}_h - \mathbf{div}(\boldsymbol{\sigma}_h) + \frac{1}{2}\mathbf{t}_h\,\mathbf{u}_h - (\boldsymbol{\vartheta}\cdot\boldsymbol{\varphi}_h)\,\boldsymbol{g}\big\|_{0,4/3;K}^{4/3} + \sum_{j=1}^{2}\big\| - \mathrm{div}(\widetilde{\boldsymbol{\sigma}}_{j,h}) + \frac{1}{2}\mathbf{u}_h\cdot\widetilde{\mathbf{t}}_{j,h}\big\|_{0,4/3;K}^{4/3}\,, \tag{5.5}$$

$$\begin{aligned}
\bar{\Psi}_K^2 :=\;& \Big\|2\mu(\boldsymbol{\varphi}_h)\mathbf{t}_{h,sym} - \frac{1}{2}(\mathbf{u}_h\otimes\mathbf{u}_h)^{\mathtt{d}} - \boldsymbol{\sigma}_h^{\mathtt{d}}\Big\|_{0,K}^2 + \sum_{j=1}^{2}\big\|\mathbb{K}_j\widetilde{\mathbf{t}}_{j,h} - \frac{1}{2}\varphi_{j,h}\mathbf{u}_h - \widetilde{\boldsymbol{\sigma}}_{j,h}\big\|_{0,K}^2\\
&+ h_K^2\|\mathbf{rot}\,(\mathbf{t}_h)\|_{0,K}^2 + \sum_{j=1}^{2} h_K^2\|\mathrm{rot}\,(\widetilde{\mathbf{t}}_{j,h})\|_{0,K}^2 + \sum_{e\in\mathcal{E}_h(K)\cap\mathcal{E}_h(\Omega)} h_e\big\|[\![\mathbf{t}_h\,\mathbf{s}]\!]\big\|_{0,e}^2\\
&+ \sum_{j=1}^{2}\Bigg\{\sum_{e\in\mathcal{E}_h(K)\cap\mathcal{E}_h(\Omega)} h_e\big\|[\![\widetilde{\mathbf{t}}_{j,h}\cdot\mathbf{s}]\!]\big\|_{0,e}^2 + \sum_{e\in\mathcal{E}_h(K)\cap\mathcal{E}_h(\Gamma)} h_e\|\widetilde{\mathbf{t}}_{j,h}\cdot\mathbf{s} - \nabla\varphi_{j,D}\cdot\mathbf{s}\|_{0,e}^2\Bigg\}\\
&+ \sum_{e\in\mathcal{E}_h(K)\cap\mathcal{E}_h(\Gamma)} h_e\|\mathbf{t}_h\mathbf{s} - \nabla\mathbf{u}_D\,\mathbf{s}\|_{0,e}^2\,,
\end{aligned} \tag{5.6}$$

and

$$\widehat{\Psi}_K^4 := h_K^4 \|\mathbf{t}_h - \nabla \mathbf{u}_h\|_{0,4;K}^4 + \sum_{j=1}^{2} h_K^4 \|\widetilde{\mathbf{t}}_{j,h} - \nabla \varphi_{j,h}\|_{0,4;K}^4$$
$$+ \sum_{e \in \mathcal{E}_h(K)\cap\mathcal{E}_h(\Gamma)} h_e \|\mathbf{u}_D - \mathbf{u}_h\|_{0,4;e}^4 + \sum_{j=1}^{2} \left\{ \sum_{e \in \mathcal{E}_h(K)\cap\mathcal{E}_h(\Gamma)} h_e \|\varphi_{j,D} - \varphi_{j,h}\|_{0,4;e}^4 \right\}, \tag{5.7}$$

so that the global a posteriori error estimator is given by

$$\Psi = \left\{ \sum_{K\in\mathcal{T}_h^b} \widetilde{\Psi}_K^{4/3} \right\}^{3/4} + \left\{ \sum_{K\in\mathcal{T}_h^b} \bar{\Psi}_K^2 \right\}^{1/2} + \left\{ \sum_{K\in\mathcal{T}_h^b} \widehat{\Psi}_K^4 \right\}^{1/4}. \tag{5.8}$$

Then, the reliability and efficiency of Ψ, whose proofs follow very closely the analysis of Section 3, are established as follows.

Theorem 5.1 *Assume that the data are sufficiently small (similarly as indicated in Lemma* 3.7*), and suppose for simplicity that* $\mathbf{u}_D$ *and* $\varphi_{j,D}$*,* $j \in \{1,2\}$*, are piecewise polynomials. Then, there exist positive constants* $C_{\mathtt{rel}}$ *and* $C_{\mathtt{eff}}$*, independent of* h*, such that*

$$C_{\mathtt{eff}}\, \Psi + \text{h.o.t.} \,\le\, \|\vec{\boldsymbol{\sigma}} - \vec{\boldsymbol{\sigma}}_h\|_{\mathbb{X}} \,\le\, C_{\mathtt{rel}}\, \Psi\,,$$

where h.o.t. *stands for one or several terms of higher order.*

5.4 The a posteriori error estimator in 3D

In this case we define for each $K \in \mathcal{T}_h^b$

$$\bar{\Psi}_K^2 := \left\|2\mu(\boldsymbol{\varphi}_h)\mathbf{t}_{h,sym} - \frac{1}{2}(\mathbf{u}_h\otimes\mathbf{u}_h)^{\mathtt{d}} - \boldsymbol{\sigma}_h^{\mathtt{d}}\right\|_{0,K}^2 + \sum_{j=1}^{2} \left\|\mathbb{K}_j\widetilde{\mathbf{t}}_{j,h} - \frac{1}{2}\varphi_{j,h}\mathbf{u}_h - \widetilde{\boldsymbol{\sigma}}_{j,h}\right\|_{0,K}^2$$
$$+ h_K^2\|\underline{\mathbf{curl}}(\mathbf{t}_h)\|_{0,K}^2 + \sum_{j=1}^{2} h_K^2 \|\mathbf{curl}\,(\widetilde{\mathbf{t}}_{j,h})\|_{0,K}^2 + \sum_{e\in\mathcal{E}_h(K)\cap\mathcal{E}_h(\Omega)} h_e \big\|[\![\mathbf{t}_h\times\boldsymbol{\nu}]\!]\big\|_{0,e}^2$$
$$+ \sum_{j=1}^{2}\left\{ \sum_{e\in\mathcal{E}_h(K)\cap\mathcal{E}_h(\Omega)} h_e \big\|[\![\widetilde{\mathbf{t}}_{j,h}\times\boldsymbol{\nu}]\!]\big\|_{0,e}^2 + \sum_{e\in\mathcal{E}_h(K)\cap\mathcal{E}_h(\Gamma)} h_e \|\widetilde{\mathbf{t}}_{j,h}\times\boldsymbol{\nu} - \mathbf{curl}_{\mathbf{s}}(\varphi_{j,D})\|_{0,e}^2 \right\}$$
$$+ \sum_{e\in\mathcal{E}_h(K)\cap\mathcal{E}_h(\Gamma)} h_e \|\mathbf{t}_h\times\boldsymbol{\nu} - \underline{\mathbf{curl}}_{\mathbf{s}}(\mathbf{u}_D)\|_{0,e}^2\,,$$

so that, letting $\widetilde{\Psi}_K^{4/3}$ and $\widehat{\Psi}_K^4$ as defined by (5.5) and (5.7), the corresponding global a posteriori error estimator is given by (5.8), and the respective reliability and efficiency result is stated analogously to Theorem 5.1.

6 Numerical results

This section presents four computational tests that illustrate the properties of the proposed family of methods. Tests 1 and 2 consider the Boussinesq equations for non-isothermal flow, and tests 3 and

4 focus on the Oberbeck-Boussinesq system. For each problem we provide a test with known closed-form solution that we use to quantify the robustness of the a posteriori error estimators (tests 1 and 4), while we consider in tests 2 and 3 application-driven problems without closed-form solution. All computations use Alfeld splits (barycentric refined meshes) $\mathcal{T}_h^{\mathtt{b}}$ created from regular partitions $\mathcal{T}_h$ of Ω, using the open-source mesh manipulator GMSH [42]. For the implementation of the numerical schemes we have used the open-source finite element library FEniCS [2]. A Newton-Raphson algorithm with null initial guess is used for the resolution of all nonlinear problems, whereas the solution of tangent systems resulting from the linearization is carried out with the multifrontal massively parallel sparse direct solver MUMPS. The condition of zero-average pressure (thanks to (2.4), translated in terms of the trace of the tensor quantity $2\boldsymbol{\sigma}+\mathbf{u}\otimes\mathbf{u}$) is imposed by means of a real Lagrange multiplier.

Errors between exact and approximate solutions are denoted as

$$e(\mathbf{u}) := \|\mathbf{u}-\mathbf{u}_h\|_{0,4;\Omega}, \quad e(\mathbf{t}) := \|\mathbf{t}-\mathbf{t}_h\|_{0,\Omega} \quad e(\boldsymbol{\sigma}) := \|\boldsymbol{\sigma}-\boldsymbol{\sigma}_h\|_{\mathbf{div}_{4/3};\Omega}, \quad e(p) := \|p-p_h\|_{0,\Omega},$$

$$e(\varphi) := \sum_{j=1}^{2}\|\varphi_j-\varphi_{j,h}\|_{0,4;\Omega}, \quad e(\widetilde{\mathbf{t}}) := \sum_{j=1}^{2}\|\widetilde{\mathbf{t}}_j-\widetilde{\mathbf{t}}_{j,h}\|_{0,4;\Omega}, \quad e(\widetilde{\boldsymbol{\sigma}}) := \sum_{j=1}^{2}\|\widetilde{\boldsymbol{\sigma}}_j-\widetilde{\boldsymbol{\sigma}}_{j,h}\|_{\mathrm{div}_{4/3};\Omega},$$

while we let $r(\star)$ denote their corresponding rates of convergence, specified for the case of adaptive computations as

$$r(\star) := -2\frac{\log(\mathsf{e}(\star)/\mathsf{e}'(\star))}{\log(\mathtt{DoF}/\mathtt{DoF}')} \qquad \forall \star \in \left\{\mathbf{u},\mathbf{t},\boldsymbol{\sigma},p,\varphi,\widetilde{\mathbf{t}},\widetilde{\boldsymbol{\sigma}}\right\},$$

where $\mathtt{DoF}$ and $\mathtt{DoF}'$ denote the numbers of degrees of freedom associated with two consecutive meshes producing errors $\mathsf{e}(\star)$ and $\mathsf{e}'(\star)$, respectively.

The local contributions of the residual-based a posteriori error estimators (3.10), (4.2), and (5.8), which come from the constitutive equations, the conservation equations, and the inter-element residuals, are used to steer the adaptive mesh-refining. We follow Algorithm 6.1, which, though explained below for (2.12) and Θ (cf. (3.10)), applies in the same way for (5.4) and Ψ (cf. (5.8)). It is designed based on the classical loop of

$$\text{solving} \to \text{estimating} \to \text{marking} \to \text{refining} \to \text{solving} \to \cdots,$$

as specified in, e.g., [32, 46]. As in [25] we need to deal with the adaptive procedure associated with the initial triangular/tetrahedral mesh at each refinement step, and perform an additional step to treat its Alfeld split and to project the estimator on a macro (parent) mesh.

6.1 Example 1: accuracy for the Boussinesq problem using uniform and adaptive mesh refinement

First we verify numerically the convergence of the mixed method applied to the Boussinesq equations by manufacturing exact solutions of (2.6) over the L-shaped domain $\Omega=(-1,1)^2\setminus(0,1)^2$

$$\mathbf{u}=\begin{pmatrix}\cos(\frac{\pi}{2}x_1)\sin(\frac{\pi}{2}x_2)\\ -\sin(\frac{\pi}{2}x_1)\cos(\frac{\pi}{2}x_2)\end{pmatrix}, \; p=\frac{1+\sin(x_1x_2)}{(x_1-0.01)^2+(x_2-0.01)^2}, \; \varphi=0.1+e^{-100[(x_1-0.01)^2+(x_2-0.01)^2]},$$

from which we can determine the exact strain rate, pseudostress, pseudo-heat and heat flux. The values of the exact velocity and temperature are used for Dirichlet data $\mathbf{u}_D$ and φ_D, and they are also used to generate matching right-hand side forcing term and heat source. We consider synthetic viscosity and conduction functions, as well as constant gravity acceleration as follows

$$\mu(\varphi)=e^{-\varphi}, \quad \mathbb{K}=\begin{pmatrix}e^{-x_1} & x_1/10\\ x_2/10 & e^{-x_2}\end{pmatrix}, \quad \text{and} \quad \boldsymbol{g}=\begin{pmatrix}0\\-1\end{pmatrix}.$$

Algorithm 6.1 – Adaptive refinement algorithm

1: **for** a given computation **start** with a coarse mesh $\mathcal{T}_h$ made of triangles (or tetrahedra) Δ **and do**
2: **Generate** the associated barycentric refinement $\mathcal{T}_h^{\mathsf{b}}$ made of triangles (or tetrahedra) K,
3: **for** the current mesh $\mathcal{T}_h^{\mathsf{b}}$ **do**
4: **solve** the discrete problem (2.12) on the new barycentric mesh $\mathcal{T}_h^{\mathsf{b}}$,
5: **end for**
6: **for** each $K \in \mathcal{T}_h^{\mathsf{b}}$ **do**
7: **compute** $\widetilde{\Theta}_K$, $\bar{\Theta}_K$, **and** $\widehat{\Theta}_K$, **and** then **compute** the local a posteriori error indicator $\Theta_K := \widetilde{\Theta}_K + \bar{\Theta}_K + \widehat{\Theta}_K$,
8: **end for**
9: **for** each $\Delta \in \mathcal{T}_h$ **do**
10: **project** the local a posteriori error indicator to the parent mesh $\Theta_\Delta := \displaystyle\sum_{K \in \mathcal{T}_h^{\mathsf{b}},\, K \subseteq \Delta} \Theta_K$,
11: **end for**
12: **if** for an element in the parent mesh $L \in \mathcal{T}_h$ (even for a boundary element) we have $\Theta_L \geq 0.2 \max_{K \in \mathcal{T}_h^{\mathsf{b}}} \Theta_K$ **then**
13: **mark** L for refinement **and** mark further elements to guarantee that the triangulation remains regular,
14: **end if**
15: **if** sufficiently many elements in the parent mesh $\mathcal{T}_h$ are marked so that they represent a given fraction of the total estimated error **then**
16: **stop**
17: **else**
18: **continue** to the next step,
19: **end if**
20: **generate** an adapted parent mesh from $\mathcal{T}_h$ through a variable metric/Delaunay automatic meshing algorithm using the local indicators Θ_Δ, targeting the equidistribution of the local error indicators in the updated parent mesh,
21: **define** the resulting mesh as $\mathcal{T}_h$ and go to step (2).
22: **end for**

Note that the exact pressure (and therefore the exact pseudostress) and the exact temperature have relatively high gradients near the reentrant corner, and we expect the accuracy of the mixed finite element scheme to deteriorate upon using uniform mesh refinement.

On each refinement level we compute approximate solutions, as well as errors and convergence rates defined as above. The error history for each field variable and the effectivity index for the estimator (3.10), $\text{eff}(\Theta) := \mathsf{e}/\Theta$ (where e denotes the total error), are supplied in Table 6.1. These results tabulate the convergence of the method when following a uniform mesh refinement versus the adaptive case. In the uniform case we generate triangular meshes and refine them uniformly, then apply for each mesh a barycentric refinement, on which we compute numerical solutions and errors. In the adaptive case we use Algorithm 6.1. In all cases we see that the convergence is suboptimal for the uniform refinement whereas optimal and super-optimal rates are seen when we apply the adaptive algorithm. In addition, we observe that the effectivity index is much more stable in the adaptive case.

To further exemplify the performance of the numerical scheme, we show in Figure 6.1 approximate solutions (discontinuous velocity magnitude, postprocessed pressure, and temperature) obtained by the adaptive method on relatively coarse meshes, together with examples of locally refined barycentric

With uniform mesh refinement

DoF	h	$e(\mathbf{u})$	$r(\mathbf{u})$	$e(\mathbf{t})$	$r(\mathbf{t})$	$e(\boldsymbol{\sigma})$	$r(\boldsymbol{\sigma})$
2899	1.0000	4.73e+00	–	9.79e+01	–	5.31e+02	–
11521	0.5000	2.37e+00	1.003	5.59e+01	0.813	2.27e+02	1.235
45937	0.2500	2.54e+00	-0.100	7.61e+01	-0.447	2.30e+02	-0.022
183457	0.1250	1.46e+00	0.799	1.05e+02	-0.459	3.59e+02	-0.641
733249	0.0625	3.24e-01	2.173	8.50e+01	0.300	1.60e+02	1.163

$e(\varphi)$	$r(\varphi)$	$e(\widetilde{\mathbf{t}})$	$r(\widetilde{\mathbf{t}})$	$e(\widetilde{\boldsymbol{\sigma}})$	$r(\widetilde{\boldsymbol{\sigma}})$	$e(p)$	$r(p)$	eff(Θ)
6.01e-01	–	3.20e+00	–	8.25e+00	–	2.78e+02	–	0.5103
8.83e-02	2.780	1.27e+00	1.336	5.23e+00	0.662	1.30e+02	1.102	0.4823
3.19e-02	1.469	4.57e-01	1.479	4.79e+00	0.125	5.07e+01	1.362	0.3673
2.08e-02	0.619	3.18e-01	0.525	3.77e+00	0.348	4.05e+01	0.323	0.2884
9.69e-04	4.427	1.11e-01	1.514	7.09e-01	2.411	2.70e+01	0.585	0.1686

With adaptive mesh refinement

DoF	h	$e(\mathbf{u})$	$r(\mathbf{u})$	$e(\mathbf{t})$	$r(\mathbf{t})$	$e(\boldsymbol{\sigma})$	$r(\boldsymbol{\sigma})$
19405	0.5143	2.42e+00	–	7.43e+01	–	2.68e+02	–
30385	0.5144	1.65e+00	1.713	6.80e+01	2.753	1.94e+02	1.041
44236	0.5153	4.34e-01	7.115	3.55e+01	3.149	1.39e+02	2.514
57601	0.5146	6.21e-02	14.722	1.65e+01	4.873	2.64e+01	12.587
77653	0.5144	7.98e-03	13.741	6.77e+00	6.139	3.89e+00	12.833

$e(\varphi)$	$r(\varphi)$	$e(\widetilde{\mathbf{t}})$	$r(\widetilde{\mathbf{t}})$	$e(\widetilde{\boldsymbol{\sigma}})$	$r(\widetilde{\boldsymbol{\sigma}})$	$e(p)$	$r(p)$	eff(Θ)
3.19e-02	–	4.42e-01	–	4.68e+00	–	5.62e+01	–	0.2957
2.14e-02	1.768	3.15e-01	1.511	3.47e+00	1.335	4.02e+01	1.499	0.2879
3.48e-03	9.689	1.26e-01	4.897	1.09e+00	6.188	3.03e+01	1.506	0.2859
3.35e-04	17.717	2.33e-02	12.759	1.03e-01	17.869	7.13e+00	10.952	0.2514
8.11e-05	9.500	4.32e-03	11.292	1.20e-02	14.381	1.77e+00	9.322	0.2812

Table 6.1: Example 1: Convergence history for the fully-mixed approximation with polynomial degree $k = 2$ and using uniform (top block) and adaptive mesh refinement guided by (3.10) (bottom block). DoF stands for the number of degrees of freedom associated with each barycentric refined mesh $\mathcal{T}_h^{\mathtt{b}}$.

meshes indicating the expected refinement near the reentrant corner of the domain, located at the origin.

6.2 Example 2: adaptive computation for the 3D thermal cavity

Next we test the adaptive algorithm in a 3D problem consisting of the stationary Boussinesq equations on the unit cube $\Omega = (0,1)^3$, where the distribution of temperature and flow patterns is driven by differentially heating the enclosure. The classical benchmark problem uses unity viscosity and thermal conductivity (see, e.g., [4, 9, 35]), while here we use the same nonlinear viscosity as in the previous example together with $\boldsymbol{g} = (0,0,\mathrm{Ra})^{\mathtt{t}}$ with a Rayleigh number of $\mathrm{Ra} = 5 \cdot 10^4$. For the thermal energy conservation, the boundary is split into two regions: Γ_1 (top and bottom edges of the box) and Γ_2 (vertical walls) where temperature and heat flux are prescribed, respectively. The boundary temperature on Γ_1 is set to $\varphi_D = 0$ on the top surface and $\varphi_D = 1$ on the bottom. On Γ_2 we consider that the remainder squares of the boundary (that is, the cavity walls) are insulated, which translates

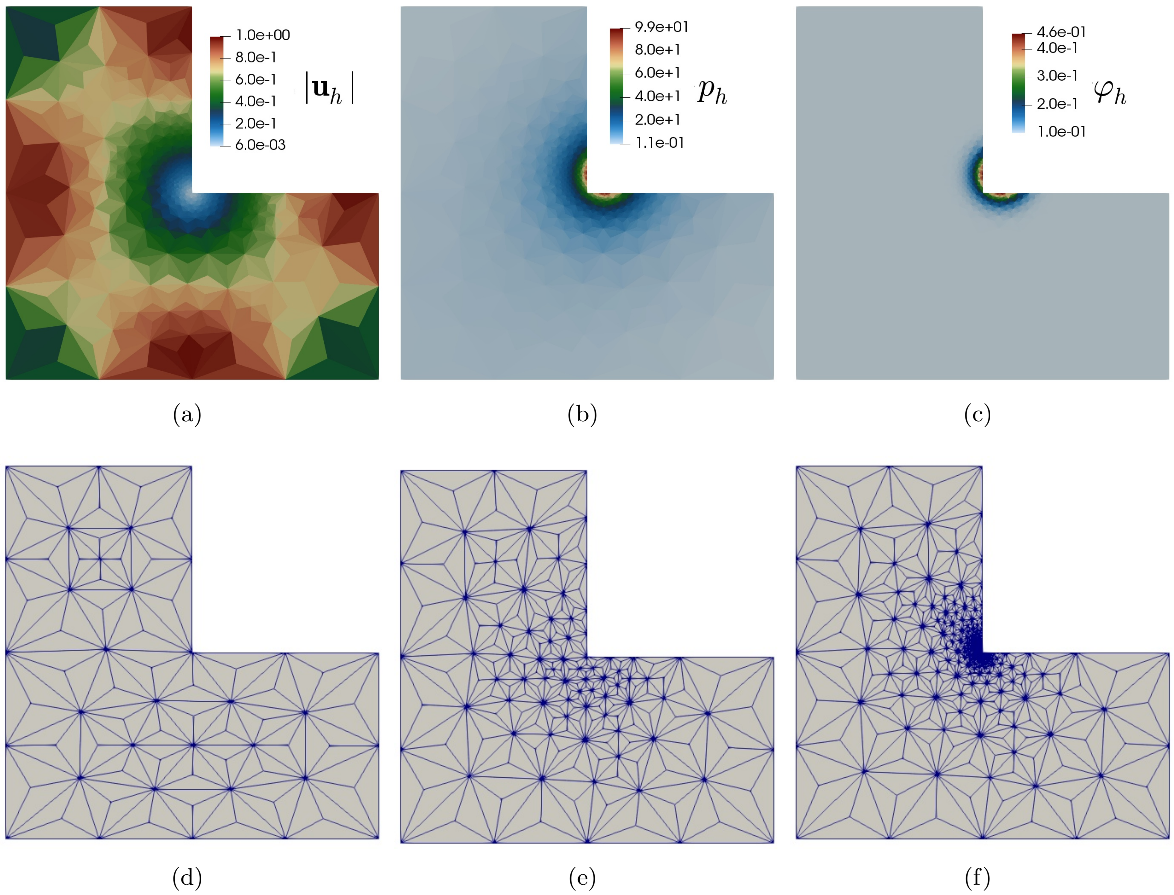

Figure 6.1: Example 1: Approximate velocity magnitude (a), postprocessed pressure (b), and temperature distribution (c) obtained using a mixed method for the Boussinesq problem with $k = 2$ and after two steps of adaptive mesh refinement. Panels (d,e,f) show samples of adaptive meshes.

in prescribing zero normal components for the heat flux $\widetilde{\boldsymbol{\sigma}}$, which is done as an essential boundary condition. Finally, no-slip velocities $\mathbf{u}_D = \mathbf{0}$ are prescribed everywhere on the boundary.

Starting with a coarse uniform tetrahedral mesh and its corresponding barycentric refinement, we compute numerical solutions using the mixed method with $k = 2$. The error estimator (4.2) guides the adaptive mesh refinement, which seems to focus the majority of the marking on the zone of higher temperature gradients. The performance of the scheme is exemplified in Figure 6.2 where we display approximate temperature, heat flux, and velocity streamlines that exhibit a qualitative agreement with the expected flow recirculation. We also show in the bottom panels of the figure, some coarse adaptively refined grids.

6.3 Example 3: adaptive Oberbeck-Boussinesq flow on a complex channel

The error estimation strategy applied to Oberbeck-Boussinesq flows is tested on a channel with three obstacles (using the domain and boundary configuration from the micro-macro models for incompressible flow introduced in [45]), and including mixed boundary conditions. On the inlet (the bottom horizontal section of the boundary defined by $(0, 1) \times \{-2\}$) we prescribe a parabolic inflow velocity

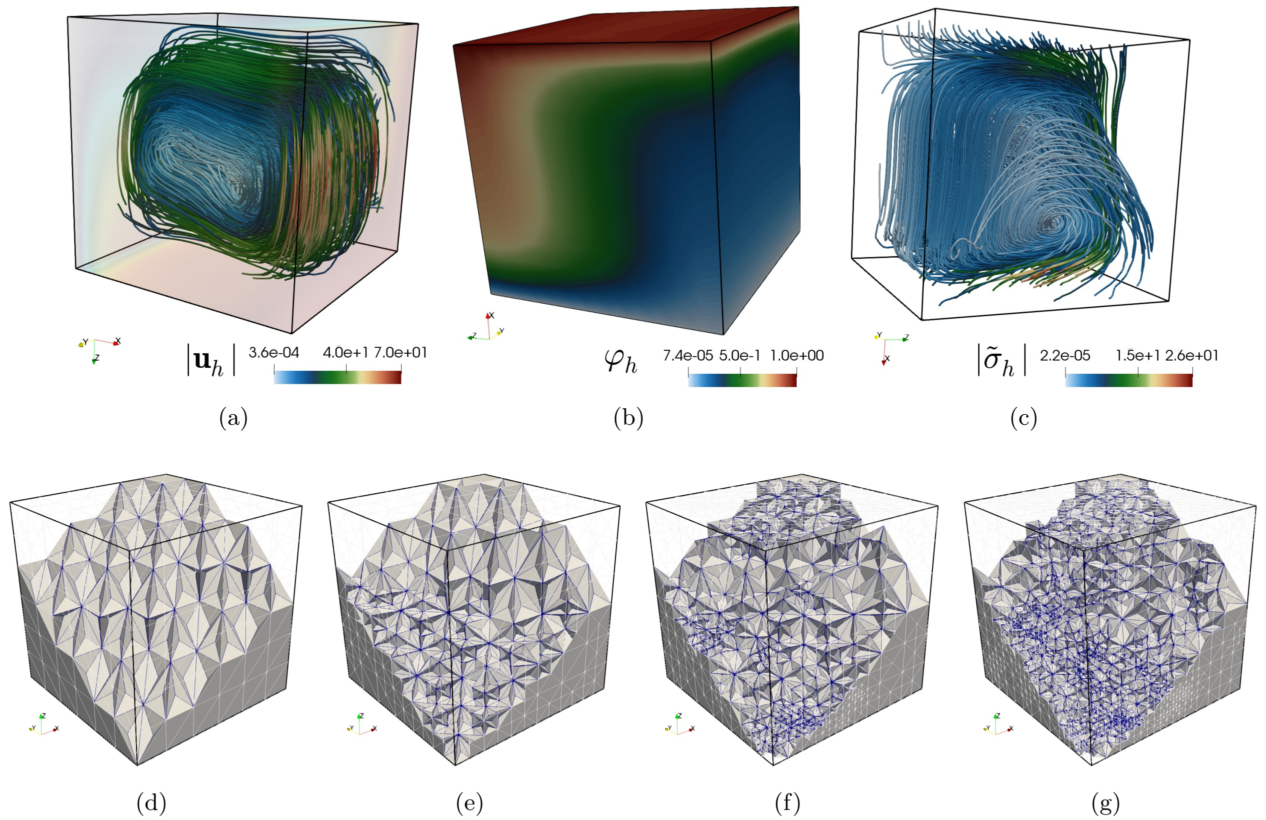

Figure 6.2: Example 2: Different angle views for approximate velocity streamlines (a), temperature distribution (b), and heat flux streamlines (c) for the Boussinesq equations modeling the differentially heated cavity. Solutions computed with a method using $k = 2$ and a barycentric tetrahedral grid obtained after four steps of adaptive mesh refinement. Panels (d,e,f,g) show samples of adaptive meshes with a crinkle clip across the geometry.

$\mathbf{u}_{D,1} = (0, x_1(1 - x_1))^{\mathtt{t}}$ and a constant concentration and temperature. On the outlet (the vertical segment on the top left part of the boundary, defined by $\{-2\} \times (0, 1))$ we impose constant concentration and temperature, and set zero normal Cauchy stress, which means that we need to impose $(\boldsymbol{\sigma} + \frac{1}{2}\mathbf{u} \otimes \mathbf{u})\boldsymbol{\nu} = \mathbf{0}$, and on the remainder of the boundary we set no-slip velocities. Zero-flux conditions are imposed for concentration on the outlet and for temperature elsewhere on the boundary. No closed-form solution is available for this problem but the global error estimator (5.8) decays with optimal order. For this test we use $k = 1$ and perform five steps of adaptive mesh refinement. The computed flow profiles and sample adaptive grids are shown in Figure 6.3.

6.4 Example 4: accuracy for the Oberbeck-Boussinesq problem in a truncated cube

We conclude our numerical tests with the verification of convergence of the mixed method and the adaptive mesh refinement applied to the Oberbeck-Boussinesq system. We use the non-convex domain

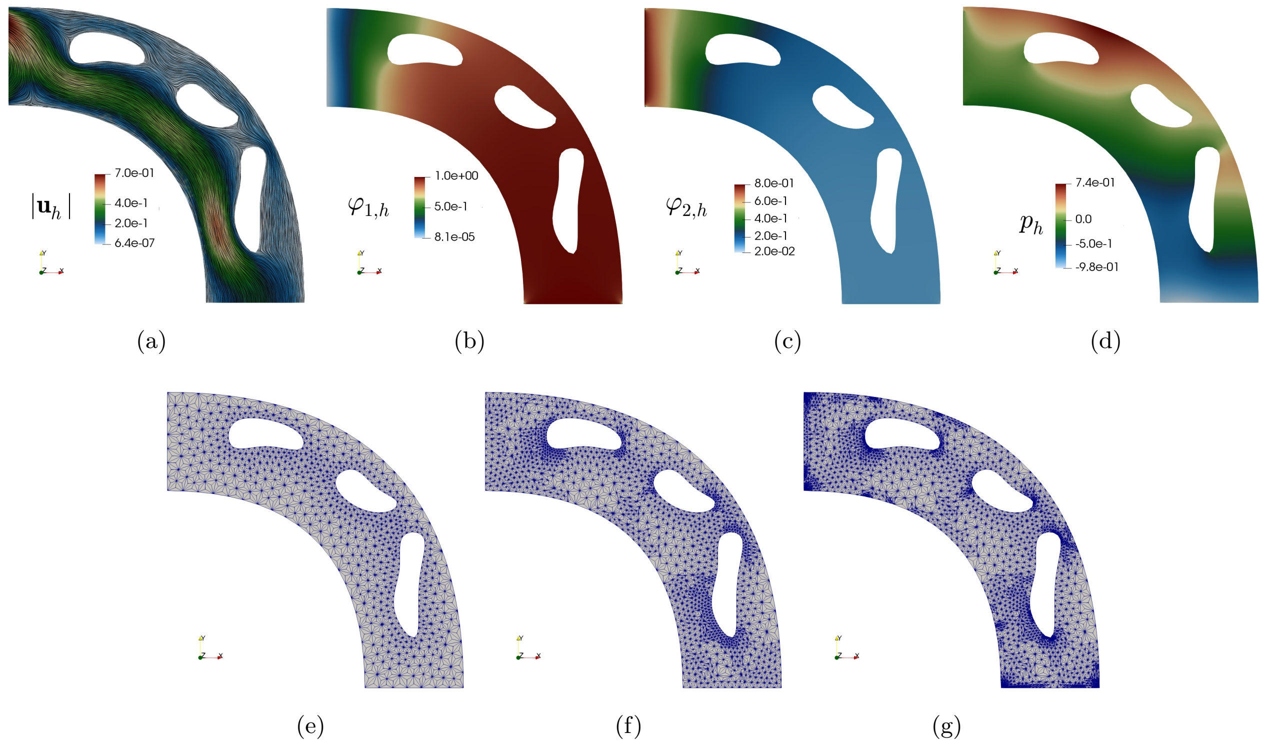

Figure 6.3: Example 3: Approximate velocity magnitude and line integral contour (a), temperature distribution (b), concentration distribution (c), and postprocessed pressure (d) for the Boussinesq-Oberbeck equations on a channel. Solutions computed with a method using $k = 1$. Panels (d,e,f) show samples of adaptive meshes.

$\Omega = (0,1)^3 \setminus [0.5,1]^3$ (with a volume of $|\Omega| = 0.875$), and consider the following closed-form solutions

$$\mathbf{u} = \begin{pmatrix} \sin^2(\pi x_1)\sin(\pi x_2)\sin(2\pi x_3) \\ \sin(\pi x_1)\sin^2(\pi x_2)\sin(2\pi x_3) \\ -[\sin(2\pi x_1)\sin(\pi x_2) + \sin(\pi x_1)\sin(2\pi x_2)]\sin^2(\pi x_3) \end{pmatrix}, \quad p = \frac{1 - x_1^2 - x_2^2 - x_3^2}{(x_1-0.55)^2 + (x_2-0.55)^2 + (x_3-0.55)^2},$$
$$\varphi_1 = 1 - \sin(\pi x_1)\cos(\pi x_2)\sin(\pi x_3), \quad \varphi_2 = \exp(-(x_1-0.55)^2 - (x_2-0.55)^2 - (x_3-0.55)^2)\,.$$

The manufactured exact velocity, concentration, and temperature are used as Dirichlet data everywhere on the boundary. The pressure has a strong gradient near the reentrant corner of the domain and therefore we expect that adaptive mesh refinement outperforms the convergence of the method using meshes successively refined in a uniform way. We select the following parameter values

$$\mu(\varphi) = \exp(-\varphi_1), \quad \gamma = 1, \quad \alpha = (1, 0.5)^{\mathtt{t}}, \quad \mathbb{K}_1 = \begin{pmatrix} \exp(-x_1) & 0 & 0 \\ 0 & \exp(-x_2) & 0 \\ 0 & 0 & \exp(-x_3) \end{pmatrix}, \quad \mathbb{K}_2 = \mathbb{I}.$$

The error history for each field variable (number of degrees of freedom associated with each mesh and experimental errors and convergence rates) and the effectivity index for the estimator (5.8) (its 3D version), $\mathrm{eff}(\Psi) := \mathtt{e}/\Psi$ (where $\mathtt{e}$ denotes the total error), are supplied in Table 6.2. As in the 2D Boussinesq case of Example 1, the lack of smoothness of the exact solution is reflected in the hindered convergence observed under uniform mesh refinement. Noticeably improved results are obtained for

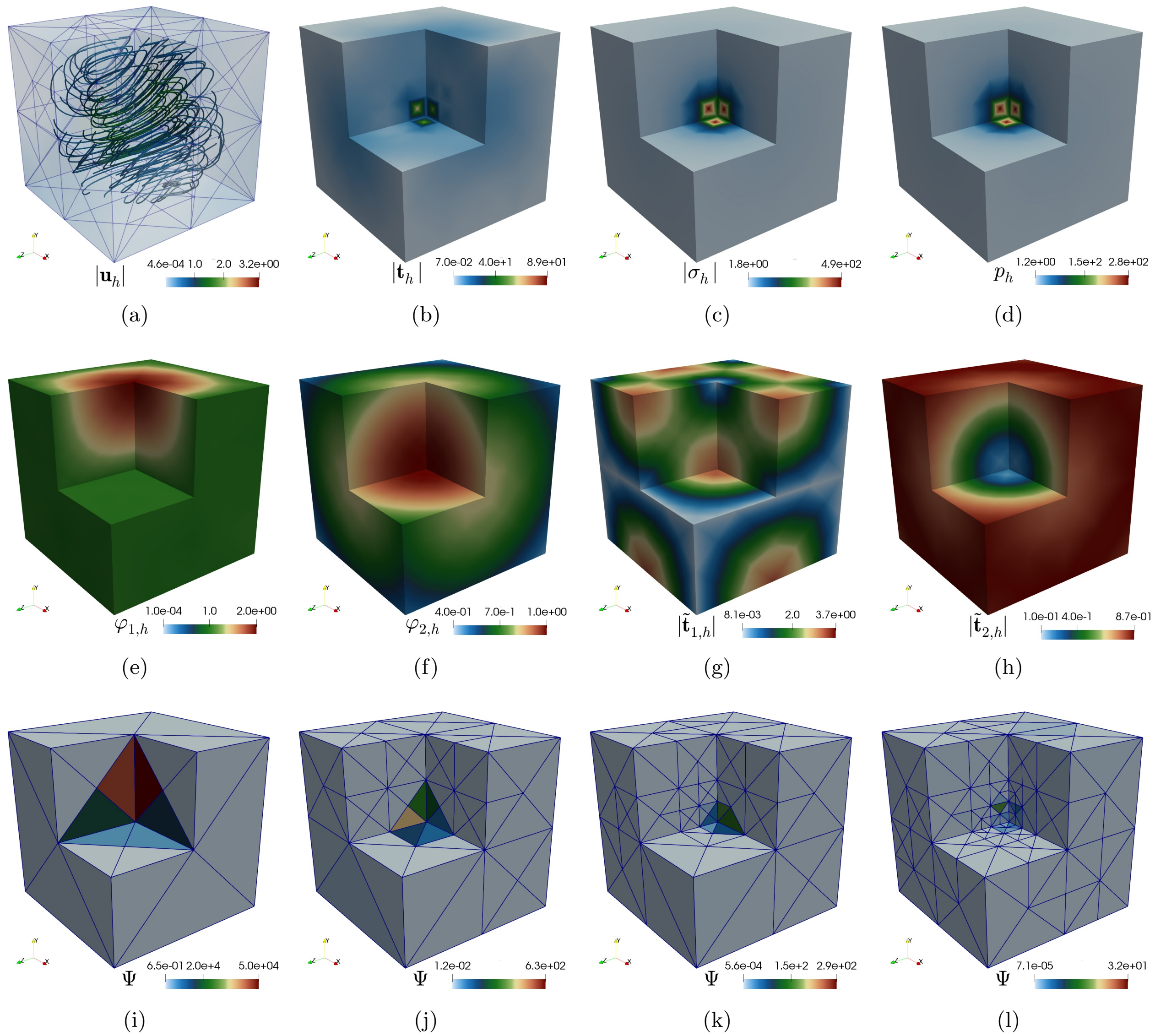

Figure 6.4: Example 4: Approximate velocity magnitude and streamlines (a), velocity gradient (b), Bernoulli tensor (c), postprocessed pressure (d), temperature (e), concentration (f), temperature gradient (g), and concentration gradient (h), obtained using $k = 2$ and an adaptive barycentrically refined tetrahedral mesh. Panels (i,j,k,l) show the repartition of the indicator on coarse sample meshes.

the case of adaptive mesh refinement. The overall mesh density is controlled through a refinement tolerance in order to produce adaptive meshes representing fewer degrees of freedom than in the uniform case. Even then the errors decay much faster for the adaptive case and the effectivity index remains in a neighborhood of 0.69, confirming the efficiency and reliability of the a posteriori error indicator. Approximate solutions are shown in Figure 6.4.

With uniform mesh refinement

DoF	h	$e(\mathbf{u})$	$r(\mathbf{u})$	$e(\mathbf{t})$	$r(\mathbf{t})$	$e(\boldsymbol{\sigma})$	$r(\boldsymbol{\sigma})$		
46251	1	0.5848	–	17.11	–	135.7	–		
368921	0.5	0.1542	1.285	11.67	0.549	96.16	0.332		
2947041	0.3056	0.1320	0.511	9.265	0.388	64.02	0.451		
8655681	0.1528	0.0944	0.603	6.304	0.410	45.78	0.398		
$e(\varphi)$	$r(\varphi)$	$e(\widetilde{\mathbf{t}})$	$r(\widetilde{\mathbf{t}})$	$e(\widetilde{\boldsymbol{\sigma}})$	$r(\widetilde{\boldsymbol{\sigma}})$	$e(p)$	$r(p)$	eff(Ψ)	It.
0.03211	–	0.6320	–	0.9353	–	6.432	–	0.7676	4
0.02031	0.694	0.4377	0.467	0.6395	0.698	3.678	0.538	0.8542	3
0.01276	0.766	0.1929	0.776	0.2684	0.819	2.353	0.692	0.6129	3
0.00715	0.983	0.1307	0.462	0.2591	0.128	2.012	0.377	0.3009	4

With adaptive mesh refinement

DoF	h	$e(\mathbf{u})$	$r(\mathbf{u})$	$e(\mathbf{t})$	$r(\mathbf{t})$	$e(\boldsymbol{\sigma})$	$r(\boldsymbol{\sigma})$		
46251	1	0.5848	–	17.11	–	235.7	–		
102181	1	0.3689	3.185	13.14	2.885	101.3	2.764		
160002	0.7071	0.1952	2.838	9.246	2.233	60.17	2.552		
334557	0.7071	0.0913	2.524	6.365	2.681	37.95	2.845		
468940	0.7071	0.0532	2.487	4.032	2.528	22.79	2.709		
667680	0.5719	0.0376	2.435	2.516	2.507	17.48	2.696		
844490	0.5673	0.0193	2.617	1.254	2.791	11.89	2.391		
$e(\varphi)$	$r(\varphi)$	$e(\widetilde{\mathbf{t}})$	$r(\widetilde{\mathbf{t}})$	$e(\widetilde{\boldsymbol{\sigma}})$	$r(\widetilde{\boldsymbol{\sigma}})$	$e(p)$	$r(p)$	eff(Ψ)	It.
0.03211	–	0.6325	–	0.9353	–	7.432	–	0.7676	4
0.02371	2.474	0.3761	3.543	0.6802	2.497	5.457	1.954	0.6541	4
0.01240	1.946	0.2189	2.413	0.3549	2.794	2.872	2.506	0.6799	5
0.00628	2.666	0.1047	2.123	0.1985	2.342	1.916	2.126	0.6701	4
0.00161	2.728	0.0722	2.401	0.1343	2.194	1.141	2.396	0.6959	4
0.00092	2.729	0.0504	2.504	0.0865	2.946	0.753	2.560	0.6954	4
0.00065	2.249	0.0299	2.538	0.0596	2.444	0.449	3.028	0.6984	4

Table 6.2: Example 4: Convergence history and Newton iteration count for the fully-mixed approximation of the Oberbeck-Boussinesq equations on a truncated cube.

References

[1] S. Agmon, *Lectures on Elliptic Boundary Value Problems.* Van Nostrand, Princeton, NJ, 1965.

[2] M.S Alnæs, J. Blechta, J. Hake, A. Johansson, B. Kehlet, A. Logg, C. Richardson, J. Ring, M.E. Rognes and G.N. Wells, *The FEniCS project version 1.5.* Arch. Numer. Softw. 3 (2015), no. 100, 9–23.

[3] K. Allali, *A priori and a posteriori error estimates for Boussinesq equations.* Int. J. Numer. Anal. Model. 2 (2005), 179–196.

[4] A. Allendes, C. Naranjo and E. Otárola, *Stabilized finite element approximations for a generalized Boussinesq problem: a posteriori error analysis.* Comput. Methods Appl. Mech. Engrg. 361 (2020), Art. 112703.

[5] J.A. Almonacid and G.N. Gatica, *A fully-mixed finite element method for the n-dimensional Boussinesq problem with temperature-dependent parameters.* Comput. Methods Appl. Math. 20 (2020), no. 2, 187–213.

[6] J.A. Almonacid, G.N. Gatica and R.Oyarzúa, *A mixed-primal finite element method for the Boussinesq problem with temperature-dependent viscosity.* Calcolo 55 (2018), no. 3, Art. 36.

[7] J.A. Almonacid, G.N. Gatica and R. Oyarzúa, *A posteriori error analysis of a mixed-primal finite element method for the Boussinesq problem with temperature-dependent viscosity.* J. Sci. Comput. 78 (2019), no. 2, 887–917.

[8] J.A. Almonacid, G.N. Gatica, R. Oyarzúa and R. Ruiz-Baier, *A new mixed finite element method for the n-dimensional Boussinesq problem with temperature-dependent viscosity.* Netw. Heterog. Media 15 (2020), no. 2, 215–245.

[9] M. Alvarez, G.N. Gatica and R. Ruiz-Baier, *An augmented mixed-primal finite element method for a coupled flow-transport problem*, ESAIM: Math. Model. Numer. Anal. 49 (2015), 1399–1427.

[10] M. Alvarez, G.N. Gatica and R. Ruiz-Baier, *A posteriori error analysis for a viscous flow-transport problem.* ESAIM: Math. Model. Numer. Anal., 50 (2016), no. 6, 1789–1816.

[11] M. Alvarez, G.N. Gatica and R. Ruiz-Baier, *A posteriori error estimation for an augmented mixed-primal method applied to sedimentation-consolidation systems.* J. Comput. Phys. 367 (2018), 322–346.

[12] T.P. Barrios, G.N. Gatica, M. González and N. Heuer, *A residual based a posteriori error estimator for an augmented mixed finite element method in linear elasticity.* M2AN Math. Model. Numer. Anal. 40 (2006), no. 5, 843–869

[13] G. Benavides, S. Caucao, G.N. Gatica and A.A. Hopper, *A Banach spaces-based analysis of a new mixed-primal finite element method for a coupled flow-transport problem.* Comput. Methods Appl. Mech. Engrg. 371 (2020), Art. 113285.

[14] R. Bürger, A. Khan, P.E. Méndez and R. Ruiz-Baier, *Divergence-conforming methods for transient doubly-diffusive flows: A priori and a posteriori error analysis.* Arxiv Preprint (2021). Available from http://arxiv.org/abs/2102.05819.

[15] J. Camaño, S. Caucao, R. Oyarzúa and S. Villa-Fuentes, *A posteriori error analysis of a momentum conservative Banach-spaces based mixed-FEM for the Navier-Stokes problem.* Preprint 2020-24, Centro de Investigación en Ingeniería Matemática (CI^2MA), Universidad de Concepción, Chile, (2020).

[16] J. Camaño, C. García and R. Oyarzúa, *Analysis of a momentum conservative mixed-FEM for the stationary Navier–Stokes problem.* Numer. Methods Partial Differential Equations 37 (2021), no. 5, 2895–2923.

[17] S. Caucao, M. Discacciati, G.N. Gatica and R. Oyarzúa, *A conforming mixed finite element method for the Navier–Stokes/Darcy–Forchheimer coupled problem.* ESAIM Math. Model. Numer. Anal. 54 (2020), no. 5, 1689–1723.

[18] S. Caucao, G.N. Gatica and R. Oyarzúa, *A posteriori error analysis of a fully-mixed formulation for the Navier–Stokes/Darcy coupled problem with nonlinear viscosity*. Comput. Methods Appl. Mech. Engrg. 315 (2017), 943–971.

[19] S. Caucao, G.N. Gatica and R. Oyarzúa, *A posteriori analysis of an augmented fully mixed formulation for the nonisothermal Oldroyd-Stokes problem*. Numer. Methods Partial Differential Equations 35 (2019), no. 1, 295–324.

[20] S. Caucao, G.N. Gatica, R. Oyarzúa and F. Sandoval, *Residual-based a posteriori error analysis for the coupling of the Navier–Stokes and Darcy–Forchheimer equations*. ESAIM Math. Model. Numer. Anal. 55 (2021), no. 2, 659–687.

[21] S. Caucao, G.N. Gatica and F. Sandoval, *A fully-mixed finite element method for the coupling of the Navier-Stokes and Darcy-Forchheimer equations*. Numer. Methods Partial Differential Equations 37 (2021), no. 3, 2550–2587.

[22] S. Caucao, R. Oyarzúa and S. Villa-Fuentes, *A new mixed-FEM for steady-state natural convection models allowing conservation of momentum and thermal energy*. Calcolo 57 (2020), no. 4, article:36.

[23] P. Clément, *Approximation by finite element functions using local regularisation*. RAIRO Modélisation Mathématique et Analyse Numérique 9 (1975), 77–84.

[24] E. Colmenares, G.N Gatica and S. Moraga, *A Banach spaces-based analysis of a new fully-mixed finite element method for the Boussinesq problem*. ESAIM Math. Model. Numer. Anal. 54 (2020), no. 5, 1525–1568.

[25] E. Colmenares, G.N. Gatica, S. Moraga and R. Ruiz-Baier, *A fully-mixed finite element method for the steady state Oberbeck-Boussinesq system*. SMAI J. Comput. Math. 6 (2020), 125–157.

[26] E. Colmenares, G.N. Gatica and R. Oyarzúa, *Analysis of an augmented mixed–primal formulation for the stationary Boussinesq problem*. Numer. Methods Partial Differential Equations 32 (2016), no. 2, 445–478.

[27] E. Colmenares, G.N. Gatica and R. Oyarzúa, *An augmented fully-mixed finite element method for the stationary Boussinesq problem*. Calcolo 54 (2017), no. 1, 167–205.

[28] E. Colmenares, G.N. Gatica and R. Oyarzúa, *A posteriori error analysis of an augmented mixed-primal formulation for the stationary Boussinesq model*. Calcolo 54 (2017), no. 3, 1055–1095.

[29] E. Colmenares, G.N. Gatica and R. Oyarzúa, *A posteriori error analysis of an augmented fully-mixed formulation for the stationary Boussinesq model*. Comput. Math. Appl. 77 (2019), no. 3, 693–714.

[30] E. Colmenares and M. Neilan, *Dual-mixed finite element methods for the stationary Boussinesq problem*. Comp. Math. Appl. 72 (2016), no. 7, 1828–1850.

[31] C. Domínguez, G.N. Gatica and S. Meddahi, *A posteriori error analysis of a fully-mixed finite element method for a two-dimensional fluid-solid interaction problem*. J. Comput. Math. 33 (2015), no. 6, 606–641.

[32] W. Dörfler, *A convergent adaptive algorithm for Poisson's equation.* SIAM J. Numer. Anal. 33 (1994), no. 3, 1106–1124.

[33] A. Ern and J.-L. Guermond, *Theory and Practice of Finite Elements.* Applied Mathematical Sciences, 159. Springer-Verlag, New York, 2004.

[34] M. Farhloul, S. Nicaise and L. Paquet, *A priori and a posteriori error estimations for the dual mixed finite element method of the Navier-Stokes problem.* Numer. Methods Partial Differential Equations 25 (2009), no. 4, 843–869.

[35] T. Fusegi and J.M. Hyun, *A numerical study of 3D natural convection in a cube: effects of the horizontal thermal boundary conditions.* Fluid Dyn. Res. 8 (1991), no. 5-6, 221–230.

[36] G.N. Gatica, *A note on stable Helmholtz decompositions in 3D.* Appl. Anal. 99 (2020), no. 7, 1110–1121.

[37] G.N. Gatica, L.F Gatica and F. Sequeira, *A priori and a posteriori error analyses of a pseudostress-based mixed formulation for linear elasticity.* Comput. Math. Appl. 71 (2016), no. 2, 585–614.

[38] G.N. Gatica, A. Márquez and M.A. Sánchez, *Analysis of a velocity-pressure-pseudostress formulation for the stationary Stokes equations.* Comput. Methods Appl. Mech. Engrg. 199 (2010), 1064–1079.

[39] G.N. Gatica, R. Oyarzúa, R. Ruiz-Baier and Y.D. Sobral, *Banach spaces-based analysis of a fully-mixed finite element method for the steady-state model of fluidized beds.* Comput. Math. Appl. 84 (2021), 244–276.

[40] G.N. Gatica, R. Ruiz-Baier and G. Tierra, *A posteriori error analysis of an augmented mixed method for the Navier-Stokes equations with nonlinear viscosity.* Comput. Math. Appl. 72 (2016), no. 9, 2289–2310.

[41] L.F. Gatica, R. Oyarzúa and N. Sánchez, *A priori and a posteriori error analysis of an augmented mixed-FEM for the Navier-Stokes-Brinkman problem.* Comput. Math. Appl. 75 (2018), no. 7, 2420–2444.

[42] C. Geuzaine and J.-F. Remacle, *Gmsh: a three-dimensional finite element mesh generator with built-in pre- and post-processing facilities.* Int. J. Numer. Methods Engrg. 79 (2009), no. 11, 1309–1331.

[43] V. Girault and P.A. Raviart, *Finite Element Methods for Navier–Stokes Equations. Theory and Algorithms.* Springer Series in Computational Mathematics, 5. Springer-Verlag, Berlin, 1986.

[44] J. Howell and N. Walkington, *Dual-mixed finite element methods for the Navier-Stokes equations.* ESAIM Math. Model. Numer. Anal. 47 (2013), no. 3, 789–805.

[45] M. Torrilhon and N. Sarna, *Hierarchical Boltzmann simulations and model error estimation.* J. Comput. Phys. 342 (2017), 66–84.

[46] R. Verfürth, *A Review of A-Posteriori Error Estimation and Adaptive Mesh-Refinement Techniques.* Wiley Teubner, Chichester, 1996.

Centro de Investigación en Ingeniería Matemática (CI²MA)

PRE-PUBLICACIONES 2021

2021-09 Felisia A. Chiarello, Luis M. Villada: *On existence of entropy solutions for 1D nonlocal conservation laws with space-discontinous flux*

2021-10 Rodolfo Araya, Cristóbal Bertoglio, Cristian Cárcamo: *Error analysis of pressure reconstruction from discrete velocities*

2021-11 Gabriel N. Gatica, Filander A. Sequeira: *An Lp spaces-based mixed virtual element method for the two-dimensional Navier-Stokes equations*

2021-12 Gabriel N. Gatica, Cristian Inzunza: *On the well-posedness of Banach spaces-based mixed formulations for nearly incompressible elasticity and Stokes models*

2021-13 Nestor Sánchez, Tonatiuh Sanchez-Vizuet, Manuel Solano: *Error analysis of an unfitted HDG method for a class of non-linear elliptic problems*

2021-14 Paulo Amorim, Raimund Bürger, Rafael Ordoñez, Luis M. Villada: *Global existence in a food chain model consisting of two competitive preys, one predator and chemotaxis*

2021-15 Raimund Bürger, Julio Careaga, Stefan Diehl, Romel Pineda: *A moving-boundary model of reactive settling in wastewater treatment*

2021-16 Sergio Caucao, Gabriel N. Gatica, Juan P. Ortega: *A fully-mixed formulation in Banach spaces for the coupling of the steady Brinkman–Forchheimer and double-diffusion equations*

2021-17 David Mora, Alberth Silgado: *A C1 virtual element method for the stationary quasi-geostrophic equations of the ocean*

2021-18 Alfredo Bermúdez, Bibiana López-Rodríguez, Francisco José Pena, Rodolfo Rodríguez, Pilar Salgado, Pablo Venegas: *Numerical solution of an axisymmetric eddy current model with current and voltage excitations*

2021-19 Raimund Bürger, Sonia Valbuena, Carlos A. Vega: *A well-balanced and entropy stable scheme for a reduced blood flow model*

2021-20 Gabriel N. Gatica, Cristian Inzunza, Ricardo Ruiz-Baier, Felipe Sandoval: *A posteriori error analysis of Banach spaces-based fully-mixed finite element methods for Boussinesq-type models*

Para obtener copias de las Pre-Publicaciones, escribir o llamar a: Director, Centro de Investigación en Ingeniería Matemática, Universidad de Concepción, Casilla 160-C, Concepción, Chile, Tel.: 41-2661324, o bien, visitar la página web del centro: http://www.ci2ma.udec.cl




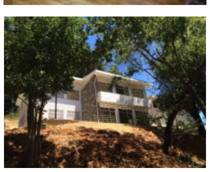
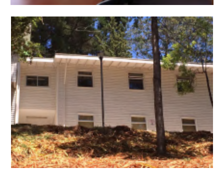

CENTRO DE INVESTIGACIÓN EN
INGENIERÍA MATEMÁTICA (CI^2MA)
Universidad de Concepción

Casilla 160-C, Concepción, Chile
Tel.: 56-41-2661324/2661554/2661316
http://www.ci2ma.udec.cl